Escola de Camins
Escola Tècnica Superior d'Enginyeria de Camins, Canals i Ports
UPC BARCELONATECH

TESIS DE MÁSTER

Máster

Máster Universitario en Ingeniería Civil

Título

Effect of asynchronous seismic action in long highway bridges

Autor

Carolina Esteves Dias

Tutor

Jesús Miguel Bairan

Intensificación

Ingeniería de Estructuras y Construcción

Fecha

30 de Junio de 2015

Carolina Esteves Dias

EFFECT OF ASYNCHRONOUS SEISMIC ACTION IN LONG HIGHWAY BRIDGES

Master Thesis in Civil Engineering supervised by Professor Jesús Miguel Bairan, presented to the Department of Construction Engineering of the Polytechnic University of Catalonia

June 2015

Universitat Politècnica de Catalunya

Content

List of Figures

List of Tables

Page

"A perfeição técnica de uma obra de Engenharia tem sempre reflexo na sua qualidade estética. A simplicidade e a justeza com que foi concebida comandam o grau de emoção que desperta naqueles que a contemplam.".

Eng. Edgar Cardoso

Abstract

The current study focus on the spatial variability of ground motion caused by a seismic action applied to large bridges. Four different bridges were studied and two different analysis were carried out on each of them: a synchronous analysis (where the seismic sign arrives at each pier's foundation at the same time) and an asynchronous one (where the seismic sign arrives at each pier's foundation with time gaps). The goal of this study is to evaluate the damage on the structure caused by both analysis carried out in each one of the four bridges and compare them, measuring the displacements of the deck, the base shear, the bending moment and the drift of the piers, in each of the cases. This study was performed considering two types of foundation ground, for both of the analysis performed, a solid rock and a compact sand, and comparing the difference of the results in each one. Both of the analysis were carried out using the software SAP2000. This study aims at showing the importance of considering the asynchrony of seismic waves and in which cases it causes more damages than a synchronous seismic sign, rather than figuring out which foundation ground is better or worse. It was concluded that the asynchronous analysis was the less favourable and that the results bring about more advantages when a better quality ground type is considered. In what matters the spatial variability of ground motion, the conclusion is that the uniform seismic excitation is not able to control the seismic design for long prestressed concrete bridges, and the influence of the multi-support excitations on the seismic responses of the long prestressed concrete bridges must be considered.

Key words: spatial variability, seismic sign, synchronous analysis, asynchronous analysis, large bridges, damages on the structure.

Resumen

El presente estudio trata la variabilidad espacial del movimiento del suelo provocado por la acción sísmica aplicada a puentes largos. Se han estudiado cuatro puentes diferentes sobre los cuales se desarrollaron dos análisis: un análisis síncrono (donde la señal sísmica llega a la cimentación de cada pila en el mismo ínstate de tiempo) y un análisis asíncrono (donde la señal sísmica llega a la cimentación de cada pila en instantes de tiempo diferentes). El objetivo de este estudio es evaluar los daños en la estructura de los cuatro puentes causados por los dos análisis realizados y comparar sus resultados en lo que toca a los desplazamientos del tablero, al cortante basal, a los momentos flectores y el desplome de las pilas. Estos análisis se han realizado considerando dos casos distintos para el suelo de fundación de los puentes, una roca y una arena densa, comparando la diferencia en los resultados que obtienen en uno y otro caso. Ambos análisis efectuados se han realizado con recurso al programa informático SAP2000. Con este estudio se pretendió comprobar la importancia de la consideración de la asincronía de las ondas sísmicas y en qué situaciones esta provoca daños mayores que una señal sísmica síncrona, conforme se tenga un mejor o un peor suelo de cimentación. Se concluyó que el análisis asíncrono es el más desfavorable y que los resultados son menos malos cuando se considera un suelo de mejor calidad. En lo que toca a la variabilidad espacial del movimiento de suelo, con la realización de este estudio ha sido posible concluir que una acción sísmica uniforme no puede controlar el dimensionamiento sísmico de un puente largo de hormigón pretensado, y que la influencia de la variabilidad espacial de la acción sísmica, en esto tipo de puentes, tiene que ser considerada.

Palabras-clave: variabilidad espacial, señal sísmico, analice síncrona, analice asíncrona, puentes largos, daños en la estructura.

1. Introduction

1.1 Explanation of the problem

Until recently, the effects of earthquakes on buildings have received more attention than the same effects on bridges. This is probably due to the social and economic consequences of earthquake damage on buildings proved to be greater than those resulting from damage on bridges. However, a study on seismic shock included in Ryall (n.d.), states that:

Bridges should be designed to absorb seismic forces without collapse to ensure that main arterial routes remain open after major seismic events. This helps the movement of aid and rescue services in the first instance and underpins the ability of the local community to recover in the long term.

According to this statement, the main point of most of the current seismic norms for bridges is to establish design and construction provisions for bridges to minimize their susceptibility to damage from earthquakes. The design earthquake motions and forces specified in those provisions are based on a low probability of their being exceeded during the normal life expectancy of a bridge. Bridges and their components designed to resist those forces may suffer damage, but there should be a low probability of collapse due to seismically induced ground shaking.

The main purpose of this thesis is the study and evaluation of the effect of the spatial variability of the ground motion on the response of bridges, particularly when the sign of seismic waves reaching the foundation of each pillar is asynchronous. Or, in other words, the moment each pillar receives a seismic sign of a different intensity and time gap. This is expected to represent a much more overwhelming effect on the structure deck rather than one coming from a synchronic seismic sign (where the seismic sign will spread the soil and reach all the pillars at the same time). However, considering all the strength acting upon pillars during an asynchronous seismic sign, a reduction on that effort is expected as the occurrence of the pillars' displacement will compensate their eagerness to deform.

In short, besides the more complete explanation of the spatial variability of the ground motion, the current investigation aims at proving that during a synchronous analysis the displacements occurring in the bridge deck will be reduced and the base shear on pillars will be higher rather than during an asynchronous analysis.

The spatial variability of the ground motion is a phenomenon which can be represented as the combined effect of three causes: the loss of coherence of the motion with distance, the wave-passage, and the local site conditions. Once the nature and amount of non-synchronism vary within very ample limits, there is the need to adopt a statistical approach to study them.

It is important to notice that the more significant the bridge's longitudinal development is, the wider the effect of the seismic asynchrony gets, as there will be more means to consider, from the origin of the seismic sign to the moment it reaches the foundation of the structure, causing time gaps and considerable changes. Therefore, one can easily come to the conclusion that the longer the bridge, the higher the impact of the asynchrony of seismic waves, which is precisely why it was chosen to perform the current study on bridges with a significant longitudinal development.

1.2 Purpose of the thesis

The purpose of this thesis is to study the behaviour of long bridges subjected to an asynchronous ground motion. For that, a comparative study to analyse the damage produced on the piers and the desk, originated by synchronous and asynchronous ground motions, will be carried out.

The study will focus on four different long bridges, with the same characteristics, all but the height of the piers and the total length of one of them. In each structure two different analyses will be performed: a synchronous and an asynchronous one, both according to Eurocode 8.

The synchronous analysis consists of applying the same seismic sign on each pier, at the exact same time. On the other hand, the asynchronous analysis consists of applying the same seismic signal on each pier as the synchronous one, only the sign arrives at different time gaps.

One should notice that both analysis, especially the asynchronous one, can become much more complex and have much more variable parameters. However, for measuring the damage originated at the piers and deck, the current study, using the simplified method of Eurocode 8, will meet the necessary purpose.

The main objective of the investigation will be the comparison of the damage caused by the analysis performed in each bridge, evaluating the displacements of the deck, the base shear and the pillars' drift, as well as the support efforts (shear and bending actions) originated in the structure.

1.3 Organization of the thesis

This thesis is composed by eight chapters. The first one is an introduction and a brief summary of all the contents of the study and the second one is a more detailed description of the issue, previous studies performed and applicable norms.

In the third chapter, there is an explanation of the analysis performed in the following chapters. The four selected cases studies are presented between the fourth and seventh chapters. The fourth chapter describes the processes of analysis used in Bridge 1 and discusses its results, while the fifth and sixth chapters focus on the display and discussion of the results obtained for Bridges 2 and 3 and for Bridge 4, in this order, since the processes of analysis are the same as the ones applied to Bridge 1. Finally, the seventh chapter is dedicated to a comparative analysis between all the studies carried out in the bridges.

The eighth and last chapter contains the conclusions of all the studies carried out and of the general issue.

2. State of knowledge

2.1 The origin of a seismic event

The unpredictability of the occurrence of a seismic event and the amount of energy that is emitted during his short but potentially devastating action, makes it one of the natural phenomena with a higher degree of danger to human life, either by failure of the structures that ensure the current type of human living, or by natural secondary events caused by seismic actions (tsunamis, volcanic eruptions, landslides, etc.).

As a naturally occurring phenomenon, with a degree of predictability still extremely low, the seismic action consists of introducing a vibration in the earth's crust as a result of natural phenomena, like the movement of tectonic plates or a volcanic eruption. Between the various causative factors of seismic activity the most relevant in terms of released energy are the earthquakes with tectonic origin.

The world globe is formed by fifteen tectonic plates, which are in constant relative movement since the formation of the earth. These movements cause an interaction between the different plates, which generate tensions. If they are traction tensions, the magma in the centre of the earth is released through the existing failures, leading to the continued formation of new tectonic plate sections. If, by the contrary, the movements are compressive tensions, the result will be landslide and torsion between the plates. Such movements can be easily observed, for example, in the continuous spacing between the European plates (Euro-Asian) and the American plates or even in the genesis of the Himalayas, where fossils of marine animals have been detected at a high altitude, which can explain the interaction between the Indian and Euro-Asian plates.

With the application forces, due to the tectonic movements previously described, the rocks forming the plates are progressively subjected to an increasing compressive stress resulting from the friction between each other, until reaching its elastic limit point, after which the breakage of the elements occurs as well as a consequent sudden release of stored energy

during the deformation. It is estimated that only 10% of the energy involved in these colossal mass movements is converted into seismic waves.

In an earthquake situation, although side effects can occur (as tsunamis, volcanic eruptions, landslides or others), the majority of earthquakes show only the effect of the soil vibration as the main element to cause damage. Its duration is extremely brief, ranging from a few seconds to, in a rare limit, a minute or a few minutes at the most.

The seismic waves, generated by breakage of tectonic plates, propagate over a much higher period of time than the event which originates them, circling the globe in about twenty minutes. Currently, the seismic waves only have energy to cause damage in structures that are at reduced distances from the epicentre. Nevertheless, sometimes a longer period of waves may cause damage in structures that are at considerable distances, especially if these structures have an impaired damping.

The location of the initial point of seismic radiation in depth is called the hypocentre and its projection in the crust is called epicentre.

There are several different kinds of seismic waves and they all move in different ways. The two main types of waves are body waves and surface waves. Body waves can travel through the earth's inner layers, but surface waves can only move along the surface of the planet like ripples on water. Earthquakes radiate seismic energy as both body and surface waves.

Traveling through the interior of the earth, body waves arrive before the surface waves emitted by an earthquake. These waves are of a higher frequency than surface waves.

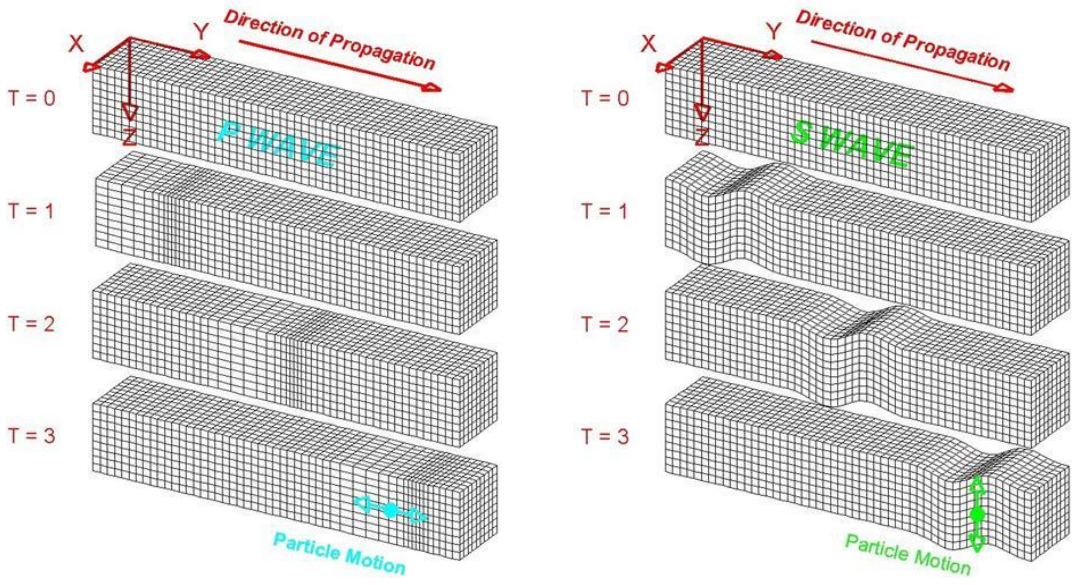

Figure 2-1: Body waves (Braile, 2006).

The first kind of body wave is the P wave or primary wave. This is the fastest kind of seismic wave, and consequently, the first to arrive at the seismic station. The P wave can move through solid rock and fluids, like water or the liquid layers of the earth. It pushes and pulls the

rock it moves through in the same way sound waves push and pull the air. P waves are also known as compressional waves, because of the pushing and pulling they do. When subjected to a P wave, particles move in the same direction the wave does, as it is exactly the same direction taken by energy.

The second type of body wave is the S wave or secondary wave, which is the second wave felled in an earthquake. An S wave is slower than a P wave and can only move through solid rock, not through any liquid medium. Seismologists were led to conclude that the Earth's outer core is a liquid considering this particular S wave property. S waves move rock particles up and down, or side-to-side, perpendicular to the direction that the wave is traveling in (the direction of wave propagation).

Surface waves, travelling only through the crust are of a lower frequency than body waves, therefore easily distinguished on a seismogram. In spite of arriving after body waves, surface waves are the ones almost entirely responsible for the damage and destruction associated to earthquakes. In deeper earthquakes the damage mentioned and the strength of surface waves are lessened.

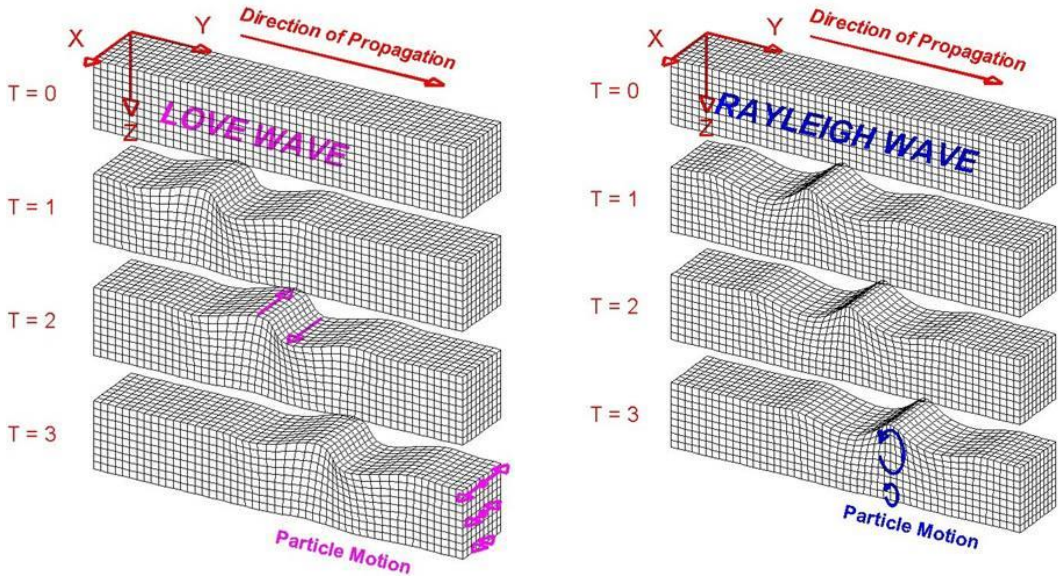

Figure 2-2: Surface waves (Braile, 2006).

The first kind of surface wave is called a Love wave, named by Augustus Edward Hough Love, a British mathematician who worked out the mathematical model for this kind of wave in 1911. It's the fastest surface wave, moving the ground from side-to-side. Confined to the surface of the crust, Love waves only produce horizontal motion.

The other kind of surface wave is the Rayleigh wave, named by John William Strutt, Lord Rayleigh, who mathematically predicted the existence of this kind of wave in 1885. The rolling of this wave along the ground is similar to a regular wave rolling across a lake or an ocean. Because it rolls, it moves the ground up and down and side-to-side in the same direction that the wave is moving. Most of the shaking felt from an earthquake is due to the Rayleigh wave, which can be much larger than the other waves.

The random nature of the seismic events makes it difficult and only partially possible to fight the damaging and devastating effects, and it can only be measured in probabilistic terms, as stated by Pennington *et al* (2007). The extent of the protection that can be provided to different categories of buildings, whose measurement is only possible through probabilities, is a matter of optimal allocation of resources and is therefore expected to vary from country to country, depending on the relative importance of the seismic risk with respect to risks of other origin and on the global economic resources.

2.2 Structural dynamic and seismic engineering bases

As fundamental elements in modern transport systems, bridges are the weakest element of the entire network during the occurrence of an earthquake.

Several recent earthquakes have shown the weaknesses of existing structures, causing the collapse or severely damaging a considerable number of important bridges, as the ones of 1989 in Loma Prieta and of 1994 in Northridge, both in California, or Hyogo-Ken Nanbu in 1995, Japan, among others. Such occurrences have shown several types of damage on the structures, depending on the ground motion experienced, the soil characteristics of the foundations and the structural characteristics. Normally, the superstructure damages aren't the main cause of the collapse. After detailed studies on the issue, it was possible to conclude that the most severe damage occurred due to the following reasons (Silva, 2009):

- Instability of the superstructure in the connections with the piers, due to improper design of the support device needed to enable the translational movement and rotation introduced by the seismic acceleration;
- Collapse of the superstructure caused by geometrical weaknesses introduced in the elements which result from the increasing complexity of the chosen solutions (such as the use of expansive unions and joints making angles with the deck axis);
- Failure on the seizing of the pillars, which are liable to fracture by cutting, with reduced propensity to deflection before yielding (note that in reinforced concrete piers, this is reflected in an improper disposal of the steel and an insufficiency of the concrete confinement);
- Occasional failures in complex structures, where special reinforcement was not properly regarded, and in areas with a considerable probability of suffering high levels of stress during a seismic event.

The task of identification and classification of the types of damage introduced by the seismic action is quite complex, and in most cases it is the result of an interaction between different variables (Kiureghian, 1996). The elements that lead to the collapse are, in most cases, hidden in the damage they caused, which implies a necessary speculation to reconstruct the seismic event. In some of the cases, even after a detailed study, it is still not possible to clearly understand the mechanisms that caused the failure. However, when the primary cause happens to be clearly identified, the generalization to other similar cases usually faces

difficulties. However, the knowledge of the causes of failure are very useful because of the large number of damage repeatedly inflicted upon the analysed structures. This procedure helps to better understand the structural operating mechanisms and identify potential weak areas in future projects thus becoming a key driver of progress in Seismic Engineering. It is also important to constantly consider the age and the philosophy underlying the design of the bridge in question as a result of the considerable evolution of the criteria and the approach of the seismic design throughout the years. The analysis of the oldest bridges should be performed regarding its strengthening, rehabilitation or replacement thus providing for new performance criteria that need to be increasingly strict.

Li and Yang (2008) state that almost all seismic design applied on bridges is performed assuming that all contact points experience the same ground motion in spite of all the evidence proving that this is not the case. These evidences cover not only the ground motion, but also the effect on structural response. As regarding ground motion, a number of strong-motion recorder arrays have been set up in the past twenty years in different parts of the world, the most renowned ones from Taiwan and California, USA, from where the spatial variation of ground motion during seismic events has been observed and measured. Indeed, the structure experiences an asynchronous motion, typically referred to as Spatial Variability of Earthquake Ground Motion (SVEGM), which comprises the differences in amplitude, phase and frequency content within ground motions recorded over extended areas.

In fact, the critical question here is not if seismic motion is actually different along an extended structure. According to Pinto (2007) and Lupoi *et al* (2005), the spatial and temporal variation of seismic ground motion has been well studied and identified and it is commonly attributed to the combination of the following:

- → finite velocity of wave travelling, providing for out of phase arrival at each support point;
- → wave coherency loss in terms of gradual reduction of their statistical dependence on distance and frequency, caused by multiple reflections, refractions and superpositioning during propagation;
- → effects on local sites.

As a result of the previously described, even in the ideal situation of a similar input motion at all points of the free surface, the presence of the foundations and the structure would locally alter the motion due to soil-structure interaction. This is caused by the changing of the free movement of the soil, a consequence of the geometry and the stiffness of the foundation's structure and also by the transmission of the inertial forces from the superstructure back into the soil.

In addition to the previous theoretical justification, Spatial Variability of Earthquake Ground Motion (SVEGM) has also been recorded in various densely instrumented arrays all over the world (Papadopoulos *et al*, 2013). Therefore, the fact that a long structure is expected to be stimulated with asynchronous and partially uncorrelated seismic forces is evident and well documented.

Asynchronous motion is an aspect not accounted for in the vast majority of the design cases, although, during the last 40 years, many methods have been suggested in order to acknowledge the consequences of SVEGM on bridges. This tendency may be a consequence of the simplicity of synchronous excitation analysis and to the false perception that SVEGM has a generally favourable effect on bridge dynamic response.

Nevertheless, as demonstrated by Vanmarcke (1996), the potential effects of SVEGM on bridge response cannot be approached in a deterministic way, mainly in cases where local soil conditions show significant variation in length. As a matter of fact, it is essential to regard the uncertainty related to the definition of the appropriate seismic motion at each support and the conditions under which asynchronous motion can become detrimental for a structure.

A significant number of studies have been performed so as to acknowledge the effects of changes in the various parameters which regulate the ground motion field as well as the impact of field characteristics on different bridge configuration. The results of these studies do not specify a clear trend regarding the beneficial or detrimental effect of asynchronous excitation on bridge response. Even in cases where the SVEGM effect could be important, the definition of some reasonable input motions and relative motions featuring the expected ones at bridge supports is undoubtedly the hardest process to come up with. In each particular case, however, the bridge support soil conditions provide an indication of whether the structure is sensitive to the phenomenon or not.

The importance of the SVEGM stirs up when local soil conditions vary significantly with length, hence increasing the probability of failure even for relatively short bridges.

The main question relies on whether the designer is able to consider reasonable variation of ground motion and what the response of a structure would be under such an asynchronous excitation in case the final response is detrimental compared to the prediction made assuming a structure uniformly excited in the time domain especially if it can be predictable during the design process.

The answer cannot be straightforward because of the complexity in predicting incoherency patterns, to add to the significant coupling between earthquake input, the dynamic characteristics of the soil-structure system (particularly in terms of the adequacy of the foundation and energy dissipation) at the soil foundation interface. To deal with the problem, modern seismic codes prescribe increased seating lengths for the deck.

A valuable set of proposals is provided to record the bridge vicinity and other specific locations on the structure and its foundation. Based on the gathered data, there is a particular investment in:

- → developing a reliable finite element model after appropriate system identification and model updating procedures;
- → evaluating the bridge sensitivity to SVEGM effects using the free field (asynchronous) ground motion excitations.

In statistical terms, the sources of ground motion spatial variability denoted as loss of coherence and wave-passage produce responses are equal or slightly lower than those

obtained when ignoring them. Including these sources in an assessment procedure would obviously lead to a rise of the global variability of the response. However, it is important to notice that this variability is well within the decision of controlling the response attainable at the present design procedure, which would necessarily result in discarding these effects for design purposes. Contrarily, when ground motion spatial variability is originated from differences in soil profiles beneath the supports, the effect on the response can be quite substantial.

2.3 Fundamental aspects of Eurocode 8 concerning the analysis and seismic design of bridges

2.3.1 Objectives and general rules of Eurocode 8

The main objective of Eurocode 8 is to ensure that in the event of earthquakes human lives are protected, damage is limited and structures important for civil protection remain operational. For that, this norm determines how to design and construct buildings and civil engineering structures in seismic regions (note that this norm does not cover special structures as nuclear power plants, offshore structures or large dams).

These objectives are expressed in two seismic verification levels that are formulated in the following two requirements that structures must obey to:

→ **No-collapse requirement**

Under the action of a rare seismic event, the structures must not collapse. This requirement is intended primarily to protect human lives from the effects of global or partial collapses of structures. In consequence, it is required that the structures maintain their integrity and a minimum capacity of supporting gravity loads during and after the occurrence of the earthquake. It is possible to assume that the structural damage can be really significant to the point of the subsequent recovery of the structure becoming economically unfeasible, but the structure should not collapse.

→ **Damage limitation requirement**

Under the action of a rather frequent seismic event, the damage on buildings should be restricted. This requirement is primarily intended to reduce economic losses. The intention behind it is to avoid structural damage and limit non-structural damage in easily and economically repairable situations.

Eurocode 8 is divided into six parts:

→ **EN 1998-1 (Part 1)** – Contains particular aspects of the seismic performance of buildings. Here we can find an approach to the definition of seismic response spectra, dimensioning

assumptions and general rules for the definition of seismic action and its combination with other actions. In case one is dealing with other type of structures apart from buildings, this approach needs the additional detail provided in the remaining parts of Eurocode 8;

- → **EN 1998-1 (Part 2)** – Contains particular aspects of the seismic performance of bridges;
- → **EN 1998-1 (Part 3)** – Contains aspects related to the seismic evaluation and repair of existing buildings;
- → **EN 1998-1 (Part 4)** – Contains details of the seismic performance of silos, tanks and pipelines;
- → **EN 1998-1 (Part 5)** – Contains specific provisions relevant to foundations, retaining structures and geotechnical aspects;
- → **EN 1998-1 (Part 6)** – Contains specific aspects of towers, masts and chimneys.

This issue will be mostly focused on Part 2 of Eurocode 8, but fitting some aspects of Part 1, as it happens with aspects related to the seismic action.

Eurocode 8 not only covers dimensioning problems, but it also displays the determination of the calculation of actions relating to earthquakes. There are two important technical reasons for treating the seismic actions in a separate order from the remaining. The first is because it differs from all others since it involves mostly dynamic forces, and not external forces applied above the foundation; and the second because seismic loads depend both on the structure and dynamic characteristics of materials, and they also depend on ground motion.

Seismic actions calculation is also very dependent on the structure ductility which leads to a complex connection between the action and the structure. This connection becomes more important when it is necessary to introduce the concept of *design based on capacity*. In this case, the calculation loads of some elements depend not only on external actions, bus also on the plastic resistance of other elements. For example, the resistance of ductile pillars must be enough to materialize sufficient strength of the beams that are connected to them.

In order to satisfy the described requirements, it is necessary to proceed to the verification of the ultimate limit states (conditions associated to collapse or other structural failure mechanism that can endanger human lives) as well as the limit states associated to damage caused by seismic action (states associated to the degradation of the upper structure). In addition to covering the issues related to the design of structures subjected to seismic action, Eurocode 8 displays methods to determine the calculation from actions introduced by ground motion.

This distinction is due to the characteristic of the seismic action as a dynamic action not involving external forces applied to the structure. The demonstration of this seismic action depends on the dynamic characteristics of the structure, its ductility, its material types and the movements and type of soil where the seismic waves are introduced.

The current method recommended by Eurocode 8 for the analysis of structures subjected to seismic action predicts the use of a single seismic action for the entire structure, which is applied to all the connection points between the structure and the soil. As such, this is a synchronous analysis.

This simplification is done implicitly when it carries out an equivalent dynamic analysis using response spectra, which are an integral part of the design method of Eurocode 8. The influence of the magnitude of the earthquake is taken into account by the recommended groups of spectral response, written in the each country's National Annex.

2.3.2 Definition of seismic actions

2.3.2.1 Soil influences

To initiate the development of response spectrum, it is necessary to start the process for characterizing the foundation soil of the structure intended to be analysed. This soil should be free from the risk of rupture, instability and have controlled permanent settlements, which can be caused by liquefaction or densification during a seismic event. Depending on the importance, displayed in Eurocode 8 by the class where the structure is settled, and the particular conditions associated to each construction, a detailed research on soil characteristics should be taken into account to enable the setting of properties with the same accuracy.

The discretization of the type of soil, present in Eurocode 8, is performed by dividing the soil into five ground types – A, B, C, D and E – and describing them by their geological and stratigraphic properties used to characterize the influence of the soil when the seismic action occurs.

This characterization of the soil obeys three physical parameters:

- $v_{s,30}$ (m/s), the average speed of the shear waves;
- N_{SPT} (blows/30 cm), which corresponds to the dynamic penetration test;
- and c_u (kPa), representing the undrained shear strength of the soil.

The regulation also defines two special ground types – S_1 and S_2 – which are soils that require a specific study. In the case of S_2, the probability of a ground failure due to seismic action must be considered; and in the case of S_1 soil type, attention should be given to a low internal damping and an abnormally enlarged linear behaviour that can cause abnormal seismic amplifications in soil-structure interaction (notice that the soils in this category have very low values of v_s).

The following table describes the different soil types and parameters used to define the ground type (this table corresponds to Table 3.1 of Eurocode 8 – part 1).

Ground type	Description of stratigraphic profile	Parameters		
		$v_{s,30}$ (m/s)	N_{SPT} (blows/30 cm)	c_u (kPa)
A	Rock or other rock-like geological formation, including at most 5 m of weaker material at the surface.	> 800	–	–
B	Deposits of very dense sand, gravel, or very stiff clay, at least several tens of meters in thickness, characterised by a gradual increase of mechanical properties with depth.	360 – 800	> 50	> 250
C	Deep deposits of dense or medium-dense sand, gravel or stiff clay with thickness from several tens many hundreds of meters.	180 – 360	15 – 50	70 – 250
D	Deposits of loose-to-medium cohesion less soil (with or without some soft cohesive layers), or of predominantly soft-to-firm cohesive soil.	< 180	< 15	< 70
E	A soil profile consisting of a surface alluvium layer with v_s values of type C or D and thickness varying between about 5 m and 20 m, underlain by stiffer material with v_s > 800 m/s.	–	–	–
S_2	Deposits consisting, or consisting a layer at least 10 m thick, of soft clays/silts with a high plasticity index (PI > 40) and high water content.	< 100 (indicative)	–	10 – 20
S_1	Deposits of liquefiable soils, of sensitive clays, or any other soil profile not included in types A – E or S_1	–	–	–

Table 2-1: Ground type.

Soil classification should be based, if possible, on the use of the values of medium cutting speeds given on 3.1.2(3) of Eurocode 8 – part 1 by:

$$v_{s,30} = \frac{30}{\sum_{i=1}^{N} \frac{h_i}{v_i}} \tag{2.1}$$

Where, h_i is the thickness of the element (m);

v_i is the speed of the cutting wave.

If the information on the values is not available, the solution is to access N_{SPT} value to make the soil classification.

The effects of the seismic acceleration at the surface depend on the magnitude of the earthquake event and the distance from the epicentre. Notice that the intensity variation promotes different changes in the soil behaviour by changing its mechanical characteristics, particularly its deformability and its damping, thereby influencing the greater or lesser amplification that the soil can admit in its surface motion.

2.3.2.2 Importance factor γ_I

The seismic acceleration calculation a_g, constituting the design seismic action A_{Ed}, is expressed in terms of the reference seismic action A_{Ek} (related to the seismic acceleration a_{gR}), and the importance factor γ_I, expressed on 2.1(3) of Eurocode 8 – part 2, by:

$$A_{Ed} = \gamma_I \cdot A_{Ek} \tag{2.2}$$

The classification of structures, in the case of bridges, is based upon the importance factor γ_I,determining the level of damage which may be acceptable to the structure in order to increase the design seismic action, considering the consequences for human lives caused by its rupture. When the bridge belongs to a highly relevant transport network, in an earthquake situation, its destruction cannot be accepted lightly, thus its importance factor will be higher than the one from a bridge that leads only to a minor road. With this procedure, it is possible to increase the design seismic action in such a way that the behaviour of the bridge lies within a stricter confidence interval and hence, the value of the design seismic action is within the parameters necessary to maintain the operability of the bridge after a seismic event.

According to the national annex of Eurocode 8 – part 2, structures are divided into three important classes represented in the following table.

Class	Description	Importance factor value (γ_I)
I	Bridges of less than average importance. A bridge shall be classified to importance class I when: the bridge is not critical for communications; and the adoption of either the reference probability of exceedance, P_{NCR}, in 50 years for the design seismic action, or of the standard bridge life of 50 years is not economically justified.	0,85
II	Bridges of average importance, with the exception of the ones which fits the class III.	1,00
III	Bridges of critical importance for maintaining communications, especially in the immediate post-earthquake period, bridges the failure of which is associated with a large number of probable fatalities and major bridges where a design life greater than normal is required.	1,30

Table 2-2: Values of the importance factor γ_I.

The contextualization of each bridge, within the categories of importance noted above, is of the responsibility of the National Annex of each country.

The reference seismic action A_{Ek} is associated to an occurrence probability of 10% in 50 years, P_{NCR}; or a return period, T_{NCR}, which in the case of Eurocode is defined by 475 years.

2.3.2.3 Response spectrum

Eurocode 8 determines that the earthquake motion at a given point on the surface is represented by an elastic ground acceleration response spectrum, henceforth called an "elastic response spectrum". The shape of the elastic response spectrum is the same for the two levels of seismic action: the no-collapse requirement and the damage limitation requirement.

The horizontal seismic action is described by two orthogonal components assumed to be independent and represented with the same response spectrum. When the earthquakes affecting a site are generated by widely differing sources, the possibility of using more than one shape of spectra should be considered to enable the design seismic action to be adequately represented. In such circumstances, different values of a_g will normally be required for each type of spectrum and earthquake.

In case a structure is classified as an important structure, where $\gamma_I > 1{,}0$, topographic amplification effects should be taken into account.

For the horizontal components of the seismic action, the elastic response spectrum $S_e(T)$ is defined by the expressions displayed on 3.2.2.2(1) in Eurocode 8 – part 1, as below:

$$0 \le T \le T_B: \qquad S_e(T) = a_g \cdot S \cdot \left[1 + \frac{T}{T_B} \cdot (\eta \cdot 2{,}5 - 1)\right] \tag{2.3}$$

$$T_B \le T \le T_C: \qquad S_e(T) = a_g \cdot S \cdot \eta \cdot 2{,}5 \tag{2.4}$$

$$T_C \le T \le T_D: \qquad S_e(T) = a_g \cdot S \cdot \eta \cdot 2{,}5 \left[\frac{T_C}{T}\right] \tag{2.5}$$

$$T_D \le T \le 4s: \qquad S_e(T) = a_g \cdot S \cdot \eta \cdot 2{,}5 \left[\frac{T_C T_D}{T^2}\right] \tag{2.6}$$

Where, $S_e(T)$ is the elastic response spectrum;

T is the vibration period of a linear single-degree-of-freedom system;

a_g is the design ground acceleration on type A ground ($a_g = \gamma_I \cdot a_{gR}$);

T_B is the lower limit of the period of the constant spectral acceleration branch;

T_C is the upper limit of the period of the constant spectral acceleration branch;

T_D is the value defining the beginning of the constant displacement response range of the spectrum;

S is the soil factor;

η is the damping correction factor with a reference value of $\eta = 1$ for a viscous damping of 5%, given by the following expression:

$$\eta = \sqrt{\frac{10}{5+\xi}} \ge 0{,}55 \tag{2.7}$$

Where ξ is the viscous damping ratio of the structure, expressed as a percentage.

The elastic response spectrum has the general shape shown in the figure below (corresponding to Figure 3.1 in Eurocode 8 – part 1).

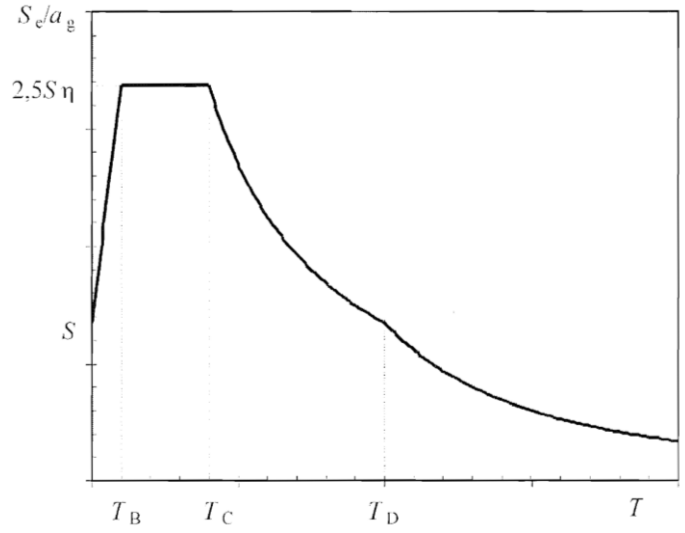

Figure 2-3: Shape of the elastic response spectrum.

The values to be ascribed to T_B, T_C, T_D and S for each ground type and type of spectrum to be used in a country may be found in each National Annex. If deep geology is not accounted for, when the earthquakes that most contribute to the seismic hazard defined for the site for the purpose of probabilistic hazard assessment have a surface-wave magnitude, M_s, greater than 5,5 (precisely the issue of the further research), the recommended spectrum and values of the parameters S, T_B, T_C and $T_D$are the following:

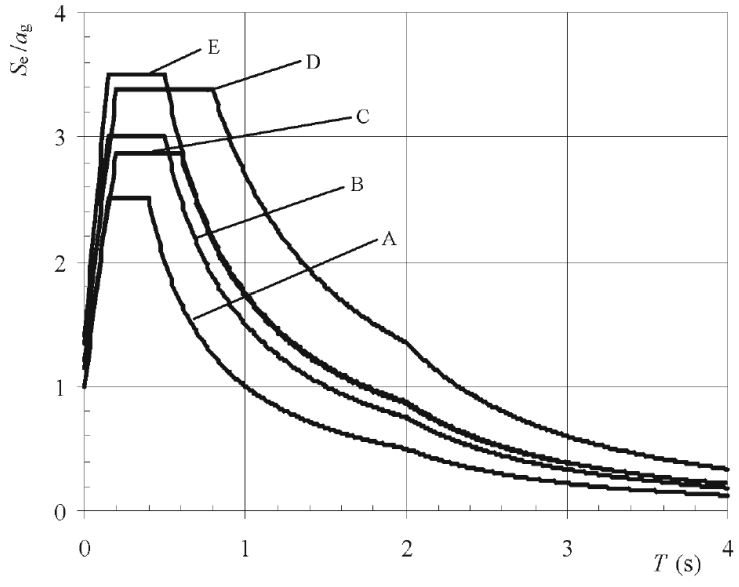

Figure 2-4: Recommended elastic response spectrum for ground types A to E (5% damping).

Ground type	S	T_B (sec)	T_C (sec)	T_D (sec)
A	1,00	0,15	0,40	2,00
B	1,20	0,15	0,50	2,00
C	1,15	0,20	0,60	2,00
D	1,35	0,20	0,80	2,00
E	1,40	0,15	0,50	2,00

Table 2-3: Values of the parameters describing the recommended elastic response spectrum.

During the seismic event, there is a vertical acceleration which can also be described in a similar way as the horizontal acceleration (this description can be found on 3.2.2.3 of Eurocode 8 – part 1). Though, since this is a very rare condition factor of the seismic behaviour of a structural element, its analysis will not be a matter to consider in the current research approach.

2.3.2.4 Design ground displacement

The design ground displacement d_g, matches the design ground acceleration, and unless special researches based on the available information indicate otherwise, it can be estimated by the following expression:

$$d_g = 0{,}025 \cdot a_g \cdot S \cdot T_C \cdot T_D$$

Where, S, T_C and T_D are defined on 2.3.2.3 of the current research.

2.3.3 Compliance criteria

2.3.3.1 Behaviour factor, q

The behaviour factor is defined globally for the entire structure and reflects its ductility capacity, i.e. the capability of the ductile members to resist, with acceptable damage but without failure, to seismic actions in the post-elastic range. The capability of ductile members to develop flexural plastic hinges is an essential requirement for the application of the values of the behaviour factor, q, for ductile behaviour.

According to Eurocode 8, the behaviour factor, q, has the following maximum values depending on the structure revealing a ductile behaviour or a limited ductile behaviour (this table corresponds to Table 4.1 in Eurocode 8 – part 2).

Type of Ductile Members	Seismic Behaviour	
	Limited Ductile	Ductile
Reinforced concrete piers:		
Vertical piers in bending	1,5	$3{,}5 \cdot \lambda(\alpha_s)$
Inclined struts in bending	1,2	$2{,}1 \cdot \lambda(\alpha_s)$
Steel piers:		
Vertical piers in bending	1,5	3,5
Inclined struts in bending	1,2	2,0
Piers with normal bracing	1,5	2,5
Piers with eccentric bracing	–	3,5
Abutments rigidly connected to the deck:		
Inn general	1,5	1,5
Locked-in structures	1,0	1,0
Arches	1,2	2,0

$\alpha_s = {}^{L_s}/_{h}$ is the shear span ratio of the pier, where: L_s is the distance from the plastic hinge to the point of zero moment; and h is the depth of the cross-section in the direction of flexure of the plastic hinge.

For $\alpha_s \geq 3$ $\lambda(\alpha_s) = 1{,}0$

$3 > \alpha_s \geq 1{,}0$ $\lambda(\alpha_s) = \sqrt{{}^{\alpha_s}/_{3}}$

Table 2-4: Maximum values of the behaviour factor, $\boldsymbol{q}$.

2.3.3.2 Ductile and limited ductile behaviour of bridges

A bridge will be designed considering its behaviour under the design seismic action to either be ductile or limited ductile (essentially elastic), depending on the seismicity of the site, on whether seismic isolation is adopted for its design, or any other constraints which may prevail. This behaviour (ductile or limited ductile) is characterized by the global force-displacement relationship of the structure, shown schematically in the following figure (corresponding to Figure 2.1 in Eurocode 8 – part 2).

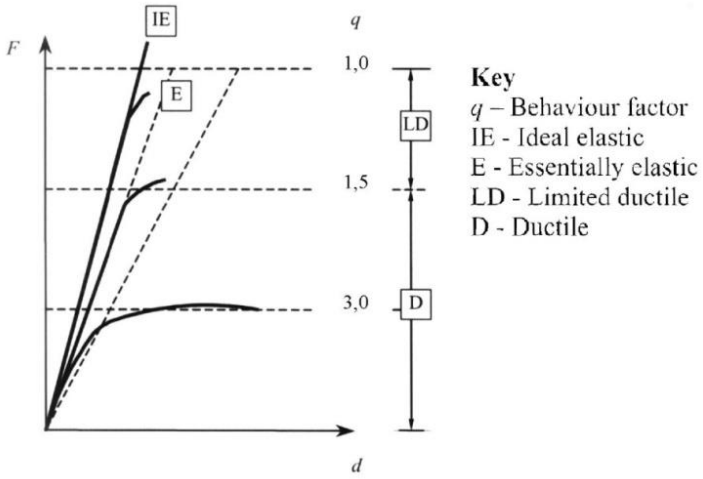

Figure 2-5: Seismic behaviour.

→ **Ductile behaviour**

In regions of moderate to high seismicity it is usually preferable, both for economic and safety reasons, to design a bridge for ductile behaviour. For that, should be provided to the bridge reliable means to dissipate a significant amount of the input energy under severe earthquakes. This is accomplished by providing for the formation of an intended configuration of flexural plastic hinges or by using isolating devices.

Bridges of ductile behaviour shall be designed so that a dependably stable partial or full mechanism can develop in the structure through the formation of flexural plastic hinges. These hinges normally form in the piers and act as the primary energy dissipating components. As far as is reasonably practicable, the location of plastic hinges should be selected at points accessible for inspection and repair.

The bridge deck shall remain within the elastic range. However, formation of plastic hinges (in bending about the transverse axis) is allowed in flexible ductile concrete slabs providing top slab continuity between adjacent simply-supported precast concrete girder spans.

Plastic hinges will not be formed in sections where the normalised axial force, η_k, exceeds 0,6, i.e. when the following expression is verified:

$$\eta_k = \frac{N_{Ed}}{A_c \cdot f_{ck}} > 0{,}6 \qquad (2.8)$$

The global force-displacement relationship will exhibit a significant force plateau at yield and ensure hysteretic energy dissipation. The ultimate displacement, d_u, is defined as the maximum displacement satisfying the following condition. The structure should be capable of sustaining at least five full cycles of deformation till the ultimate displacement in two possible situations:

→ without initiation of failure of the confining reinforcement for reinforced concrete sections, or local buckling effects for steel sections;
→ without a drop of the resisting force for steel ductile members or without a drop exceeding 20% of the ultimate resisting force for reinforced concrete ductile members.

Supporting members (piers or abutments) connected to the deck through sliding or flexible mountings should (within the research's scope), in general, remain within the elastic range.

Note that Eurocode 8 does not provide for specific rules for elements with pre-stressing, so that such elements are protected from flexural plastic hinges when the seismic event occurs.

→ **Limited ductile behaviour**

In structures with limited ductile behaviour, a yielding region with significant reduction in secant stiffness has no need for appearing under the design seismic action. In terms of force-displacement characteristics, the formation of a force plateau is not required, while deviation from the ideal elastic behaviour provides for some hysteretic energy dissipation. Such behaviour matches a value of the behaviour factor $q \leq 1{,}5$.

Notice that for bridges where the seismic response may be dominated by higher mode effects (for example cable-stayed bridges), or where the detailing of plastic hinges for ductility may not be reliable to have an elastic behaviour, the adoption of a behaviour factor of $q = 1$ will be recommended.

2.3.4 Methods of analysis

2.3.4.1 Linear dynamics analysis – Response spectrum method

The Response Spectrum Analysis is an elastic calculation of the dynamic responses peak of all significant modes of the structure, using the ordinates of the site-dependent design spectrum. The global response is obtained by statistical combination of the maximum modal contributions. This analysis can be applied in all cases in which a linear analysis is allowed.

The earthquake action effects will be determined from an appropriate discrete linear model (Full Dynamic Model), idealised in accordance to the laws of mechanics and the principles of structural analysis, and compatible with an associated idealisation of the seismic action. In general this model is a space model.

To apply this method, there are three steps to solve:

- **Determination of significant modes**

For this analysis, all modes with a significant contribution to the total structural response shall be taken into account. However, one must realize it's not easy to consider every significant mode and for that, Eurocode predicts two simplified requirements to verify this condition:

1) bridges in which the total mass, M, can be considered as a sum of "effective modal masses" M_i, and if the sum of effective modal masses for the modes considered, $(\sum M_i)_c$,

amounts to at least 90% of the total mass of the bridge, the previous criterion is deemed to be satisfied;

2) however, if condition 1) cannot be satisfied, after taking all modes with $T \geq 0{,}033\ sec$ into account, the number of modes considered may be deemed acceptable provided that both of the following conditions are satisfied:

→ $(\sum M_i)_c / M \geq 0{,}70$;

→ the final values of the seismic action effects multiplied by $M/(\sum M_i)_c$.

- **Combination of modal responses**

To apply the action resulting from all the modes considered it is necessary to combine them.

The generic rule to obtain the probable maximum value of a seismic action effect E, is the "Square Root of the Sum of Squares" (SRSS) of the modal responses E_i. In this rule, as the name implies, the response of a given magnitude can be estimated by the square root of the sum of squares of the magnitude of such response for each mode. This rule is given by the following expression:

$$E = \sqrt{\sum E_i^2} \tag{2.9}$$

This action effect is expected to act with positive and negative signs.

The SRSS rule has satisfactory results since the natural periods of two modes aren't very close. Eurocode considers that two natural periods, T_i, T_j, will be considered as closely spaced natural periods if they satisfy the condition:

$$\frac{0{,}1}{0{,}1+\sqrt{\xi_i \xi_j}} \leq \rho_{ij} = \frac{T_i}{T_j} \leq 1 + 10\sqrt{\xi_i \xi_j} \tag{2.10}$$

Where, ξ_i and ξ_j are the viscous damping ratios of modes i and j, respectively.

When this happens, it is more appropriate to use another modal combination rule called "Complete Quadratic Combination" (CQC) translated by the expression:

$$E = \sqrt{\sum_i \sum_j E_i r_{ij} E_j} \tag{2.11}$$

Where, $i = 1 \ldots n$;

$j = 1 \ldots n$;

r_{ij} is the correlation factor, given by: $r_{ij} = \dfrac{8\sqrt{\xi_i \xi_j}(\xi_i + \rho_{ij}\xi_j)\rho_{ij}^{3/2}}{\left(1-\rho_{ij}^2\right)^2 + 4\xi_i \xi_j \rho_{ij}\left(1-\rho_{ij}^2\right) + 4\left(\xi_i^2 + \xi_j^2\right)\rho_{ij}^2}$.

ξ_i, ξ_j are the viscous damping ratios i corresponding to modes i and j.

- **Combination of the components of the seismic action**

The probable maximum action effect, E, considering the simultaneous occurrence of the components of the seismic action along the horizontal axes x and y and the vertical axis z, can

be determined through the application of the SRSS rule to the maximum action effects E_x, E_y and E_z due to independent seismic action along each axis given by:

$$E = \sqrt{E_x^2 + E_y^2 + E_z^2} \tag{2.12}$$

2.3.4.2 Fundamental mode method

In this method, equivalent static seismic forces are derived from the inertia forces corresponding to the fundamental mode and natural period of the structure in the direction under consideration, using the relevant ordinate of the site's dependent design spectrum. The method also includes simplifications regarding the shape of the first mode and the estimation of the fundamental period.

Depending on the particular characteristics of the bridge, this method shall be applied using three different approaches for the model, namely, the rigid deck model, the flexible deck model and the individual pier model.

For the combination of the components of seismic action the SRSS rule will be applied.

This method can be applied in all situations in which the dynamic behaviour of the structure can be sufficiently approximated by a single model of a dynamic degree of freedom. This condition is considered to be satisfied in the following situations:

1) In the longitudinal direction of approximately straight bridges with continuous deck, when the seismic forces are carried by piers, the total mass of which is less than 20% of the mass of the deck;
2) In the transverse direction of case 1), if the structural system is approximately symmetric towards the centre of the deck, i.e. when the theoretical eccentricity, e_o, between the centre of stiffness of the supporting members and the centre of mass of the deck does not exceed 5% of the length, L, of the deck;
3) In the case of piers carrying simply supported spans, if no significant interaction between piers is expected and the total mass of each pier is less than 20% of the tributary mass of the deck.

- **Rigid deck model**

This model should only be applied, when, under the seismic action, the deformation of the deck within a horizontal plane is negligible compared to the horizontal displacements of the pier tops. This condition is always met in the longitudinal direction of approximately straight bridges with continuous deck. In the transverse direction the deck should be assumed rigid either if $L/B \leq 4{,}0$, or if the following condition is satisfied:

$$\frac{\Delta_d}{d_a} \leq 0{,}20 \tag{2.13}$$

Where, L is the total length of the continuous deck;

B is the width of the deck;

Δ_d and d_a are, respectively, the maximum difference and the average of the displacements in the transverse direction of all pier tops under the transverse seismic action, or under the action of a transverse load of similar distribution.

In this model, the earthquake effects are determined by applying a horizontal equivalent static force at the deck given by the expression:

$$F = M \cdot S_d(T) \tag{2.14}$$

Where, M is the total effective mass of the structure, equal to the mass of the deck plus the mass of the upper half of the piers;

$S_d(T)$ is the spectral acceleration of the design spectrum corresponding to the fundamental period, T, of the bridge, estimated as:

$$T = 2\pi\sqrt{\frac{M}{K}} \tag{2.15}$$

Where, $K = \sum K_i$ is the stiffness of the system, equal to the sum of the stiffnesses of the resisting members.

In the transverse direction, force F may be distributed along the deck proportionally to the distribution of the effective masses.

- **Flexible deck model**

The flexible deck model, contrarily to what happened with the rigid desk model, will be applied when expression (2.13) is not satisfied.

The fundamental period of the structure in the horizontal direction can be estimated by the Rayleigh quotient, using a generalized single-degree-of-freedom system, as follows:

$$\mathrm{T} = 2\pi\sqrt{\frac{\sum M_i d_i^2}{g\sum M_i d_i}} \tag{2.16}$$

Where, M_i is the mass at the i-th modal point;

d_i is the displacement in the direction under examination when the structure is acted upon by forces gM_i acting at all nodal points in the horizontal direction considered.

The earthquake effects will be determined by applying horizontal forces, F_i, at all nodal points given by:

$$F_i = \frac{4\pi^2}{gT^2} S_d(T) d_i M_i \tag{2.17}$$

Where, T is the period of the fundamental mode of vibration for the horizontal direction;

M_i is the mass concentrated at the i-th point;

d_i is the displacement of the i-th nodal point in an approximation of the shape of the first mode;

$S_d(T)$ is the spectral acceleration of the design spectrum;

g is the acceleration of gravity.

- **Individual pier model**

In some cases, the seismic action in the transverse direction of the bridge is mainly resisted by the piers, without significant interaction between adjacent piers. In such cases the seismic action effects acting in the i-th pier may be approximated by applying on it an equivalent static force:

$$F_i = M_i \cdot S_d(T_i) \tag{2.18}$$

Where, M_i is the effective mass attributed to pier i;

$T_i = 2\pi\sqrt{\frac{M_i}{K_i}}$ is the fundamental period of the same pier, considered independent from the rest of the bridge.

2.3.4.3 Other methods

Eurocode 8 – Part 2 also contains other three methods of analysis of the seismic action on bridges, namely Alternative Linear Methods, Non-Linear Dynamic Time-History Analysis, and Static Non-Linear Analysis.

However, these methods will not be included in the scope of the current research.

2.3.5 Spatial variability of seismic ground motion

2.3.5.1 Random vibrations method

According to Annex D of Eurocode 8 – Part 2, spatial variability is a phenomenon that can be described by means of a vector of zero-mean random processes. This vector, under the assumption of stationary, is defined by means of its symmetric $n \times n$ matrix of auto- and cross-power spectral density function:

$$G(\omega) = \begin{bmatrix} G_{11}(\omega) & G_{12}(\omega) & \cdots & G_{1n}(\omega) \\ & G_{21}(\omega) & \cdots & G_{2n}(\omega) \\ & & \cdots & \cdots \\ & & & G_{mn}(\omega) \end{bmatrix} \quad (2.19)$$

Where, n is the number of supports.

To continue the explanation of this analysis, it is useful to introduce the following non-dimensional function called coherency function:

$$\gamma_{ij}(\omega) = \frac{G_{ij}(\omega)}{\sqrt{G_{ii}(\omega)G_{jj}(\omega)}} \quad (2.20)$$

The value of the modulus of $\gamma_{ij}(\omega)$ at all frequencies is bounded by zero and one, and it provides a measure of the linear statistical dependence of the two processes at stations i and j. In this simplified model, the combination of all the asynchronous ground motion is taken into account by this linear statistical dependence.

For the purposes of structural analysis, it is necessary to generate samples of the vector of random processes, the equation (2.19) mentioned above. To accomplish this, matrix $G(\omega)$ is first decomposed into the product between matrix $L(\omega)$ and the transpose of its complex conjugation, which can be displayed as the following equation:

$$G(\omega) = L(\omega) \cdot L^{*T}(\omega) \quad (2.21)$$

According to Eurocode, previous studies have shown that a sample of the acceleration motion at the generic support i is obtained from the series:

$$a_i(t) = 2\sum_{j=1}^{i}\sum_{k=1}^{N}\left|L_{ij}(\omega_k)\right|\sqrt{\Delta\omega}\cos\left[\omega_k t - \theta_{ij}(\omega_k) + \emptyset_{jk}\right] \quad (2.22)$$

Where, N is the total number of frequencies $\omega_k$into which the significant bandwidth of $L_{ij}(\omega)$ is discretized;

$\Delta\omega = \frac{\omega_{max}}{N}$ and the angles $\emptyset_{jk}$ are, for any j, a set of N independent random variables uniformly distributed between zero and 2π.

Based on this brief introduction, Eurocode 8 – Part 2 describes three different ways to determine the structural response to spatial varying ground motions. In this assignment only the two first methods will be approached, and described in the following topics.

- **Linear random vibration analysis**

A linear random vibration analysis will either use modal analysis of frequency-dependent transfer matrices or input given by matrix $G(\omega)$. The elastic action effects are assumed to be the mean values from the probability distribution of the largest extreme value of the response for the duration consistent with the seismic event underlying the establishment of a a_g.

The determination of the design values is achieved by dividing the elastic effects by the appropriate behaviour factor, q. In turn, ductile response is assured by conformity to the relevant rules of Eurocode 8 – Part 2.

- **Time history analysis with samples of correlated motions**

The time-history analysis is a simplified method to study the asynchronous ground motion along the time. Here, Eurocode predicts two ways to perform a time-history analysis: linear time-history analysis and non-linear time-history analysis.

→ Linear time-history analysis

Linear time-history analysis can be performed by using motions generated as indicated by equations (2.21) and (2.22), starting from power spectra consistent with the elastic response spectra at the supports.

The number of samples used should be such as to yield stable estimates of the mean of maximum responses of interest. The elastic action effects are assumed as the mean values of the above maxima. The design values are determined by dividing the elastic action effects by the appropriate behaviour factor, q, and ductile response is assured in conformity to the relevant rules present on Eurocode 8 – Part 2.

→ Non-linear time-history analysis

Non-linear time-history analysis can be performed by using sample motions, also generated as indicated by equations (2.21) and (2.22), starting from power spectra consistent with the elastic response spectra at the supports. And again, the number of samples used will be such as to yield stable estimates of the mean of the maximum responses of interest.

The design values of the action effects, E_d, are assumed as the mean values of the above maxima. The comparison between action effect, E_d, and design resistance, R_d, is performed in accordance to Eurocode 8 – Part 1.

2.3.5.2 Simplified method

Eurocode 8 – Part 2 predicts that, for bridge sections with a continuous deck, the analysis of the spatial variability of the seismic action will be considered when at least one of the two following conditions is fulfilled:

- Soil properties along the bridge vary to the extent that more than one ground types (as specified in point 2.3.2.1 of the current study) match the supports of the bridge's deck.
- Soil properties along the bridge are approximately uniform, but the length of the continuous deck exceeds an appropriate limiting length, L_{lim} (the Eurocode recommends that $L_{lim} = \frac{L_g}{1{,}5}$ where the length L_g is a tabled value which represents the distance beyond which the ground motions may be considered as completely uncorrelated).

The spatial variation of the seismic action can be estimated by pseudo-static effects of appropriate displacement sets, imposed at the foundation of the supports of the bridge's deck. These sets should reflect probable configurations of the spatial variability of the seismic motion at free field and should be selected so as to induce maximum values of the seismic action effect under investigation. These requirements are deemed to be satisfied, by imposing each of the following two sets of horizontal displacements, applied separately, in each horizontal direction of the analysis, on the relevant support foundations or on the soil end of the relevant spring representing the soil stiffness. The effects of the two sets don't need to be combined.

→ **Set A:**

Consists of relative displacements, applied simultaneously with the same sign (+ or −) to all supports of the bridge in the horizontal direction considered, and it can be expressed by:

$$d_{ri} = \varepsilon_r \cdot L_i \leq d_g\sqrt{2} \tag{2.23}$$

Where, $\varepsilon_r = \frac{d_g\sqrt{2}}{L_g}$;

d_g is the design ground displacement corresponding to the ground type of support i, according to point 2.3.2.4;

L_i is the distance (projection on the horizontal plane) of support i from a reference support $i = 0$, that can be conveniently selected at one of the end supports;

L_g is the distance beyond which the ground motions may be considered as completely uncorrelated. The recommended values for L_g are given in the following table (which corresponds to Table 3.1N of Eurocode 8 – Part 2), depending on the ground type:

Ground Type	*A*	*B*	*C*	*D*	*E*
L_g (m)	600	500	400	300	500

Table 2-5: Distance beyond which ground motions may be considered uncorrelated.

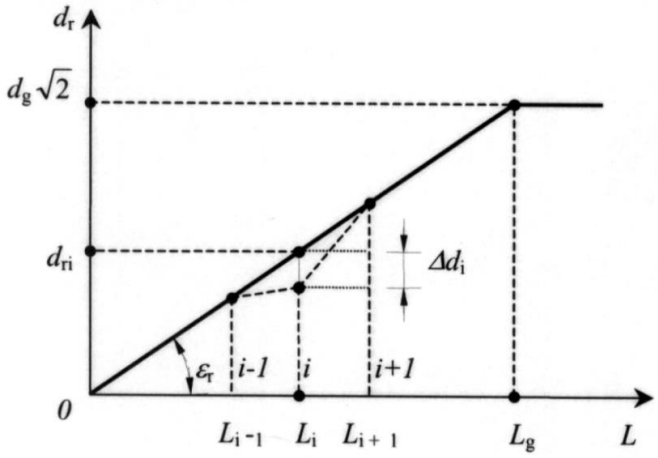

Figure 2-6: Displacements of Set A.

→ **Set B:**

It covers the influence of ground displacements occurring in opposite directions at adjacent piers. This is accounted for by assuming displacements Δd_i of any intermediate support i (> 1) relative to its adjacent supports $i-1$ and $i+1$ considered undisplaced (as one can observe in *Figure 2-6*), which can be represented by the expression:

$$\Delta d_i = \pm \beta_r \cdot \varepsilon_r \cdot L_{\alpha v,i} \tag{2.24}$$

Where, $L_{\alpha v,i}$ is the average of the distances $L_{i-1,i}$ and $L_{i,i+1}$ of intermediate support i to its adjacent supports $i-1$ and $i+1$, respectively. For the end supports (0 and n) $L_{\alpha v,0} = L_{01}$ and $L_{\alpha v,n} = L_{n-1,n}$;

β_r is a factor accounting for the magnitude of ground displacements occurring in opposite directions at adjacent supports. The recommended values are: $\beta_r = 0{,}5$, when all three supports have the same ground type; $\beta_r = 1{,}0$, when the ground type at one of the supports is different than at the other two;

ε_r is the same as defined above, for set A. If a change of ground type appears between two supports, the maximum value of ε_r should be used.

Set B consists of the following configuration of imposed absolute displacements with opposed sign at adjacent supports i and $i+1$, for $i = 0$ to $n-1$ (see *Figure 2-7*). The absolute displacements are given by the expressions:

$$d_i = \pm \frac{\Delta d_i}{2} \tag{2.25}$$

$$d_{i+1} = \pm \frac{\Delta d_{i+1}}{2} \tag{2.26}$$

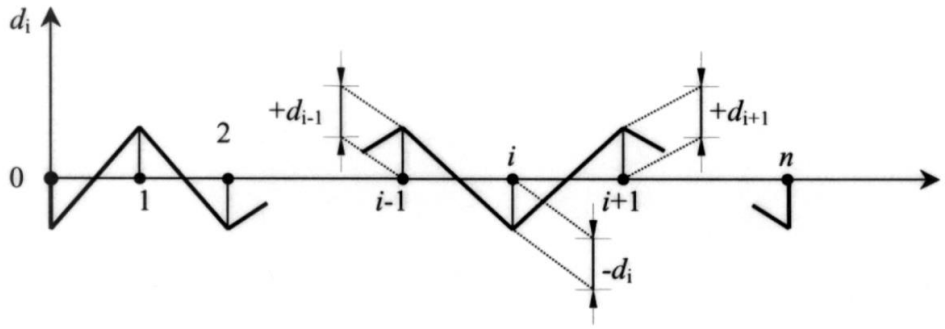

Figure 2-7: Displacement Set B.

In each horizontal direction the most severe effects resulting from the pseudo static analyses are expected to be combined with the relevant effects of the inertia response, by using the SSRS rule. The result of this combination constitutes the effects of the analysis in the considered direction.

2.4 Caltrans – Seismic Design Criteria

The California Department of Transportation (Caltrans) is an executive department within the U.S. State of California. Caltrans manages the state highway system (which includes the California Freeway and Expressway System) and is actively involved with public transportation systems throughout the state. This research will only consider the contents of the norm Seismic Design Criteria on bridges designed by and for Caltrans.

The Caltrans Seismic Design Criteria specifies the minimum seismic design requirements that are necessary to achieve the desired performance of ordinary bridges. When a seismic event occurs, it is expected that ordinary bridges designed by these specifications remain standing but some may suffer significant damage. This regulation identifies the minimum requirements for seismic design. Each bridge presents a unique set of design challenges and the designer must determine the appropriate methods and level of refinement necessary to analyse each bridge's design specificities.

This norm is a compilation of new and existing seismic design criteria documented in several publications. The main purpose of this document is to update all the structure design manuals on a periodic basis to look into the current state of practice for seismic bridge design. Once the information is included in the design manuals, the Seismic Design Criteria serves as a forum to document Caltrans' latest changes to the seismic design methodology.

2.4.1 Definition of ordinary standard bridge

The Caltrans Seismic Design Criteria determines that ordinary bridges accomplish the following requirements:

- Each span length is less than 300 feet (91,44 meters);
- Bridges with single superstructures on either a horizontally curved, vertically curved, or straight alignment;
- Constructed with precast or cast-in-place concrete girder, concrete slab superstructure on pile extensions, column or pier walls, and structural steel girders composite with concrete slab superstructure which are supported on reinforced concrete substructure elements;
- Horizontal members either rigidly connected, pin connected, or supported on conventional bearings;
- Bridges with dropped bent caps or integral bent caps;
- Columns and pier walls supported on spread footings, pile caps with piles or shafts;
- Bridges supported on soils which may or may not be susceptible to liquefaction and/or scour;
- Spliced precast concrete bridge system emulating a cast-in-place continuous structure;
- Fundamental period of the bridge system is greater than or equal to 0,7 seconds in the transverse and longitudinal directions of the bridge.

The bridges which don't meet these requirements or features shall be classified as either ordinary non-standard or important bridges and require project-specific design criteria which are beyond the scope of the norm in study.

2.4.2 Demands on structure components

2.4.2.1 Design spectrum

Caltrans predicts that, for structural applications, seismic demand shall be represented using an elastic 5% damped response spectrum. Generally, the design spectrum is defined as the greater of:

- a probabilistic spectrum based on a 5% in 50 years probability of exceedance (or 975 year return period);
- a deterministic spectrum based on the largest median response resulting from the maximum rupture of any fault in the vicinity of the bridge site;
- a statewide minimum spectrum defined as the median spectrum generated by a magnitude 6,5 earthquake on a strike-slip fault located 12 kilometres from the bridge site.

The spectrum design development has several aspects which require special knowledge related to the determination of fault location and interpretation of the site profile and geologic

setting for incorporation of site effects. Consequently, Geotechnical Service or a qualified geo-professional is responsible for providing final design spectrum recommendations.

Topic 2.1.1 of the Caltrans Seismic Design Criteria indicates several design tools, with the respective website links, which are available to the engineer for use in preliminary and final specification of the design spectrum.

2.4.2.2 Ground motion

As Eurocode 8, Caltrans also predicts the attention given to horizontal and vertical ground motion.

- **Horizontal ground motion**

An earthquake ground shaking hazard has a random orientation which can or cannot be equally probable in all horizontal directions. The method for obtaining the maximum demand on bridge members resulting from the directionality of ground motion depends on the method of analysis and complexity of the bridge.

For ordinary standard bridges, the analytical methods described by Caltrans will be applied, as for complex bridges, which are beyond the scope of this norm, the recommendation lies on the use of nonlinear time history analysis using multiple ground motions applied in two or three orthogonal directions of the bridge, accounting thus for the uncertainty in ground motion direction.

- **Vertical ground motion**

The superstructure of an ordinary standard bridge, where the site peak ground acceleration is $0{,}6g$ or greater, will be designed to resist the applied vertical force.

For non-standard and important bridges, the effect of the vertical loads should be determined by a case-by-case study.

Note that the vertical ground motion is rarely a condition factor of the seismic structural behaviour and because of that its analysis will not be performed in this study.

2.4.3 Capacity of structure components

According to Caltrans, all columns, pier walls and piles or pile-extensions in slab bridges, in soft or liquefiable soils, are designated and detailed as seismic-critical members with a ductile behaviour.

Seismic-critical members should sustain damage during a seismic event without leading to structural collapse or loss of structural integrity. Caltrans defines a ductile member as any

member that is intentionally designed to deform inelastically for several cycles without significant degradation of strength or stiffness.

Other bridge members, as the beams or the slab of the deck, can also be designed and designated as seismic-critical if they are to experience seismic damage.

The remaining components of the bridge, not designated as seismic-critical, will be designed to remain elastic in a seismic event.

2.4.4 Methods of Analysis

Seismic analysis goal is to evaluate the forces, deformations and capacities of the structural system and its individual components.

For ordinary standard bridges, to estimate the displacement demands, the appropriate analytical tools are the equivalent static analysis and the linear elastic dynamic analysis. On the contrary, in what concerns establishing displacement capacities, also, an inelastic static analysis should also be used on ordinary standard bridges.

2.4.4.1 Equivalent Static Analysis (ESA)

This analysis will be applied to estimate displacement demands for structures where a more sophisticated dynamic analysis will not provide for additional information of the structural behaviour. ESA is best suited for structures or individual frames with well-balanced spans and uniformly distributed stiffness where the response can be captured by a predominant translational mode of vibration.

In this method, the initial stiffness of each bent is obtained from a pushover analysis of a simple model of the bent in the transverse direction or a bridge frame in the longitudinal direction. The initial stiffness is expected to correspond to the slope of the line passing through the origin and the first structural plastic hinge on the force-displacement curve. The displacement demand, corresponding to the period in each direction, is then obtained from the design response spectrum.

2.4.4.2 Elastic Dynamic Analysis (EDA)

The EDA will be used to estimate the displacement demands for structures where ESA does not provide for an adequate level of sophistication to estimate the dynamic behaviour. In this

analysis, a linear elastic multi-modal spectral analysis should be carried out by using the appropriate response spectrum. The number of degrees of freedom and the number of modes considered in the analysis must be sufficient to capture at least 90% of the mass participation in the longitudinal and transverse directions.

It should be pointed out that EDA is used in the present context for purposes of estimating the demand displacement and not the design forces. In this method, the normalized modal displacements at each degree of freedom are multiplied by participating factors and spectral responses.

Sources of non-linear response that are not captured by the present method include the effects of the surrounding soil, yielding of structural components and opening and closing of expansion joins.

2.4.4.3 Inelastic Static Analysis (ISA)

Commonly referred as “push over” analysis, the ISA is used to determine the reliable displacement capacities of a structure or frame.

This analysis will be performed by using expected material properties of modelled members. ISA is an incremental linear analysis, which captures the overall non-linear behaviour of the elements, including soil effects, by pushing them laterally to initiate plastic action. Each increment pushes the frame laterally until the potential collapse mechanism is achieved.

2.4.5 Analysis of asynchronous ground motion

Caltrans does not contain any specific information about how to design a bridge under an asynchronous ground motion. What it does have is a specification about how to design a large bridge. Notice that an asynchronous seismic behaviour is much more significant in a large bridge than in a small one, due to the fact that, in a large one, it is more likely that the seismic signal between each pier are different, than in a small one.

For that, Caltrans uses the following figure (corresponding to Figure 5.5.2-1 of the Caltrans Seismic Design Criteria) representing a large bridge, and the demand for an analysis by frames, i.e. instead of a single large bridge there are n small ones.

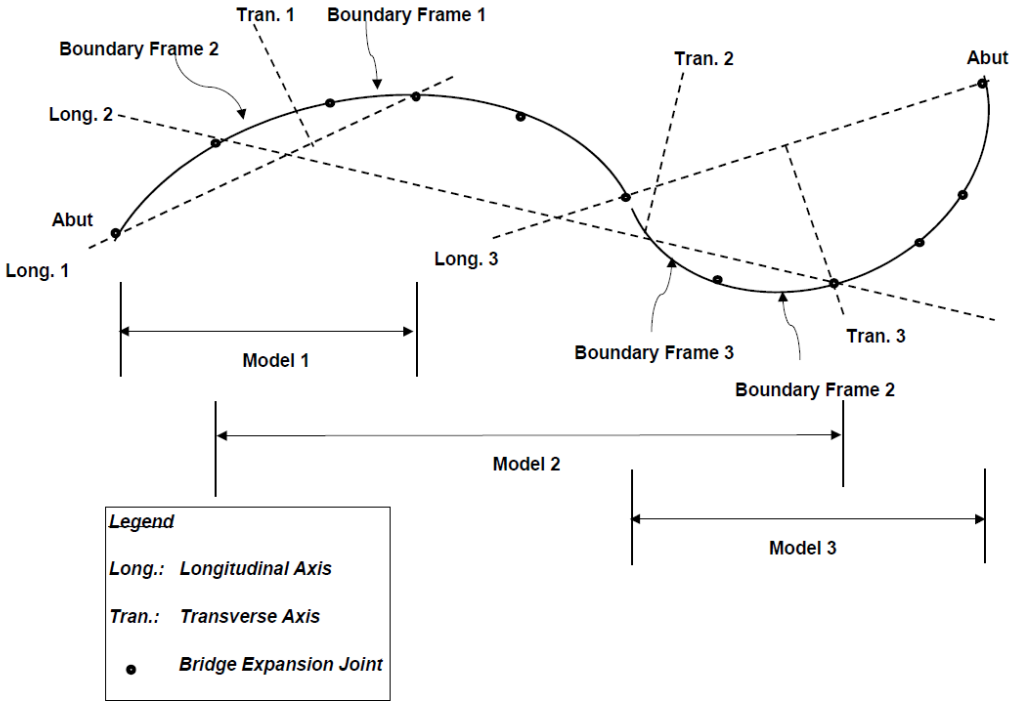

Figure 2-8: Caltrans' modelling technique for large bridges.

According to Caltrans, this multi-frame analysis will include a minimum of two boundary frames or one frame and an abutment beyond the considered frame.

2.5 Historical Evolution and Comparative Analysis of Bridge Codes: Eurocode 8 and Caltrans

The European practice in seismic design is quite recent, with a few cases of damages on bridges due to seismic events. In Europe, the interest in seismic design of bridges starts growing due to the potential of disastrous effects in case of a large-scale earthquake and its penalties in the export market. With regard to the former reason, several bridges in Italy are potentially subjected to considerable earthquake risk, among several others in European countries with a large population and non-negligible exposure.

In the beginning, national codes in Europe which included seismic provisions for bridges were very few and with minimal considerations. It was through the development of Eurocode 8 – Part 1 that concerted efforts were dedicated to the development of seismic design guidelines for bridges in Europe. With the subsequent versions of Eurocode 8, particularly Eurocode 8 – Part 2 dedicated to bridges, this project of the European Union became more robust, comprehensive and reflecting a somewhat different approach to other codes.

The current version of Eurocode 8 – Part 2 reflects the most recent view of the European earthquake engineering community. The approach consists of using ductility to reduce design forces, to detail potential plastic hinge zones for high levels of curvature ductility and to protect other bridge components by applying capacity design factors.

In USA the situation is quite different, due to the higher number of seismic events they experience. The Association of American State Highways and Transportation Officials (AASHTO) has been issuing seismic provisions for many years and its current version is based on the load and resistance factor design philosophy.

However, the status of bridges in California and the repeated relatively poor performance of bridges in Californian earthquakes led the California Department of Transportation (Caltrans) to develop its own design guidance. The Caltrans guidelines are based on the patterns and type of damage in bridges on the state earthquakes as, for example, the earthquake in San Francisco in 1971, where the interchange between the Golden State and Antelope Valley Freeways suffered total collapse. There were many other cases of heavy damage, partial and total collapse of bridges and elevated roads such as this particular one in the heavily populated California state. This prompted major investment in research of design and strengthening of reinforced concrete bridges in particular and an extensive strengthening programme was initiated.

This sequence of events leads to the continuing state support for development of the Caltrans design and strengthening guidelines. It was therefore deemed appropriate that the subsequent comparison of bridge codes should include Caltrans guidelines as a USA representative as opposed to AASHTO.

From a brief comparison between Eurocode 8 and Caltrans, it is possible to state that European regulation is supported on other researches and theoretical tests, while USA's and particularly California's norms are based upon the previous experiences.

To consolidate this analysis, the table included in Elnashai and Mwafy (n.d.) is enclosed below to demonstrate the approach on the seismic analysis of bridges by both Eurocode 8 and Caltrans. The information displayed in this table is the most relevant for the approach and respects the original text.

Provisions	Eurocode 8	Caltrans
1. General		
Performance criteria	No collapse (ultimate limit state) under the design seismic event. Minor damage (service limit state) under frequent earthquakes.	Implied. Structural integrity to be maintained and collapse during strong shaking to be prevented.
Design philosophy	Sufficient ductility and strength to be provided according to the intended seismic behaviour. Brittle types of failure to be avoided in all structures.	Adequate ductility capacity to be provided and failure of non-ductile and inaccessible elements to be prevented.
2. Seismic loading		
Design spectrum	Normalised elastic response spectra with variable corner periods. Site dependent power spectrum representation is permitted.	Acceleration response spectrum (ARS) curves. Modified or site-specific ARS curve is permitted.

Return period	The recommended value is 475 years.	Deterministic approach. Maximum credible earthquake (MCE) with mean attenuation given by ARS curves.
Geographic variation	Set by national authorities. No agreed-up on zonation maps for Europe.	Contour maps of peak rock acceleration developed for MCE and attenuation as a function of distance from fault.
Importance considerations	Recommended three categories (greater than average, average and less than average). Set by national authorities.	Not addressed directly by design specifications.
Site effects	Five basic types and two additional profiles for soft soils. Spatial variability must be considered for bridges with total length >600m and where abrupt change in soil.	Five soil profiles, based on shear wave velocity, and a profile for soil requiring site-specific evaluation.
Damping	Spectra normalised to 5%. Damping correction factor may be used.	5% of critical.
Duration considerations	Specifications for artificial time histories.	Not considered directly.
3. Analysis		
Selection guidelines	Based on bridge regularity and anticipated performance.	Based on structure complexity.
Equivalent static	Fundamental mode method is applicable for simple and regular bridges.	Static horizontal force applied to individual frames. Suitable for ordinary standard bridges.
Elastic dynamic	Multi-modal response spectrum analysis. 3D lumped mass space frame.	Multi-modal response spectrum analysis. 3D lumped mass space frame.
Inelastic static	May be applied to the entire bridge structure or to individual components.	Used to determine the reliable displacement capacities of a structure as it reaches its limit of structural stability.
Inelastic dynamic	Used only in combination with a standard response spectrum analysis to provide insight into the post-elastic response.	Not covered.
Directional combinations	$Case\ 1 = L + 0{,}3T + 0{,}3V$ $Case\ 2 = 0{,}3L + T + 0{,}3V$ $Case\ 3 = 0{,}3L + 0{,}3T + V$	$Case\ 1 = L + 0{,}3T$ $Case\ 2 = 0{,}3L + T$ A combined vertical/horizontal load analysis is not required for standard bridges.
Vertical ground motion	May be omitted in zones of low to moderate seismicity. Need to be investigated in exceptional cases in high seismicity zones.	A case-by-case determination is required for non-standard bridges.
4. Seismic effects		
Design forces	Consider ductility class and ground motion.	Consider ductility and risk.
a) Ductile components	Elastic force reduction factor (behaviour factor, q) depends on structure type and component.	Resist the internal forces generated when the structure reaches its collapse limit state.
b) Non-ductile components	Capacity design with protection factors.	Capacity design.
Displacements	Use secant stiffness at yield for members with plastic hinges.	Use cracked stiffness.
Minimum seat width	States that unseating should be avoided.	Evaluated from seismic action and spans.
5. Concrete design		
Columns (flexure)	Capacity design. Ultimate strength design.	Capacity design. Ultimate strength design.
Column (shear)	Verifications of shear resistance are carried out in accordance with Eurocode 8 – Part 1, with additional safety factors.	Demand based on capacity design. Shear capacity based on contribution from concrete and transverse reinforcement. Concrete contribution at plastic hinges is reduced to zero for members in tension.
Footings	Mainly covered in Eurocode 8 – Part 5.	Capacity design for seismic loading. Ultimate strength design.
Superstructure and pier joints	Capacity design in ductile structures.	Designed to transmit the maximum forces produced when the column has reached its over strength capacity.
Caps	Capacity design in ductile structures.	Capacity design rule to ensure plastic hinge in columns not caps.
Superstructure	Capacity design in ductile structures.	Protected by capacity design.

Shear keys	Capacity design in ductile structures.	Abutment shear keys designed as sacrificial elements to protect stability of abutment.
Anchorage of column reinforcing steel	Mainly covered in Eurocode 8 – Part 1.	Provisions for anchorage length.
Splices of column reinforcing steel	Not permitted in plastic hinge regions.	Not allowed in plastic hinge zones.
6. Steel design		
	Covered for the substructure and superstructure.	Seismic criteria for structural steel bridges are being developed independently and will be incorporated into the future releases.
7. Foundation design		
Spread footings	Mainly covered in Eurocode 8 – Part 5.	Ultimate soil-bearing capacity under seismic loading.
Pile footings	Mainly covered in Eurocode 8 – Part 5.	Provisions for pile foundations in competent and marginal soil.
Liquefaction	Mainly covered in Eurocode 8 – Part 5.	Not explicitly addressed. Soil should have low potential for liquefaction, lateral spreading, or scour.
8. Miscellaneous design		
Restrainers	Required if minimum seat length without restrainers not met in ductile structures. Required for limited ductility and isolated bridges.	Designed to remain elastic and restrict movement to allowable levels at expansion joints.
Base isolation	Specific chapters devoted to seismic isolation and elastomeric bearings.	Special case.
Active/passive control	Under development.	Not used.

Table 2-6: Comparison of the seismic codes Eurocode 8 and Caltrans.

Considering the research to be performed, the table displayed should be expanded to additional information on the subject of asynchronous ground motion, where Eurocode 8 predicts three different methods to approach this topic: time-history analysis, linear random vibration analysis, and response spectrum for multiple-support input. In what concerns Caltrans, it does not provide for any specific method to treat the topic (it merely states that, if it is a large bridge, a multi-frame analysis will be applied).

A brief review of seismic design codes and general practice in Europe and the USA indicates that the situation is far from consistent, although both of them use ductile response and capacity design principles.

In both considered cases, seismic design codes are constantly being updated, hence the statements made above should be considered as time-qualified.

3. Description of the case studies

In the current research, four different long bridges will be analysed with the main purpose of comparing the damage caused by a synchronous and an asynchronous seismic sign on each bridge. Three of these bridges are 200 meters long and have different pier height, being part of a previous study included in Pinto (2007), and the other one is 400 meters long.

All the bridges considered have the same length between pillars, 50 meters, and the same type of deck and piers. The deck is a continuous coffin section, made of concrete C40/50 while the piers have a constant rectangular section, also made of concrete C40/50. As for the connection type, the pillars are built-in both at the bridge's baseline and the deck. The connection between the abutments and the deck is easily supported, enabling the rotary motion over itself from the horizontal axis downright of the bridge and the translatory motion towards the downright development of the bridge.

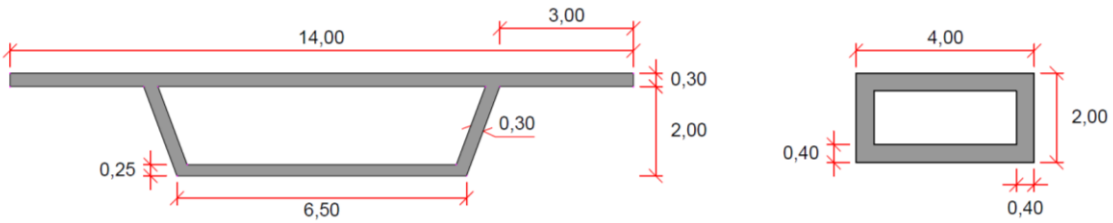

Figure 3-1: Deck section and pier section.

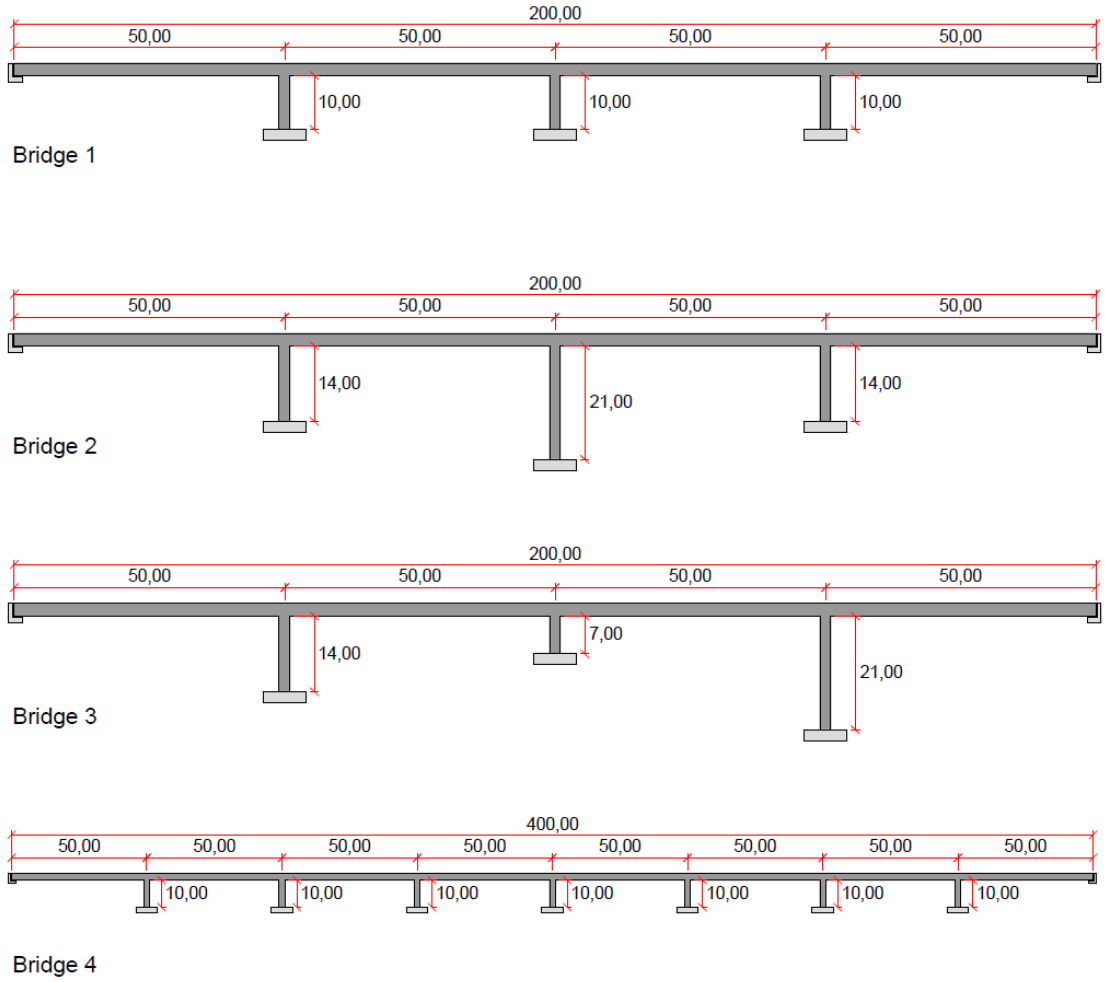

Figure 3-2: Case study bridges.

The current study aims at comparing the effects of the enforcement of a synchronous analysis through the response spectrum method described earlier in 2.3.2.3, and of an asynchronous analysis through the simplified method on each of the bridges in order to analyze the spatial variability of seismic ground motion, as described previously in 2.3.5.2. The study will particularly focus on the displacements on the deck, the base shear, the bending moment on the pillars' platform and the pillars' drift tolerated by the structure without becoming plastic. Both methods, of synchronous and asynchronous analysis are thoroughly described in Eurocode 8.

Each analysis will be carried out considering two possible scenarios according to the type of ground of the foundation. In both situations, the whole bridge structure laying on a single ground will be considered. The ground types contemplated are ground type A, defined in Eurocode 8 as a rocky ground, and ground type C composed by compact sand or stiff clay.

The main purpose is to establish the comparison between the results obtained from each bridge, by checking the variation of magnitude values of the base shear, of the displacement on the deck, of the moment of flexure on the pillars' platform and of the pillars' drift, obtained for each ground type and for each type of analysis.

In order to carry out this case study, it is necessary to know the peak ground acceleration (PGA). To meet this purpose, a single seismic sign – the El Centro North-South component – was considered in all the analysis carried out in the four selected bridges, with the following seismogram:

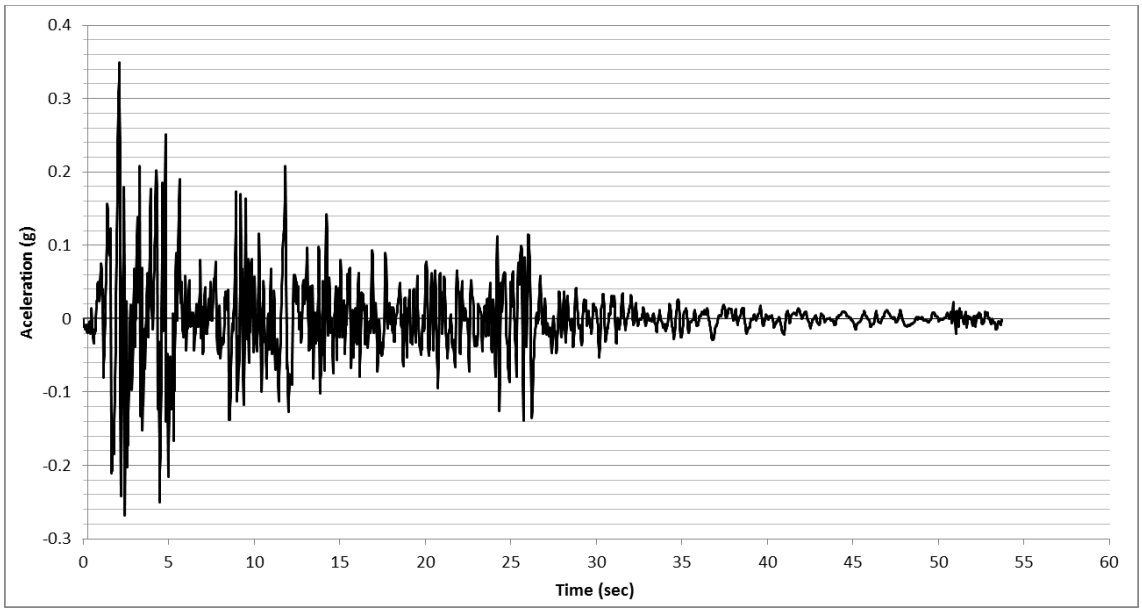

Figure 3-3: Seismogram of El Centro earthquake, North-South component.

The El Centro seismic sign was particularly chosen for the analysis because it is a widely known seismogram, with a large number of studies performed concerning the El Centro earthquake which on May 18, 1940, in the Imperial Valley in the southeaster of Southern California near the international border of the USA and Mexico. This seismic event had a magnitude of $6{,}9$ on Richter scale and a PGA of $0{,}35g$.

The following four chapters are entirely dedicated to the study of the bridges previously described and to the analysis of the results achieved.

As one can observe in Figure 3-2, Bridges 2, 3 and 4 can be regarded as deriving from Bridge 1, considering that Bridges 2 and 3 are a variation of the terrain's topography and Bridge 4 is a variation of the total longitude of the bridge. For this particular reason, though all bridges are submitted to the same study, the description of the results will be divided into three different chapters. Considering that the procedures used to carry out this study are the same for all the selected bridges, the option was to thoroughly explain the steps taken to analyse Bridge 1, whereas for the other bridges there will be an explanation of the results with associated comments.

Attention should be drawn to the fact that all values from both analysis here displayed are absolute, as the seismic action causes a fluctuation in the structure which leads to a deformation on one side or the other, turning the results into either positive or negative values.

4. Analysis of a long bridge

As explained previously, this chapter will display the synchronous and the asynchronous analysis carried out on Bridge 1, according to Eurocode 8. The response spectrum will be the method used for the synchronous analysis, while the asynchronous analysis will be performed by means of the simplified method to consider spatial variability of seismic ground motion, having the displacements calculated on both the sets, A and B, which are anticipated in Eurocode 8. These will be subsequently combined with the seismic action and then it will become possible to conclude which combination is actually causing a greater effort.

Thereafter, the effect on whether to consider the spatial variability of seismic ground motion or not, i.e., the consequences of choosing between a synchronous or an asynchronous analysis will be compared, by using the result obtained from the synchronous analysis and the more adverse combination of the asynchronous analysis.

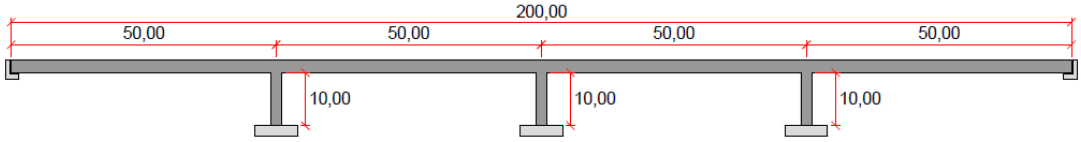

Figure 4-1: Bridge 1.

4.1 Displacements of the piers resulting from the seismic action

This stage consists on presenting the performed calculation to determine the displacements which the asynchronous seismic action brings in the structure, according to the specifications in Eurocode 8.

Prior to the analysis there was the need to calculate the displacements in the base of the piers, according to both sets (A and B) as displayed in 2.3.5.2. To achieve this calculation, it was necessary to calculate the design seismic action a_g, which is given, as stated before, by the expression:

$$a_g = \gamma_I \cdot a_{Rg} \tag{4.1}$$

Where, $\gamma_I = 1$, because this bridge it regarded as a bridge of average importance;

$a_{Rg} = 3{,}50\ m/sec^2$, which is the maxim acceleration of El Centro seismogram. This value is obtained by multiplying the maximum acceleration of El Centro seismogram represented in *Figure 3-3*, which is given in g by the gravity acceleration: $a_{Rg} \cdot g = 0{,}35 \cdot 10 = 3{,}50\ m/sec^2$.

After obtaining this figure it was them possible to calculate the design ground displacement d_g, described in 2.3.2.4, which can be represented by the expression:

$$d_g = 0{,}0025 \cdot a_g \cdot S \cdot T_C \cdot T_D \tag{4.2}$$

Where, $a_g = 3{,}50\ m/sec^2$, as explained before;

S, T_C and T_D are tabled values and it depends on whether it is a ground type A or a ground type B. These values can be found on *Table 2-3* of the current study.

This was then followed by the calculation of the value of ε_r, given by the following expression, included in 2.3.5.2:

$$\varepsilon_r = \frac{d_g\sqrt{2}}{L_g} \tag{4.3}$$

Where, d_g, is given before;

L_g is a tabled value, depending on the ground type, which can be found in the *Table 2-5*, of this work.

Arriving at this point, the necessary data are gathered for the calculation of the displacements in the base of the piers, according to either set A or B.

Displacements of set A

The displacements of set A, as explained in 2.3.5.2 can be represented by the expression:

$$d_{ri} = \varepsilon_r \cdot L_i \leq d_g\sqrt{2} \tag{4.4}$$

As soon as all the necessary coefficients are obtained, the results for Bridge 1 will be the following:

	Abutment 1	Pier 1	Pier 2	Pier 3	Abutment 2
d_{ri} (m)	**0,0000**	**0,0082**	**0,0164**	**0,0247**	**0,0329**
$\varepsilon_r \cdot L_i$ (m)	–	0,0082	0,0164	0,0247	0,0329
ε_r	–	1,6x10^{-4}	1,6x10^{-4}	1,6x10^{-4}	1,6x10^{-4}
L_i (m)	–	50,00	100,00	150,00	200,00
$d_g\sqrt{2}$ (m)	–	0,0986	0,0986	0,0986	0,0986

Table 4-1: Displacements of set A, for ground type A.

	Abutment 1	Pier 1	Pier 2	Pier 3	Abutment 2
d_{ri} (m)	**0,0000**	**0,0213**	**0,0425**	**0,0638**	**0,0851**
$\varepsilon_r \cdot L_i$ (m)	–	0,0213	0,0425	0,0638	0,0851
ε_r	–	4,3x10^{-4}	4,3x10^{-4}	4,3x10^{-4}	4,3x10^{-4}
L_i (m)	–	50,00	100,00	150,00	200,00
$d_g\sqrt{2}$ (m)	–	0,1702	0,1702	0,1702	0,1702

Table 4-2: Displacements of set A, for ground type C.

Displacements of set B

The displacements of set B, also explained in 2.3.5.2, are given by the expression:

$$d_i = \pm\frac{\Delta d_i}{2} = \pm\frac{\beta_r \cdot \varepsilon_r \cdot L_{av,i}}{2} \tag{4.5}$$

The results are the following:

	Ground type A	Ground type C
Δd_i (m)	**0,0041**	**0,0106**
β_r	0,50	0,50
ε_r	1,64x10^{-4}	4,25x10^{-4}
$L_{av,i}$ (m)	50,00	50,00

Table 4-3: Displacements Δd_i, of set B, for ground types A and C.

	Ground type A d_i (m)	Ground type C d_i (m)
Abutment 1	0,0000	0,0000
Pier 1	0,0021	0,0053
Pier 2	-0,0021	-0,0053
Pier 3	0,0021	0,0053
Abutment 2	0,0000	0,0000

Table 4-4: Displacements of set B, for ground type A and C.

The achievement of the displacements of either set A or B for both ground types will be followed by the need to check which of the situations (set A or set B) is more adverse in what concerns displacements of the deck and base shear for each ground type.

4.2 Modelling of Bridge 1

In order to determine which of the sets, A or B, causes major displacements of the deck and the greater base shear, SAP2000 was the programme consulted.

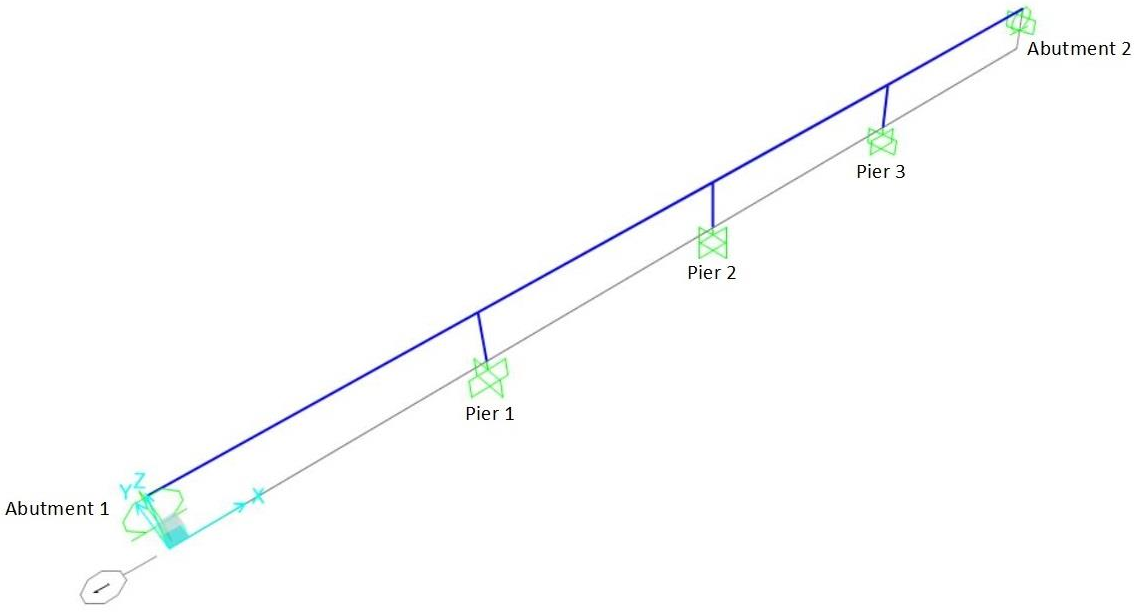

Figure 4-2: Modelling of Bridge 1 in SAP2000.

After modelling Bridge 1 in SAP2000, considering the correct definition of materials and the structure's geometry, the response spectrum (represented in *Figure 4-3*) and the displacements of both set A and B concerning ground type A were applied. This was followed by the combination of the actions of the response spectrum with the displacements of set A and the combination of the response spectrum with the displacements of set B, according to rule SRSS. This is the right moment to understand which of the combinations causes the major displacements of the deck and the greatest base shear. It is important to state that the combination which causes the major displacements is not necessarily the same which causes the greatest base shear.

For ground type C the whole previous process was repeated.

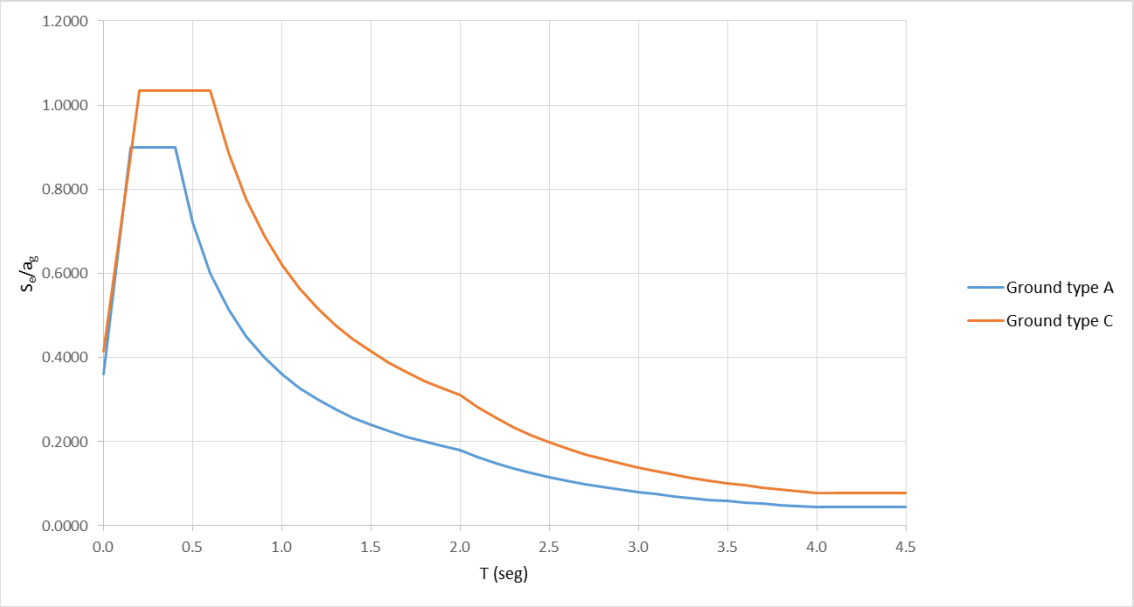

Figure 4-3: Response spectrums of ground types A and C, according to Eurocode 8.

After carrying out the analysis with SAP2000, the vibration modes of the structure and the deformations of each action and of each combination involved were attained for both ground types, as displayed in *Figures 4-4* to *4-14*, and the numerical values thereafter represented and duly commented.

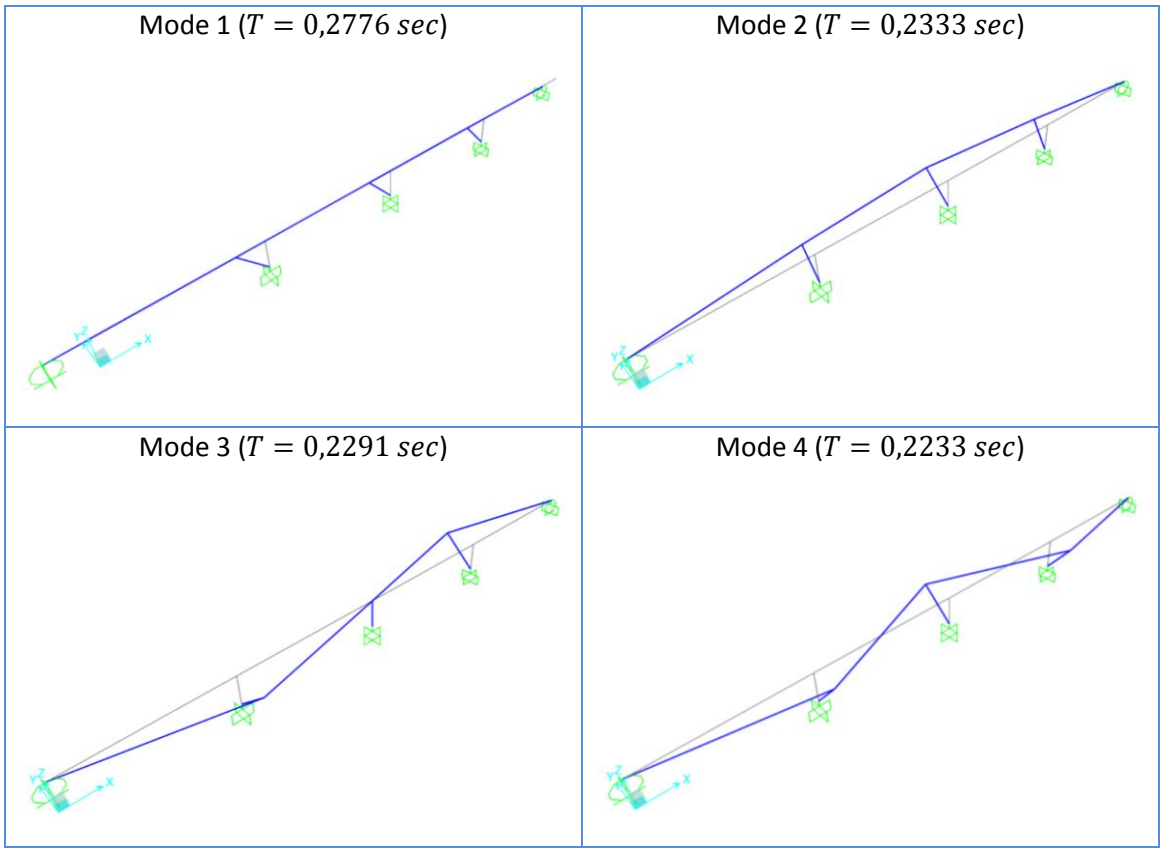

Figure 4-4: First four vibration modes of Bridge 1.

Ground type A

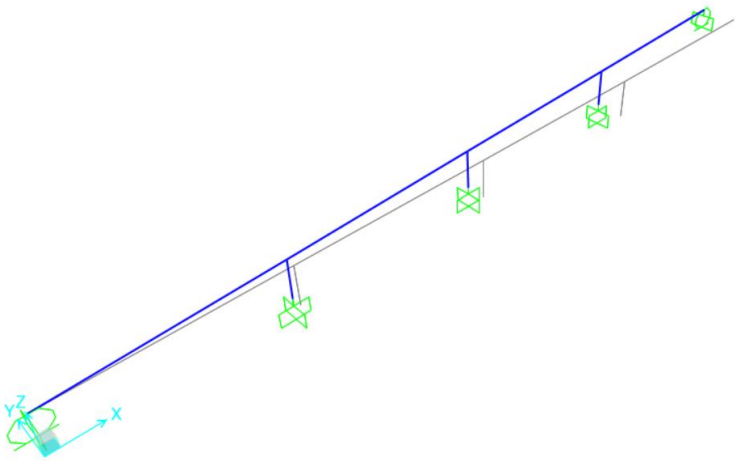

Figure 4-5: Deformation of Bridge 1 caused by the displacements of set A for ground type A.

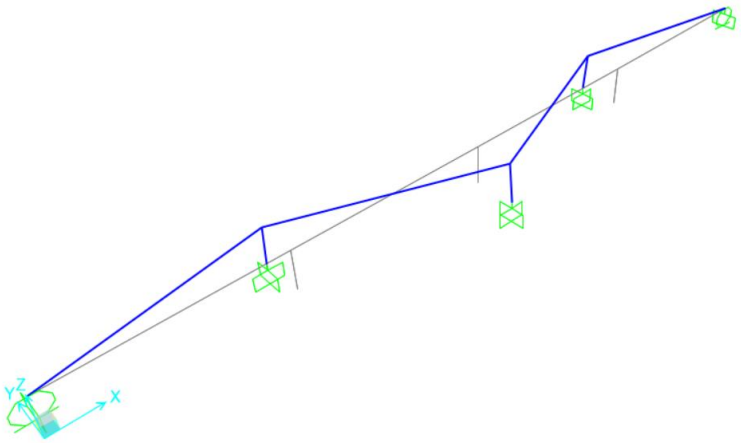

Figure 4-6: Deformation of Bridge 1 caused by the displacements of set B for ground type A.

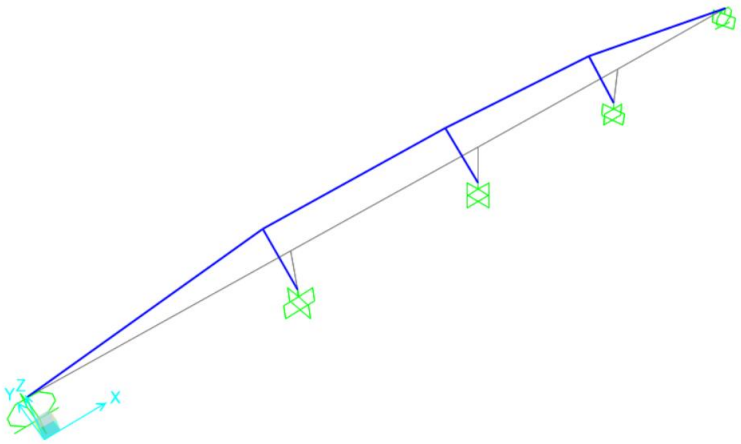

Figure 4-7: Deformation of Bridge 1 caused by the response spectrum for ground type A.

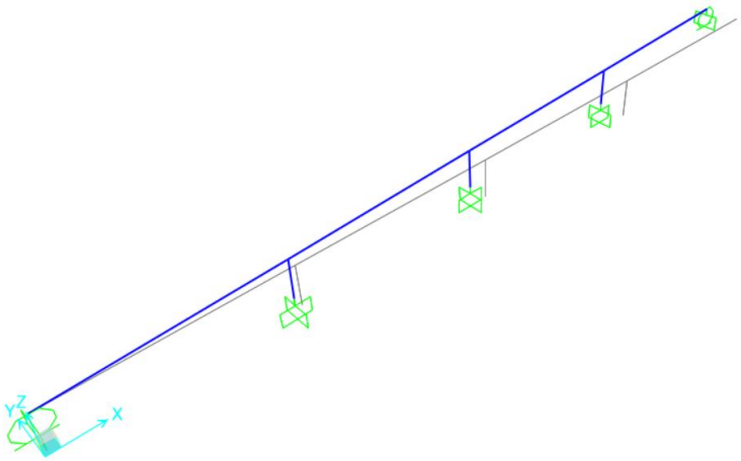

Figure 4-8: Deformation of Bridge 1 caused by the combination of the actions of the response spectrum and the displacements of set A for ground type A.

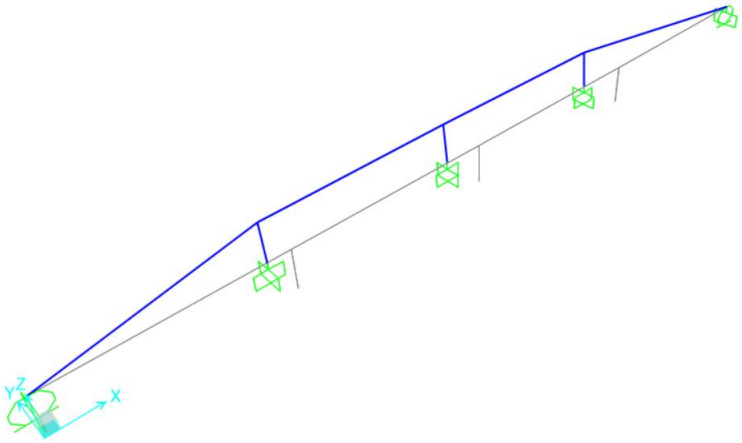

Figure 4-9: Deformation of Bridge 1 caused by the combination of the actions of the response spectrum and the displacements of set B for ground type A.

Ground type C

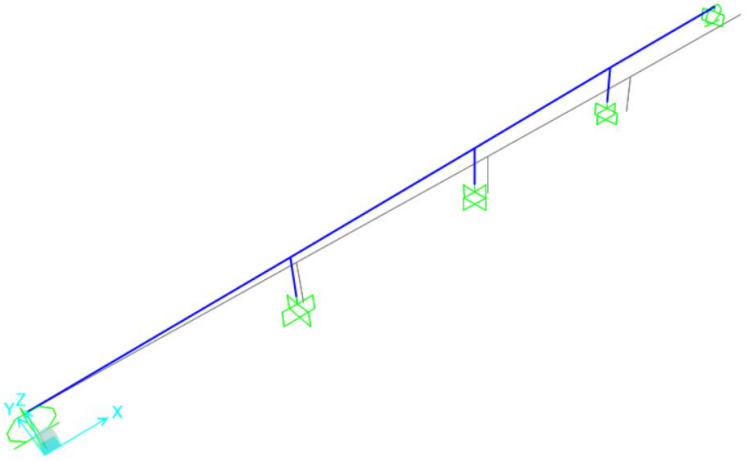

Figure 4-10: Deformation of Bridge 1 caused by the displacements of set A for ground type C.

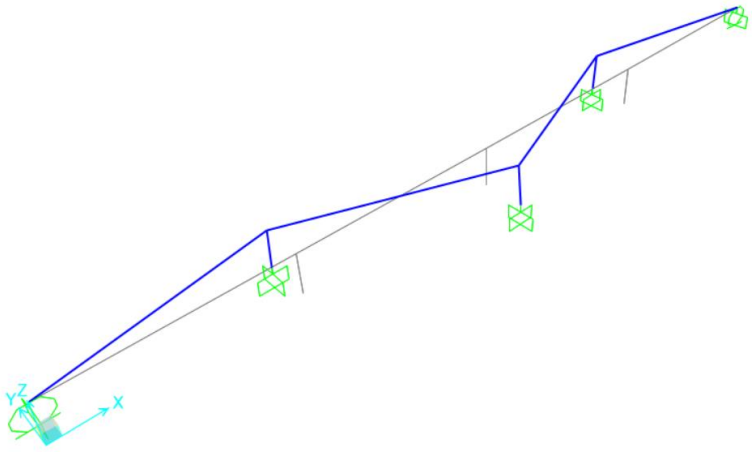

Figure 4-11: Deformation of Bridge 1 caused by the displacements of set B for ground type C.

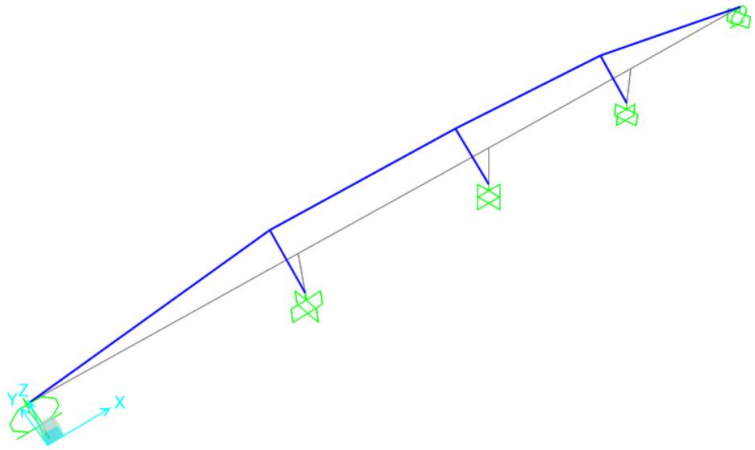

Figure 4-12: Deformation of Bridge 1 caused by the response spectrum for ground type C.

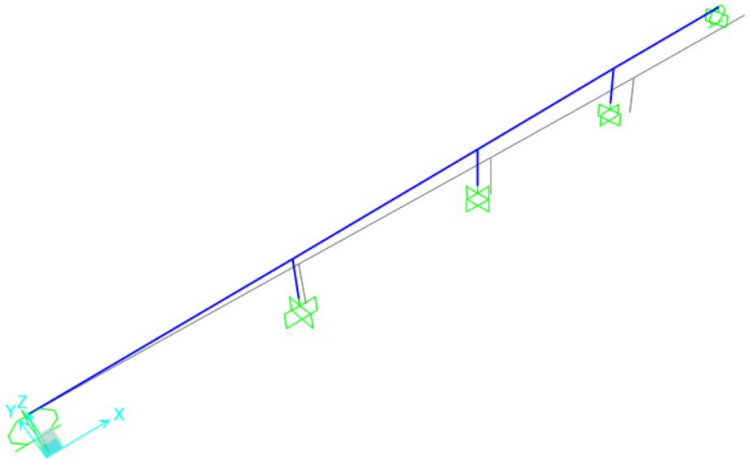

Figure 4-13: Deformation of Bridge 1 caused by the combination of the actions of the response spectrum and the displacements of set A for ground type C.

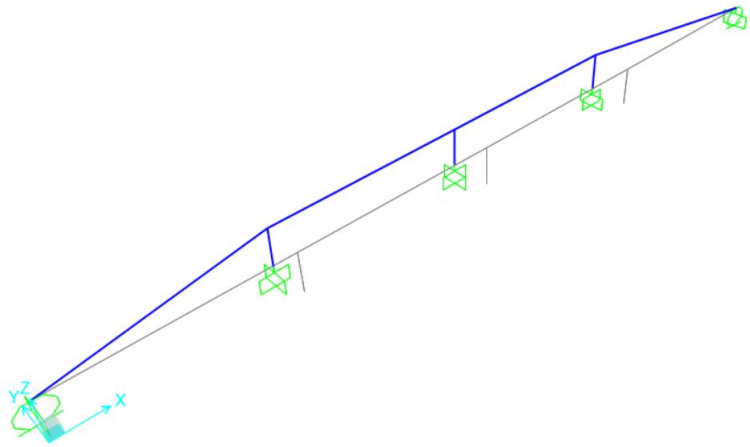

Figure 4-14: Deformation of Bridge 1 caused by the combination of the actions of the response spectrum and the displacements of set B for ground type C.

4.3 Synchronous analysis

The synchronous analysis matches the situation in which the action of the response spectrum for each ground type is taken singly. It is important to remark that during the analysis no displacement in the bases of the piers was dictated, except for the superstructure of the bridge which moved only due to the action of the spectrum. This analysis is represented in *Figures 4-7* and *4-12* previously displayed, whether it concerns a ground type A or a ground type C.

The results obtained from base shears, displacements of the deck, bending moments and drift of piers are displayed afterwards.

4.3.1 Base shears and displacements of the deck

The following values of base shear and displacement of the deck for both ground type A and B were withdrawn from the analysis performed in SAP2000 considering the single action of the response spectrum.

	Base shear (kN)	Displacements of the deck (m)
Abutment 1	13,63	0,0000
Pier 1	792,41	0,0012
Pier 2	888,23	0,0013
Pier 3	792,41	0,0012
Abutment 2	13,63	0,0000

Table 4-5: Values of base shear and displacements of the deck considering the single action of the response spectrum for ground type A.

	Base shear (kN)	Displacements of the deck (m)
Abutment 1	15,67	0,0000
Pier 1	911,27	0,0014
Pier 2	1021,47	0,0015
Pier 3	911,27	0,0014
Abutment 2	15,67	0,0000

Table 4-6: Values of base shear and displacements of the deck considering the single action of the response spectrum for ground type C.

By observing the tables, it is possible to conclude that whether for base shear or displacements of the deck, ground type C originates higher values than ground type A. The cause for this result lays in the characteristics of ground C which is weaker and does not provide the best support base to the cementation as ground type A does, since it is rocky.

Attention must be called to the fact that in displacements of the deck for a synchronous analysis, the difference between considering a ground type A or a ground type C is not that much relevant (less than 1 mm). However, when base shears on piers are taken into account, the choice between a ground type A or a ground type C becomes more determinant (around 120 kN).

From the results displayed, the action of the response spectrum on both ground types causes a major effort and a higher displacement on pier 2.

4.3.2 Shear forces and bending moments

The action of the response spectrum on Bridge 1 results in the following diagrams of shear forces and bending moments for ground type A and ground type C.

Ground type A

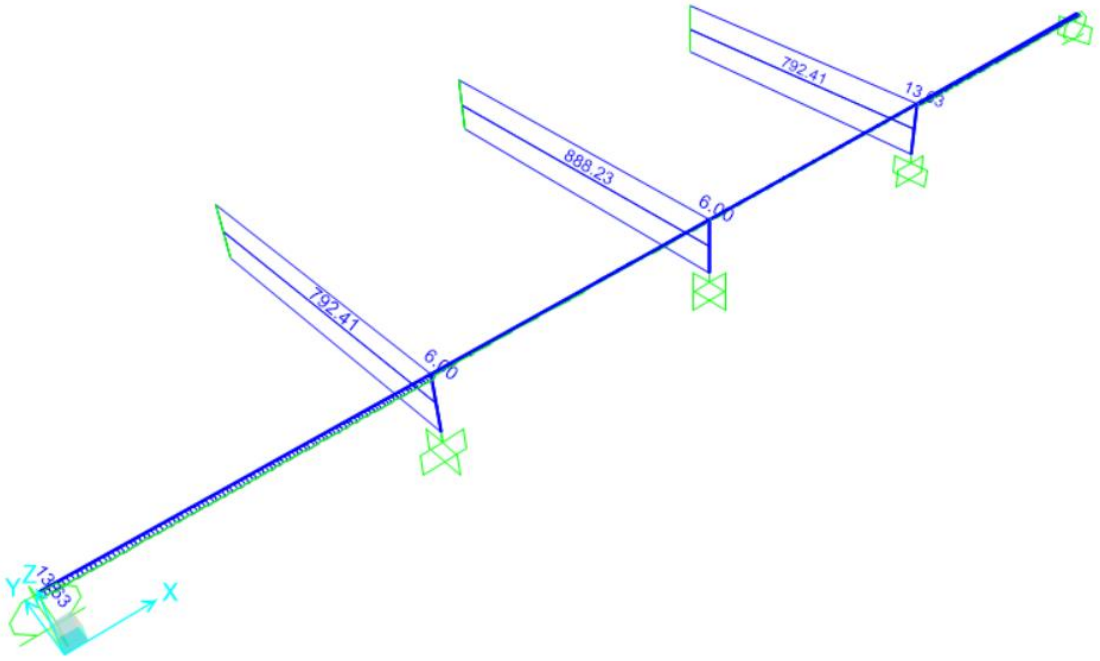

Figure 4-15: Diagrams of shear forces on Bridge 1, caused by the single action of the response spectrum for ground type A.

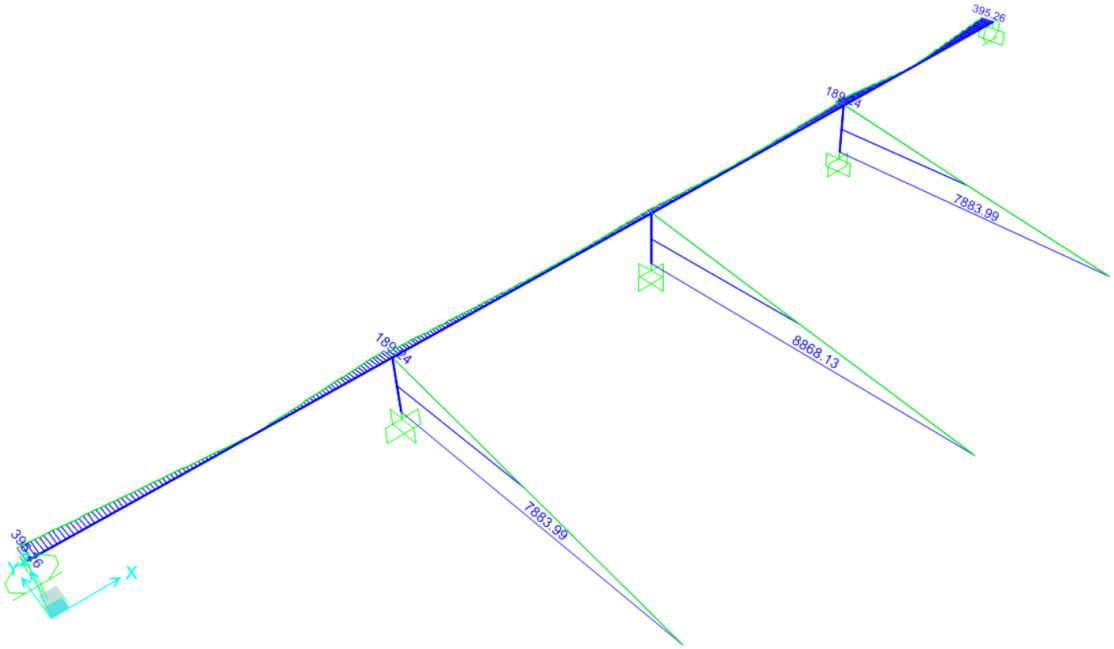

Figure 4-16: Diagrams of bending moments on Bridge 1, caused by the single action of the response spectrum for ground type A.

Piers	V (kN)	M (kN.m)
Top of pier 1	792,41	41,89
Base of pier 1	792,41	7883,99
Top of pier 2	888,23	25,88
Base of pier 2	888,23	8868,13
Top of pier 3	792,41	41,89
Base of pier 3	792,41	7883,99

Table 4-7: Values of shear forces and bending moments of the piers in Bridge 1, caused by the single action of the response spectrum for ground type A.

Deck	V (kN)	M (kN.m)
Abutment 1	13,63	395,26
Pier 1, left	13,63	287,47
Pier 1, right	6,01	189,24
Pier 2, left	6,01	126,37
Pier 2, right	6,01	126,37
Pier 3, left	6,01	189,24
Pier 3, right	13,63	287,47
Abutment 2	13,63	395,26

Table 4-8: Values of shear forces and bending moments of the deck in Bridge 1, caused by the single action of the response spectrum for ground type A.

Ground type C

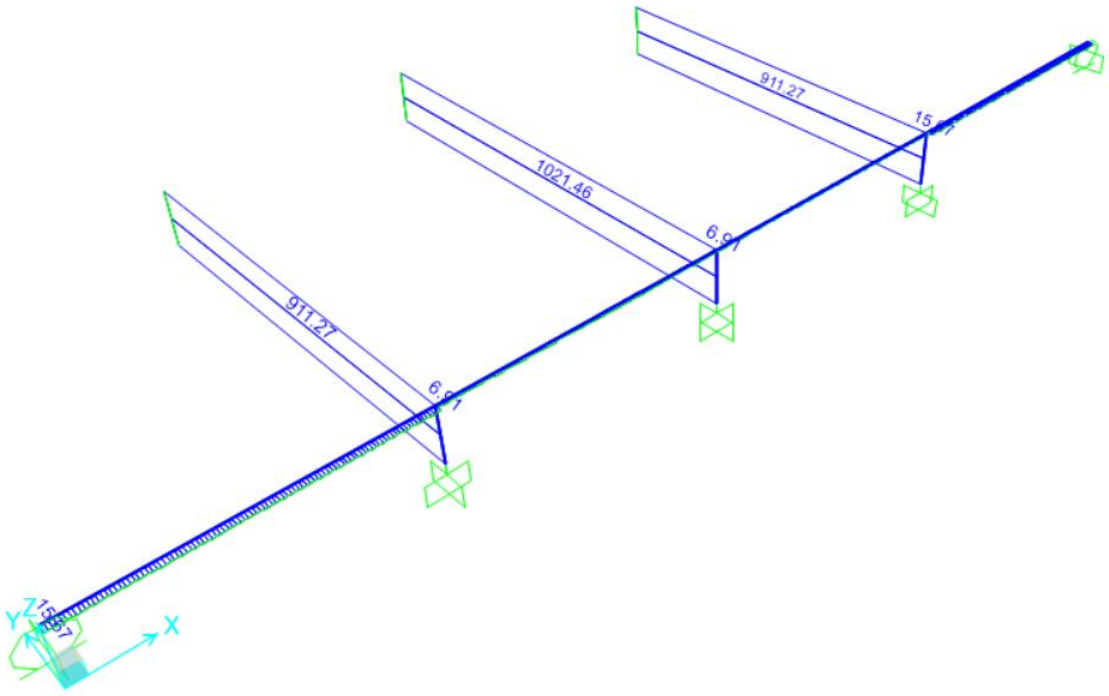

Figure 4-17: Diagrams of shear forces on Bridge 1, caused by the single action of the response spectrum for ground type C.

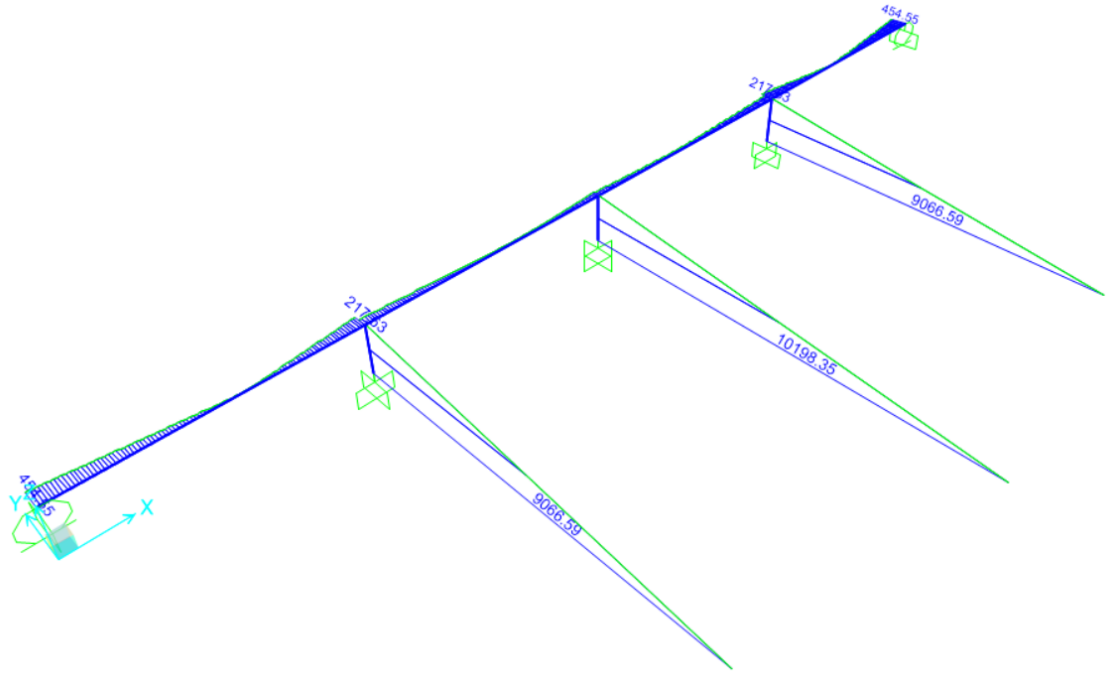

Figure 4-18: Diagrams of bending moments on Bridge 1, caused by the single action of the response spectrum for ground type C.

Piers	V (kN)	M (kN.m)
Top of pier 1	911,27	48,17
Base of pier 1	911,27	9066,59
Top of pier 2	1021,47	29,76
Base of pier 2	1021,47	10198,35
Top of pier 3	911,27	48,17
Base of pier 3	911,27	9066,59

Table 4-9: Values of shear forces and bending moments of the piers in Bridge 1, caused by the single action of the response spectrum for ground type C.

Deck	V (kN)	M (kN.m)
Abutment 1	15,67	454,55
Pier 1, left	15,67	330,59
Pier 1, right	6,91	217,63
Pier 2, left	6,91	145,32
Pier 2, right	6,91	145,32
Pier 3, left	6,91	217,63
Pier 3, right	15,67	330,59
Abutment 2	15,67	454,55

Table 4-10: Values of shear forces and bending moments of the deck in Bridge 1, caused by the single action of the response spectrum for ground type C.

As it would be expected, the values of shear force obtained for each pier match the values of base shear in both situations.

From the observation of the results it is possible to conclude that whether for ground type A or ground type C for this kind of load, piers are the elements which endeavor the highest forces, much higher than the deck's.

The comparison between the tables leads to the conclusion that the values for ground type C are higher than for ground type A.

4.3.3 Drifts of the piers

A calculation of the pier's drift was carried out in order to evaluate the importance of the seismic action on the pier, based on the following expression:

$$\theta = \frac{|\delta_d - \delta_f|}{H} \cdot q \tag{4.6}$$

Where, δ_d is the displacement of the deck;

δ_f is the displacement of the foundation;

q is the behaviour factor, which considered $q = 1$, i.e., an elastic linear behaviour;

H is the height of the pier.

In the expression 4.6, the module of the difference between displacements is taken into account as the seismic action brings about an oscillation to one side and the other of the structure, and therefore the absolute value of that difference is the only that really matters.

Considering the diagram in *Figure 4-19*, the drift of piers matches angle θ whose deformation causes with the vertical axis, deducting the foundation's displacement. It is important to state that since it is a very short angle, the distortion undergone by the pier is negligible and it is possible to assume that it deforms as represented in the figure.

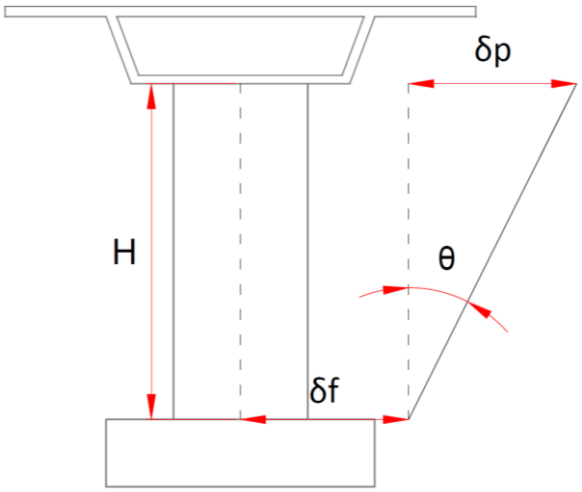

Figure 4-19: Drift of the piers.

The results achieved from the synchronous analysis were the following:

	High (m)	δ_d (m)	δ_f (m)	q	θ (rad)
Pier 1	10,00	0,0012	0,0000	1,00	**$1{,}18 \times 10^{-4}$**
Pier 2	10,00	0,0013	0,0000	1,00	**$1{,}33 \times 10^{-4}$**
Pier 3	10,00	0,0012	0,0000	1,00	**$1{,}18 \times 10^{-4}$**

Table 4-11: Drift of the piers due to the application of the response spectrum for ground type A.

	High (m)	δ_d (m)	δ_f (m)	q	θ (rad)
Pier 1	10,00	0,0014	0,0000	1,00	**$1{,}36 \times 10^{-4}$**
Pier 2	10,00	0,0015	0,0000	1,00	**$1{,}53 \times 10^{-4}$**
Pier 3	10,00	0,0014	0,0000	1,00	**$1{,}36 \times 10^{-4}$**

Table 4-12: Drift of the piers due to the application of the response spectrum for ground type C.

The results show that the drift of the piers is not significant, which has to do with the piers not being too high and having a really sturdy, stiff section which hinders them from deforming too much. The rather insignificant displacement on the deck (around 1 mm) is another factor contributing to the shortage of the drift of piers.

The greatest drift is connected to the main pier, with the drifts of outward piers being shorter yet showing the same value. The difference between the drift of the piers when considering a ground type A or a ground type C is not significant though the highest values relate to ground type C.

4.4 Asynchronous analysis

To carry out the asynchronous analysis, the behavior of the most adverse situation was considered from either the combination of the action of the response spectrum with the displacements of set A and the combination of the action of the response spectrum with the displacements of set B, both in terms of base shears and displacements of the deck. This analysis is represented in *Figures 4-8*, *4-9*, *4-13* and *4-14* previously displayed, whether it concerns a ground type A or a ground type C.

As it had happened with the synchronous analysis, the results achieved from base shears, displacements of the deck, transverse force, bending moments and the drift of piers are displayed below.

4.4.1 Base shears and displacements of the deck

The analysis carried out in SAP2000 contemplated the behavior of the combination of the action of the response spectrum with the displacements of set A and the combination of the action of the response spectrum with the displacements of set B, except for the values of base shear and displacement of the deck for both ground type A and ground type B displayed below.

Ground type A

	Base shear (kN)	Displacements of the deck (m)
Abutment 1	67,63	0,0000
Pier 1	794,15	0,0082
Pier 2	888,23	0,0165
Pier 3	794,05	0,0248
Abutment 2	67,20	0,0329

Table 4-13: Values of base shear and displacements of the deck considering the combination of the response spectrum for ground type A with the displacements of set A.

	Base shear (kN)	Displacements of the deck (m)
Abutment 1	44,51	0,0000
Pier 1	798,47	0,0023
Pier 2	895,23	0,0024
Pier 3	798,47	0,0023
Abutment 2	44,51	0,0000

Table 4-14: Values of base shear and displacements of the deck considering the combination of the response spectrum for ground type A with the displacements of set B.

Ground type C

	Base shear (kN)	Displacements of the deck (m)
Abutment 1	172,99	0,0000
Pier 1	921,48	0,0211
Pier 2	1021,47	0,0425
Pier 3	921,25	0,0640
Abutment 2	172,55	0,0851

Table 4-15: Values of base shear and displacements of the deck considering the combination of the response spectrum for ground type C with the displacements of set A.

	Base shear (kN)	Displacements of the deck (m)
Abutment 1	108,08	0,0000
Pier 1	944,39	0,0051
Pier 2	1059,66	0,0051
Pier 3	944,39	0,0051
Abutment 2	108,08	0,0000

Table 4-16: Values of base shear and displacements of the deck considering the combination of the response spectrum for ground type C with the displacements of set B.

By observing the tables, particularly ground type A, it is possible to conclude that the combination used by the displacements of set A clearly causes major displacements of the deck.

However, in what concerns the base shear undergone by piers, the most adverse situation is the one which comprises the behavior of the displacements of set B.

The results seem quite logic, as described before in 4.1, since the displacements of set A are higher than the displacements of set B and they all occur in the same direction. It is logic, therefore, that the results show higher displacements with the values of set A. On the other hand, when the values of set B are employed, the results concerning displacements of the deck are not as high since they have alternate directions, though there is a major overload of those same values related to base shear. This appends for both ground types.

It is important to remark that the values concerning both the base shear and the displacements of the deck, as occurred before during the synchronous analysis, are higher for ground type C than for ground type A.

4.4.2 Shear forces and bending moments

During the asynchronous analysis, the action of the combination of the response spectrum with the displacements of set B (where higher shear forces were attained) results in the diagrams of shear force and bending moment displayed below, whether it concerns a ground type A or a ground type C.

Ground type A

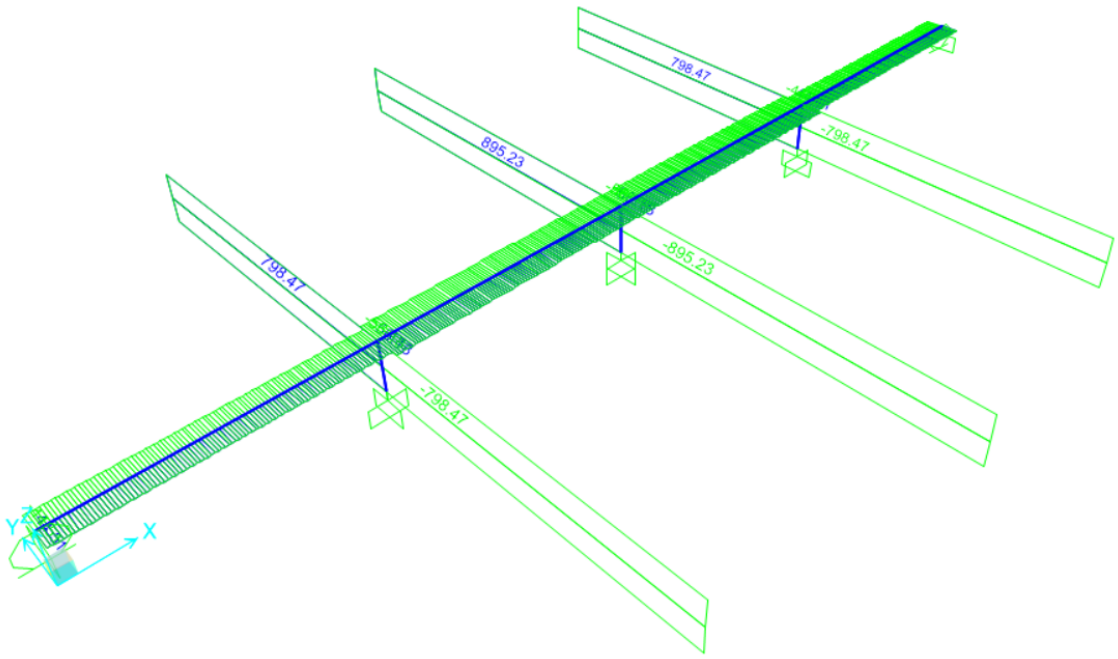

Figure 4-20: Diagrams of shear forces on Bridge 1, caused by the combination of the response spectrum for ground type A with the displacements of set B.

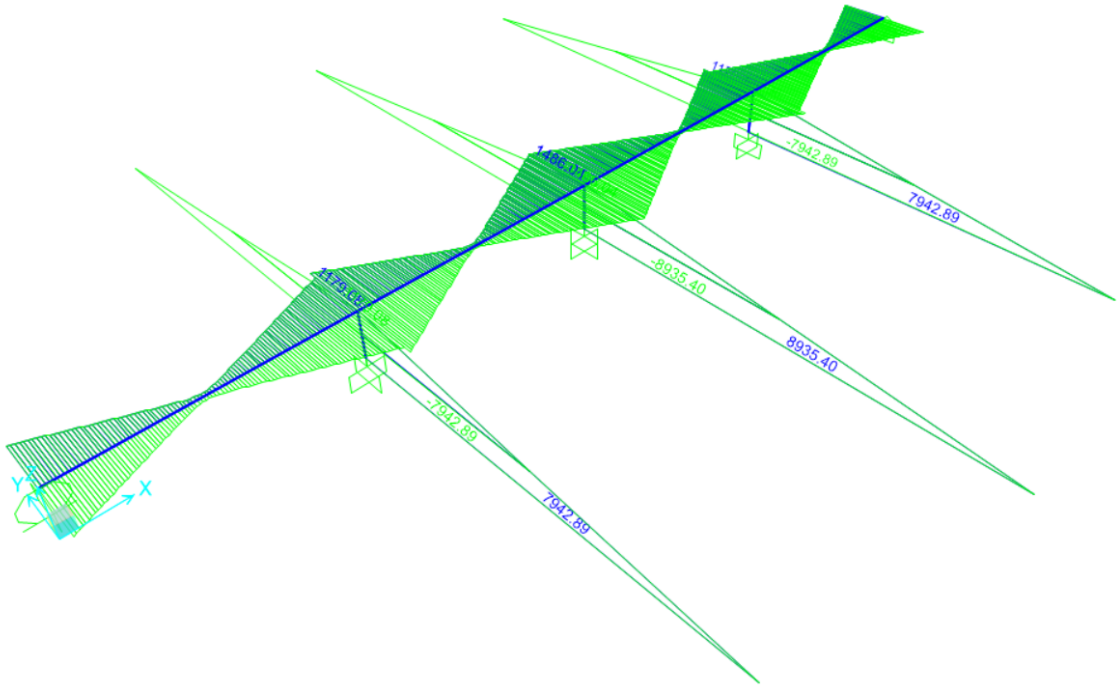

Figure 4-21: Diagrams of bending moments on Bridge 1, caused by the combination of the response spectrum for ground type A with the displacements of set B.

Piers	V (kN)	M (kN.m)
Top of pier 1	798,47	45,11
Base of pier 1	798,47	7942,89
Top of pier 2	895,23	34,48
Base of pier 2	895,23	8935,40
Top of pier 3	798,47	45,11
Base of pier 3	798,47	7942,89

Table 4-17: Values of shear forces and bending moments of the piers of Bridge 1, caused by the combination of the response spectrum for ground type A with the displacements of set B.

Deck	V (kN)	M (kN.m)
Abutment 1	44,51	1052,17
Pier 1, left	44,51	1179,08
Pier 1, right	56,18	1325,84
Pier 2, left	56,18	1486,04
Pier 2, right	56,18	1486,04
Pier 3, left	56,18	1325,84
Pier 3, right	44,51	1179,08
Abutment 2	44,51	1052,17

Table 4-18: Values of shear forces and bending moments of the deck of Bridge 1, caused by the combination of the response spectrum for ground type A with the displacements of set B.

Ground type C

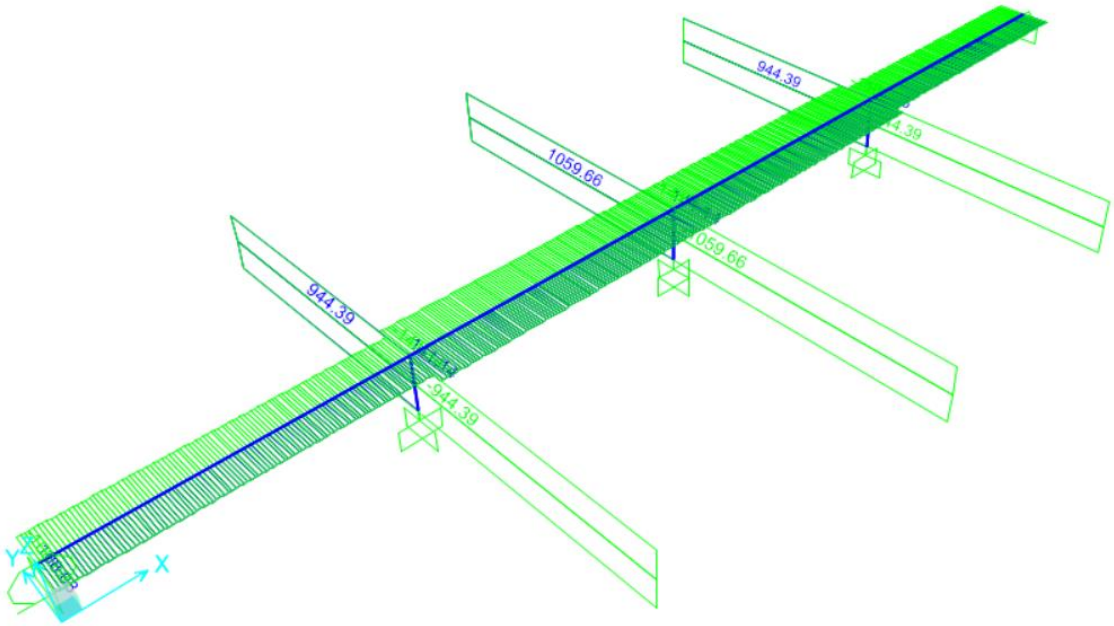

Figure 4-22: Diagrams of shear forces on Bridge 1, caused by the combination of the response spectrum for ground type C with the displacements of set B.

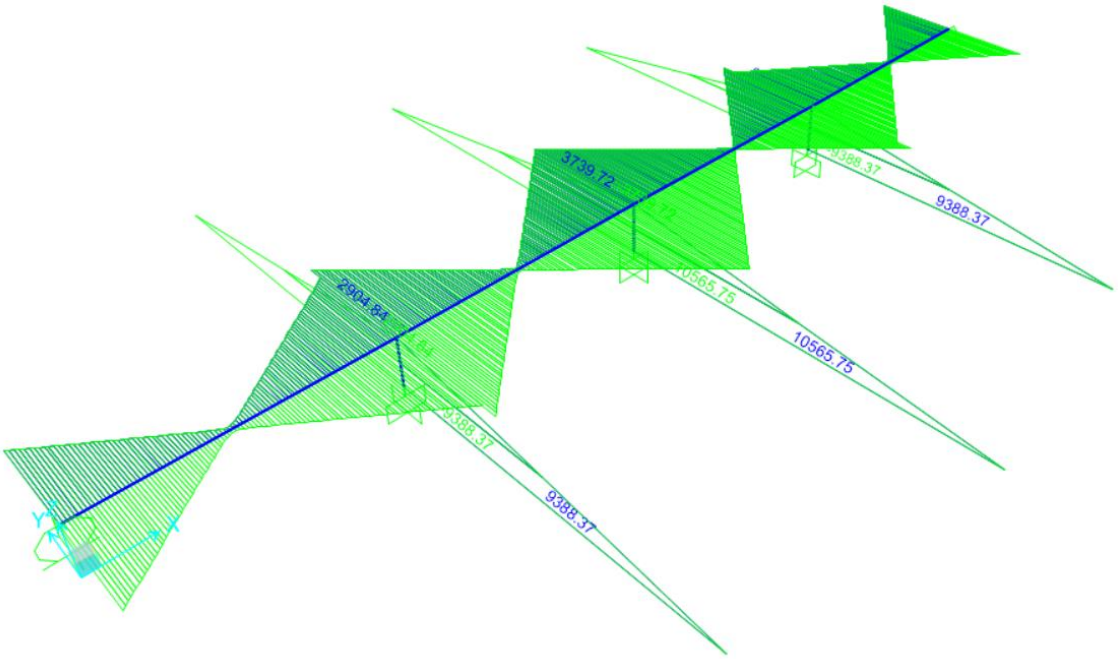

Figure 4-23: Diagrams of bending moments on Bridge 1, caused by the combination of the response spectrum for ground type C with the displacements of set B.

Piers	V (kN)	M (kN.m)
Top of pier 1	944,39	64,08
Base of pier 1	944,39	9388,37
Top of pier 2	1059,66	64,75
Base of pier 2	1059,66	10565,75
Top of pier 3	944,39	64,08
Base of pier 3	944,39	9388,37

Table 4-19: Values of shear forces and bending moments of the piers of Bridge 1, caused by the combination of the response spectrum for ground type C with the displacements of set B.

Deck	V (kN)	M (kN.m)
Abutment 1	108,08	2502,60
Pier 1, left	108,08	2904,84
Pier 1, right	141,15	3319,05
Pier 2, left	141,15	3739,72
Pier 2, right	141,15	3739,72
Pier 3, left	141,15	3319,05
Pier 3, right	108,08	2904,84
Abutment 2	108,08	2502,60

Table 4-20: Values of shear forces and bending moments of the deck of Bridge 1, caused by the combination of the response spectrum for ground type C with the displacements of set B.

The tables above show that the values of efforts for ground type A are weaker than the values for ground type C. This difference is particularly obvious when it refers to the moments of the deck.

In this asynchronous analysis the efforts on the deck are quite significant, especially in what concerns ground type C, a clear contrast to what happened in the synchronous analysis. It is on the main pier the higher efforts are concentrated.

4.4.3 Drifts of the piers

By using the same method of calculation as in the synchronous analysis, the results for the drift of the piers came to be the displayed below.

	High (m)	δ_d (m)	δ_f (m)	q	θ (rad)
Pier 1	10,00	0,0082	0,0082	1,00	**$8{,}00\times10^{-7}$**
Pier 2	10,00	0,0165	0,0164	1,00	**$5{,}60\times10^{-6}$**
Pier 3	10,00	0,0248	0,0247	1,00	**$1{,}04\times10^{-5}$**

Table 4-21: Drift of the piers due to the application of the combination of the response spectrum for ground type A with the displacements of set A.

	High (m)	δ_d (m)	δ_f (m)	q	θ (rad)
Pier 1	10,00	0,0211	0,0213	1,00	**$1{,}59 \times 10^{-5}$**
Pier 2	10,00	0,0425	0,0425	1,00	**$2{,}90 \times 10^{-6}$**
Pier 3	10,00	0,0640	0,0638	1,00	**$2{,}15 \times 10^{-5}$**

Table 4-22: Drift of the piers due to the application of the combination of the response spectrum for ground type C with the displacements of set A.

The values attained for the drift of piers are quite low. They are lower than the values attained with the synchronous analysis as what is really being considered is a displacement of the foundation, the input of deformations to the piers is not that higher as in the previous situation.

The main pier is the one enduring the major drift in both ground types.

4.5 Comparison of both analysis

The results of the comparison between both analysis carried out in this bridge is displayed in the graphics below, where it is possible to observe the values attained for each parameter measured in both ground types and for both analysis.

Figure 4-24 shows that the displacements attained from the synchronous analysis are much weaker than the values attained from the asynchronous analysis. The reason for this to happen is that in the synchronous analysis there are no enforced displacements resulting from the seismic action, whereas in the asynchronous analysis, the displacements inflicted on the deck are higher precisely because of those displacements resulting from the seismic action.

Attention should be drawn to the fact that the influence of the ground type is much more relevant when the asynchronous analysis is being performed, rather than the synchronous analysis, having ground C as the ground type attaining the highest values.

The conclusion is, therefore, that in what concerns displacements of the deck in Bridge 1, it becomes more critical when the asynchronous analysis for ground type C is being carried out.

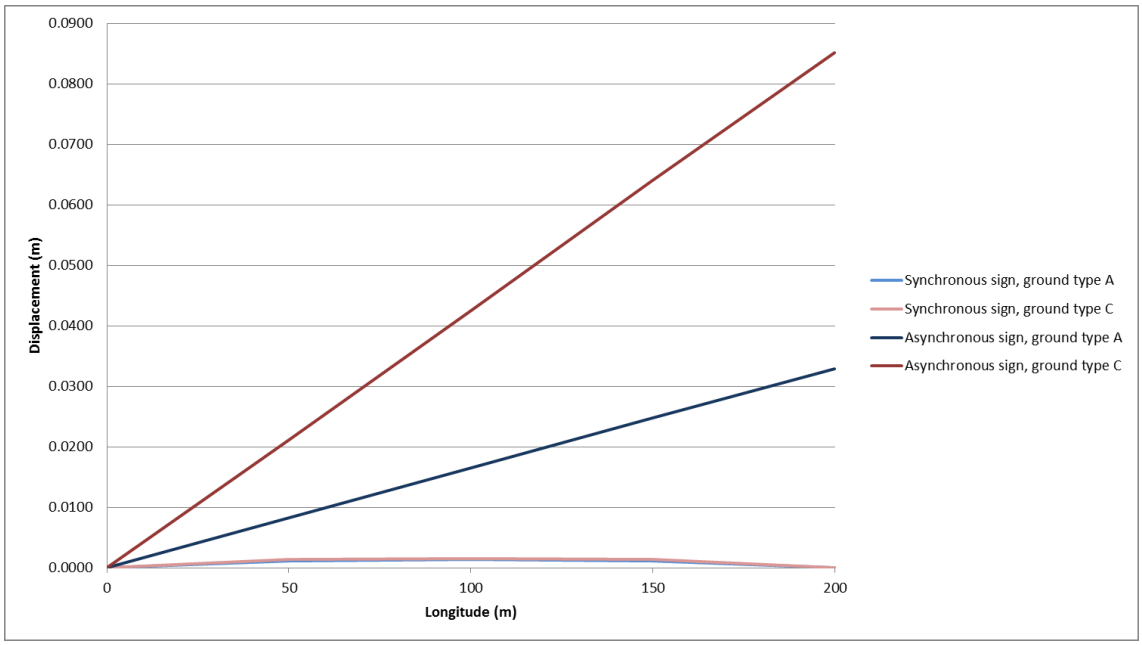

Figure 4-24: Displacements of the deck of Bridge 1.

As for the shear force and bending moment undergone by each pier, as shown in *Figures 4-25* and *4-26*, the gap between the attained values in the synchronous and asynchronous analysis is quite lower than what happens with displacements. Hence, it is through an asynchronous analysis that the higher values are attained. However, it is important to state that for the same ground type, the difference between the values attained from each analysis is irrelevant, especially in the asynchronous analysis, whereas the difference between dealing with a ground type A or a ground type C is much more significant than the difference between adopting a synchronous or an asynchronous analysis.

Whether it is about a shear force or a bending moment of the piers, the main pier is clearly the one which strives the most, followed by the sideward piers.

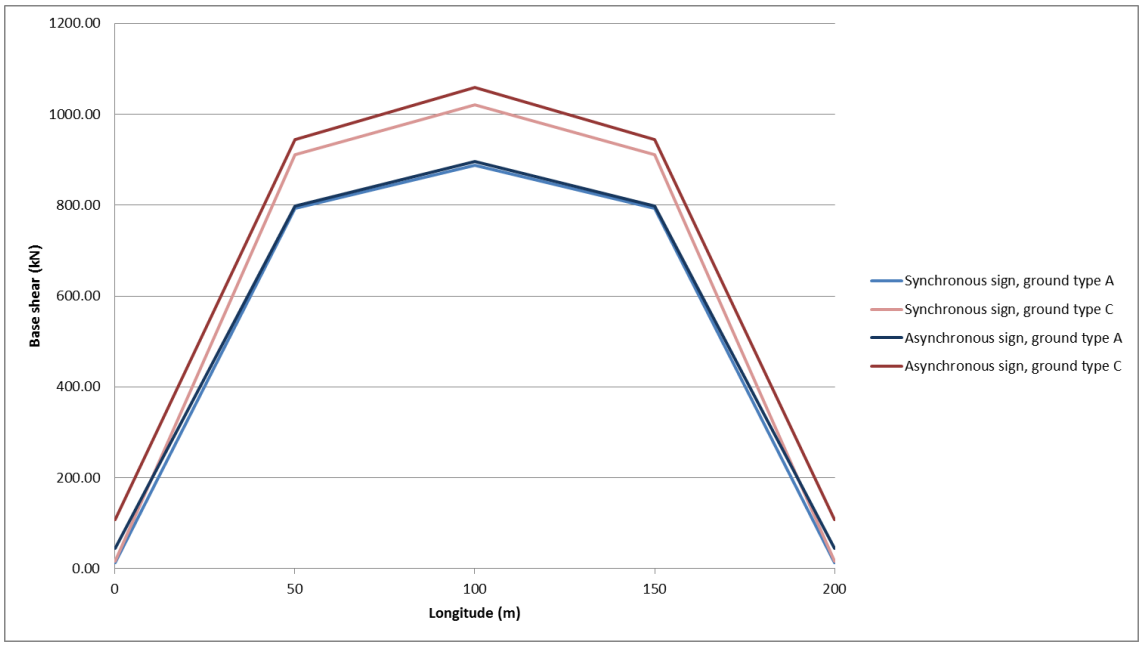

Figure 4-25: Base shear of Bridge 1.

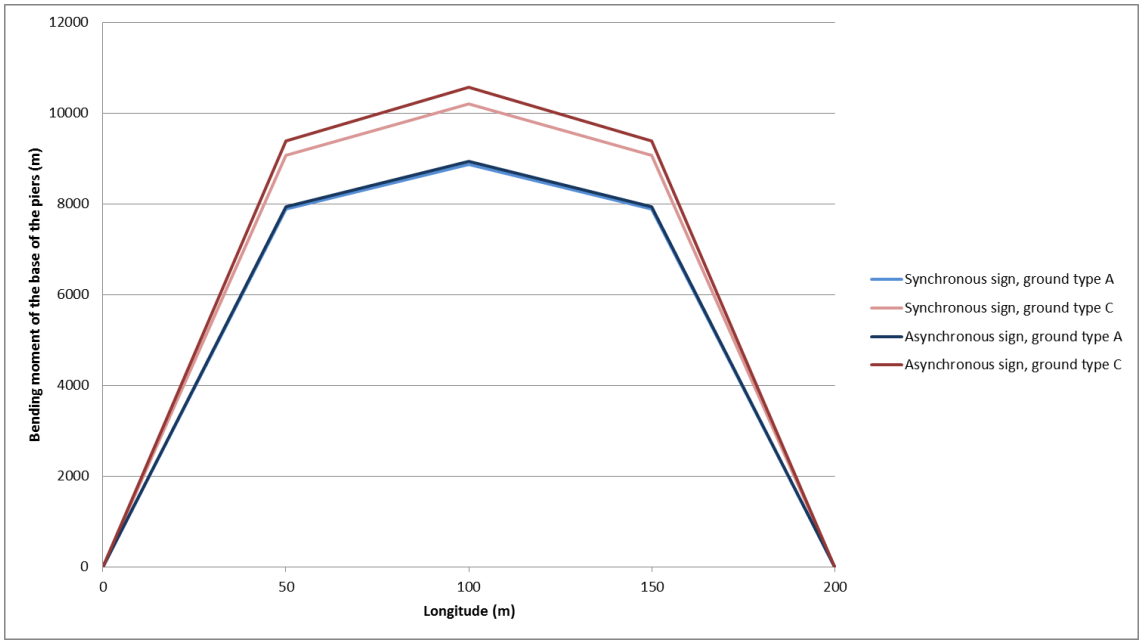

Figure 4-26: Bending moments of the base of the piers of Bridge 1.

In what concerns the bending moment of the deck, as it can be observed in *Figure 4-27*, it reaches the highest value during the asynchronous analysis for ground C, on pier 2.

There is a great difference between the synchronous and the asynchronous analysis, with the last one having more disadvantages over the first. As for considering a ground type A or C, in the synchronous analysis the difference is hardly none, whereas in the asynchronous analysis it really matters (about 2300 kN in pier 2).

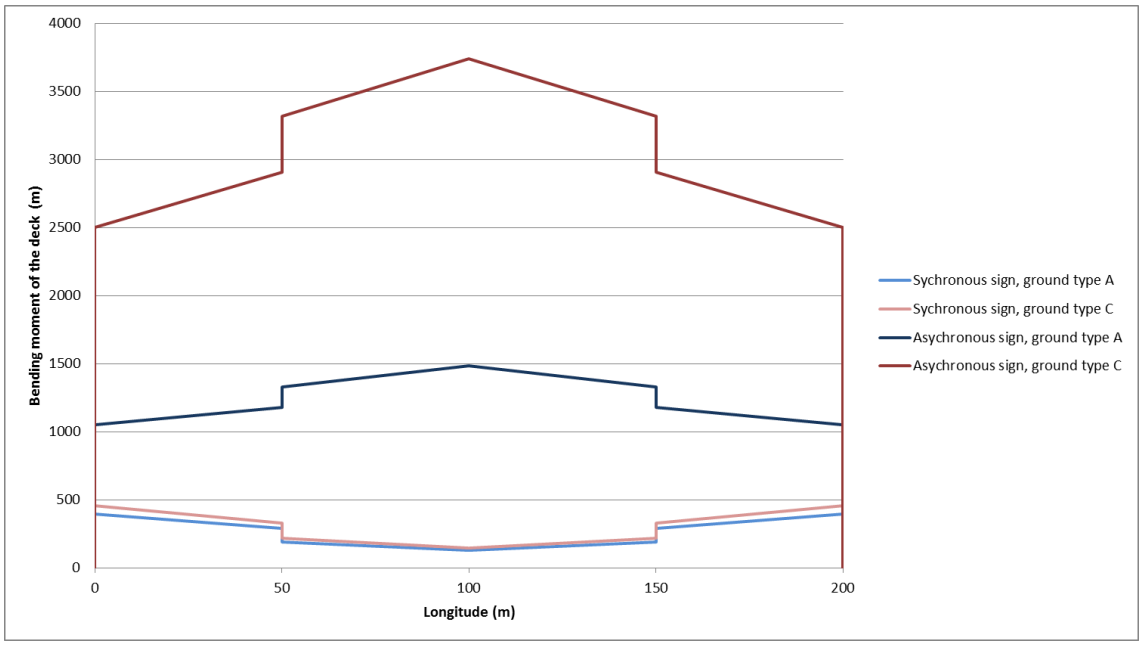

Figure 4-27: Bending moments of the deck of Bridge 1.

5. Effect of the topographic variation

5.1 Long bridge crossing a valley

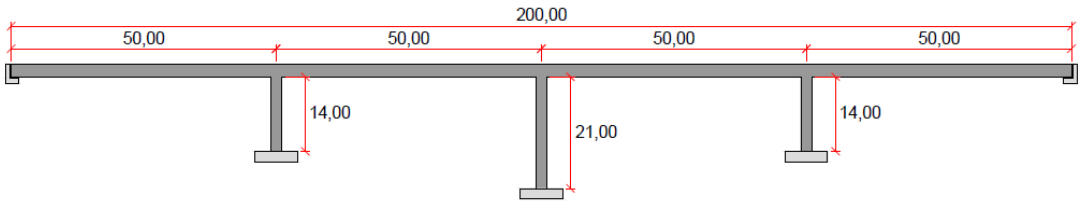

Figure 5-1: Bridge 2.

5.1.1 Displacements of the piers resulting from the seismic action

The calculation of the displacements of the piers resulting from the seismic action, determined according to Eurocode 8, is thoroughly explained in 4.1 of the current study. In what concerns Bridge 2, considering that the distance between spans equals the Bridge 1's, the results attained for these displacements are the same in both situations and exempt the repeated display of the values.

5.1.2 Modelling of Bridge 2

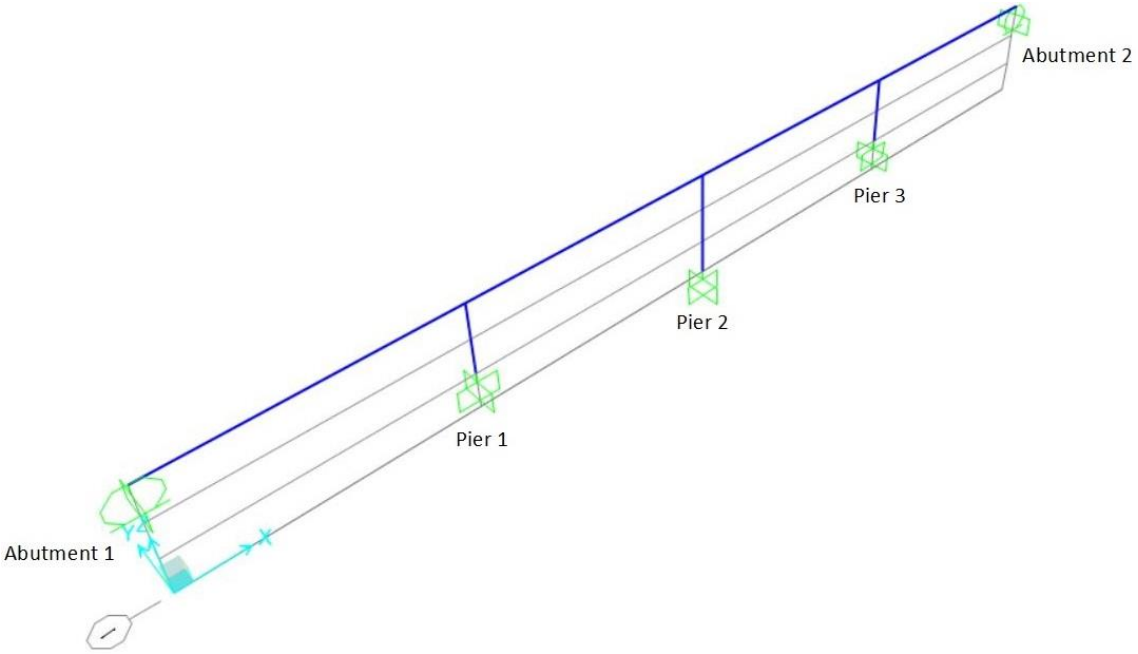

Figure 5-2: Modelling of Bridge 2 in SAP2000.

Having Bridge 2 model in SAP2000, as well as the actions of the response spectrum, of the sets A and B and theirs respective combinations for both ground types, the vibration and deformation modes for each of the considered loads were attained and displayed below.

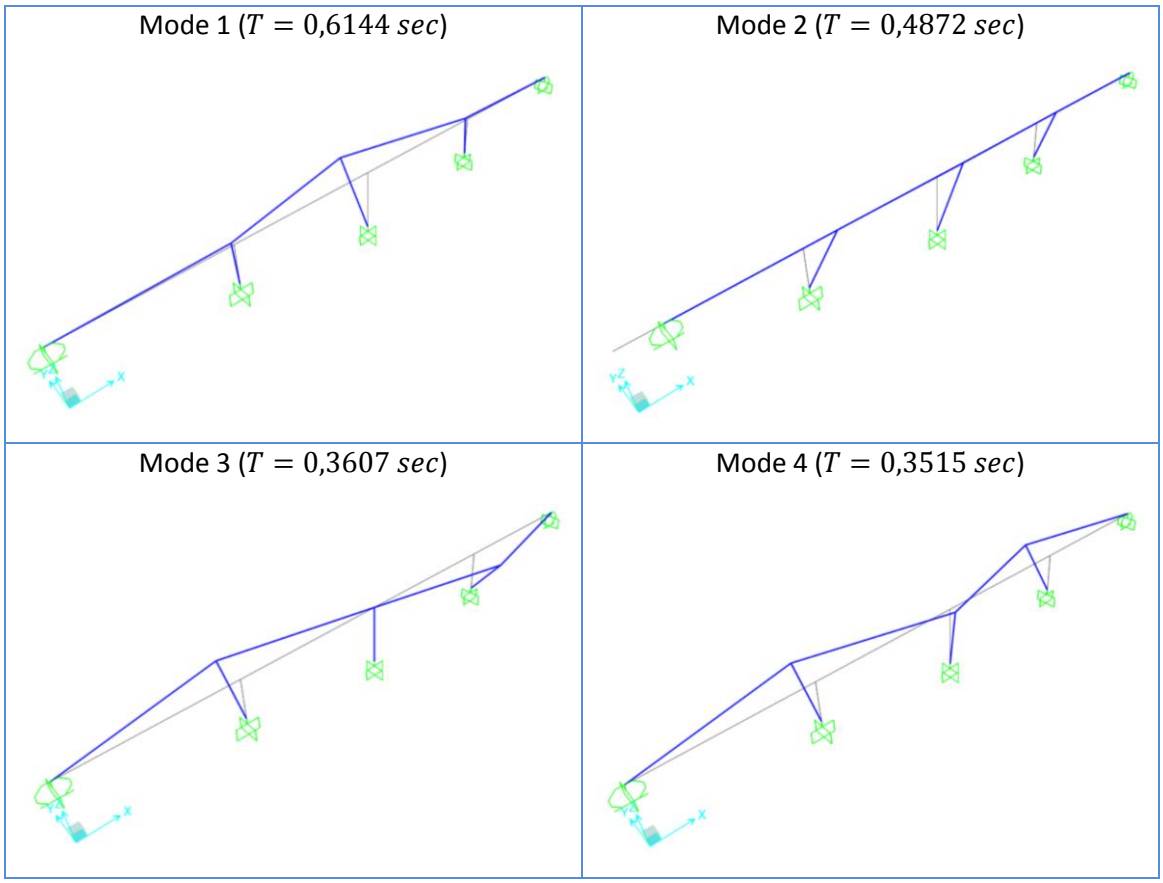

Figure 5-3: First four vibration modes of Bridge 2.

Ground type A

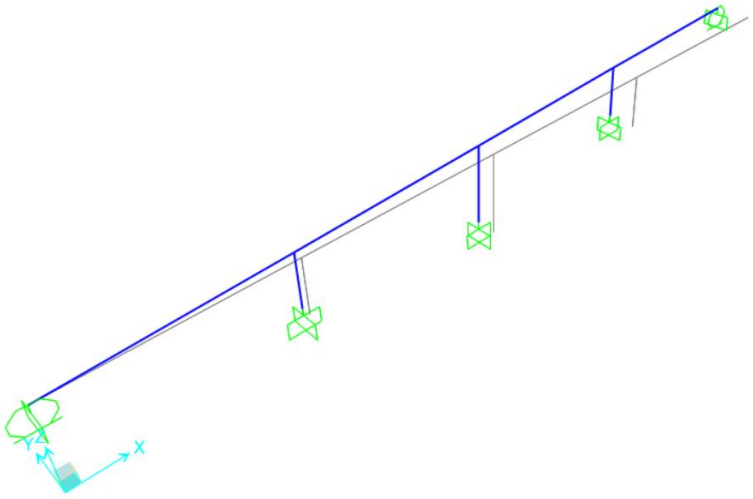

Figure 5-4: Deformation of Bridge 2 caused by the displacements of set A for ground type A.

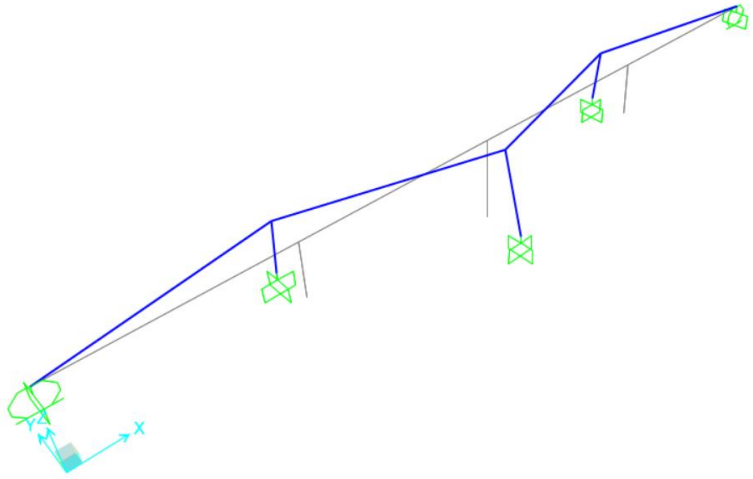

Figure 5-5: Deformation of Bridge 2 caused by the displacements of set B for ground type A.

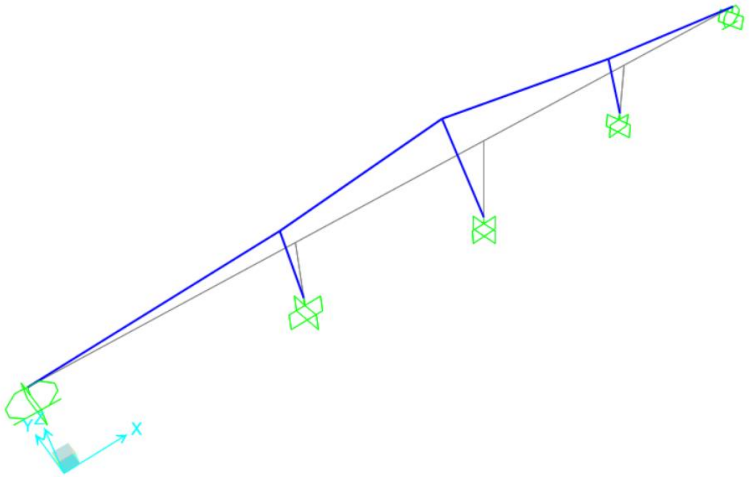

Figure 5-6: Deformation of Bridge 2 caused by the response spectrum for ground type A.

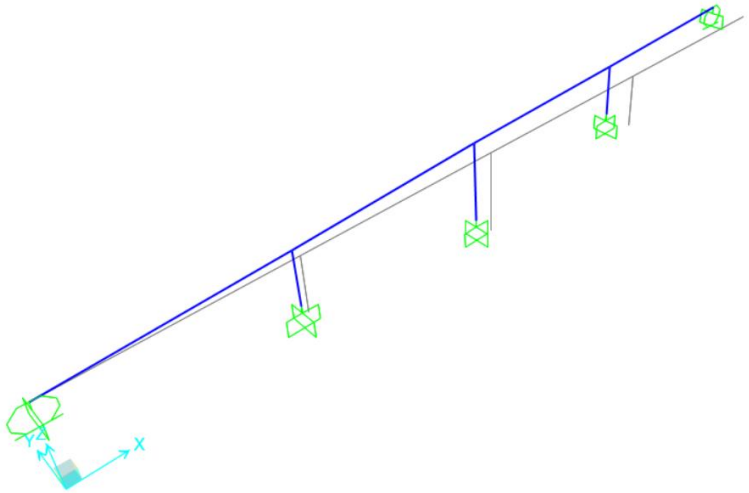

Figure 5-7: Deformation of Bridge 2 caused by the combination of the actions of the response spectrum and the displacements of set A for ground type A.

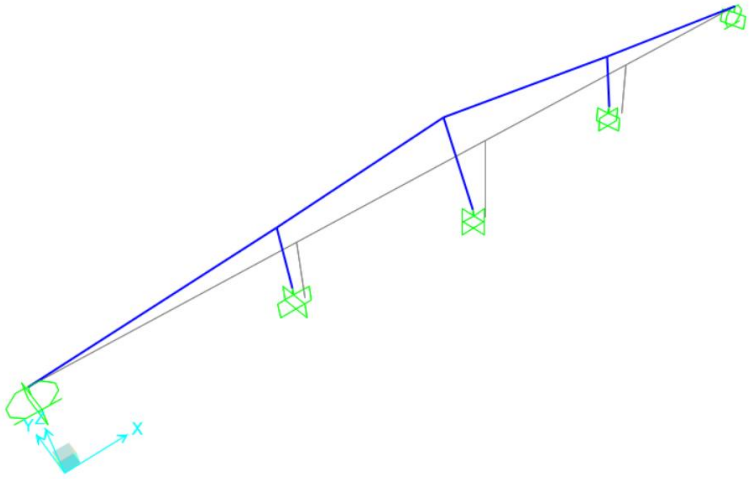

Figure 5-8: Deformation of Bridge 2 caused by the combination of the actions of the response spectrum and the displacements of set B for ground type A.

Ground type C

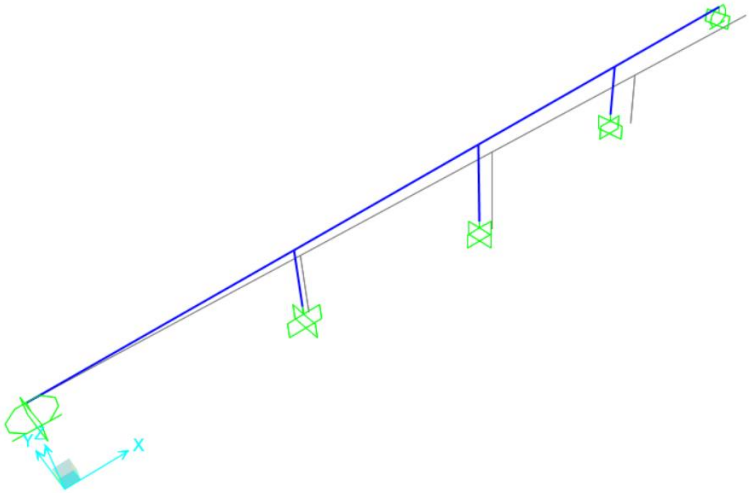

Figure 5-9: Deformation of Bridge 2 caused by the displacements of set A for ground type C.

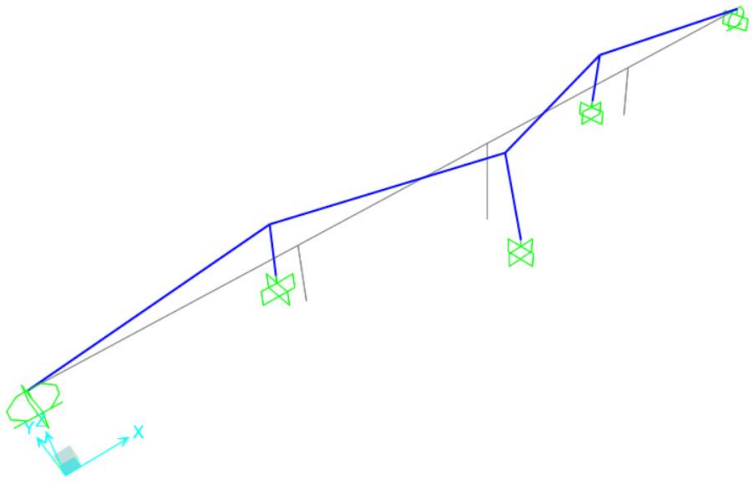

Figure 5-10: Deformation of Bridge 2 caused by the displacements of set B for ground type C.

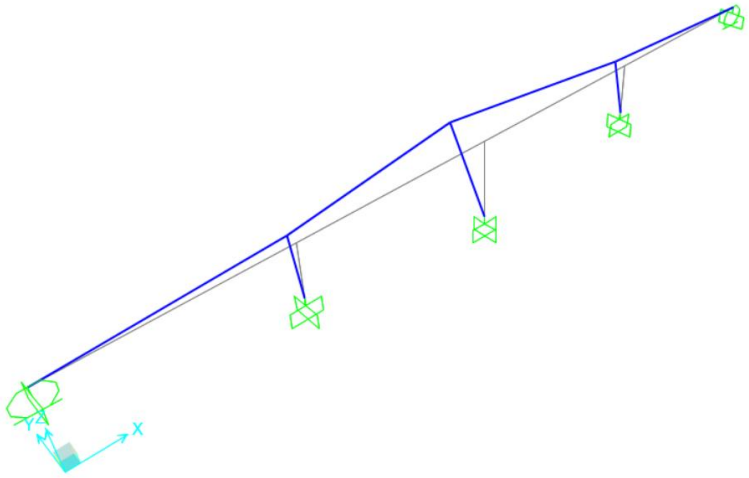

Figure 5-11: Deformation of Bridge 2 caused by the response spectrum for ground type C.

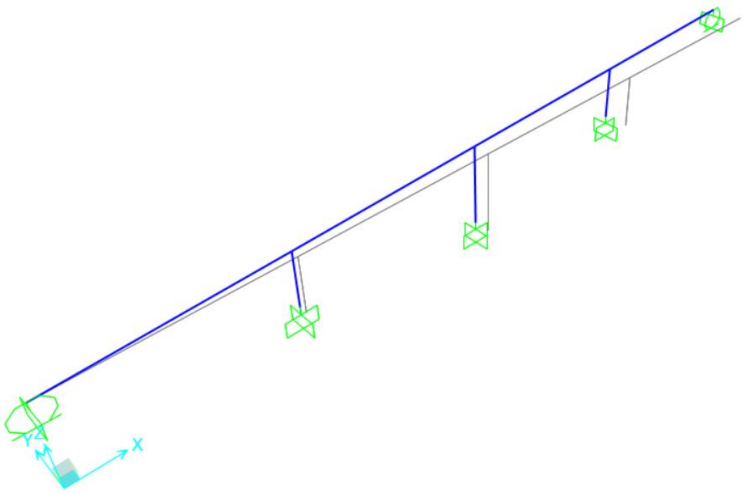

Figure 5-12: Deformation of Bridge 2 caused by the combination of the actions of the response spectrum and the displacements of set A for ground type C.

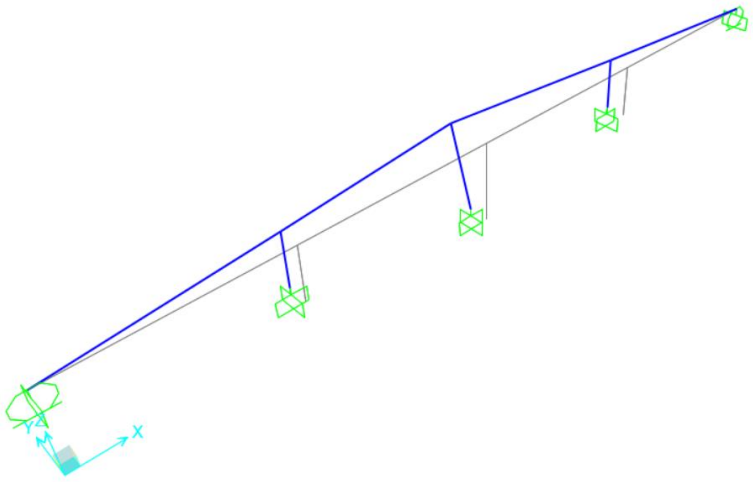

Figure 5-13: Deformation of Bridge 2 caused by the combination of the actions of the response spectrum and the displacements of set B for ground type C.

5.1.3 Synchronous analysis

The synchronous analysis is represented in *Figures 5-6* and *5-11* previously presented, whether it is a ground type A or a ground type C.

5.1.3.1 Base shears and displacements of the deck

The results attained from the structure's analysis in SAP2000, in what concerns base shears and displacements of the deck for each of the ground types, are displayed in the table below.

	Base shear (kN)	Displacements of the deck (m)
Abutment 1	50,33	0,0000
Pier 1	691,62	0,0026
Pier 2	563,49	0,0068
Pier 3	691,62	0,0026
Abutment 2	50,33	0,0000

Table 5-1: Values of base shear and displacements of the deck considering the single action of the response spectrum for ground type A.

	Base shear (kN)	Displacements of the deck (m)
Abutment 1	64,84	0,0000
Pier 1	819,29	0,0031
Pier 2	937,69	0,0113
Pier 3	819,29	0,0031
Abutment 2	64,84	0,0000

Table 5-2: Values of base shear and displacements of the deck considering the single action of the response spectrum for ground type C.

The values in the tables above lead to the conclusion that, whether for ground type A or ground type C, the displacement of the deck on the main pier is much more extensive than the same displacement on outward piers, as the main pier is 7 m longer than the others, which makes it more flexible. In this case, the difference between considering a ground type A or C is not that significant.

In what concerns base shears, it is possible to observe that ground type C gathers the highest values. Considering the values of base shears on piers 1 and 3, it also becomes clear that when it refers to ground type A the base shear of pier 2 decreases, whereas when it comes to ground type C, it increases.

5.1.3.2 Shear forces and bending moments

The efforts attained by the synchronous analysis of Bridge 2 and the related diagrams are all included in the table below.

Ground type A

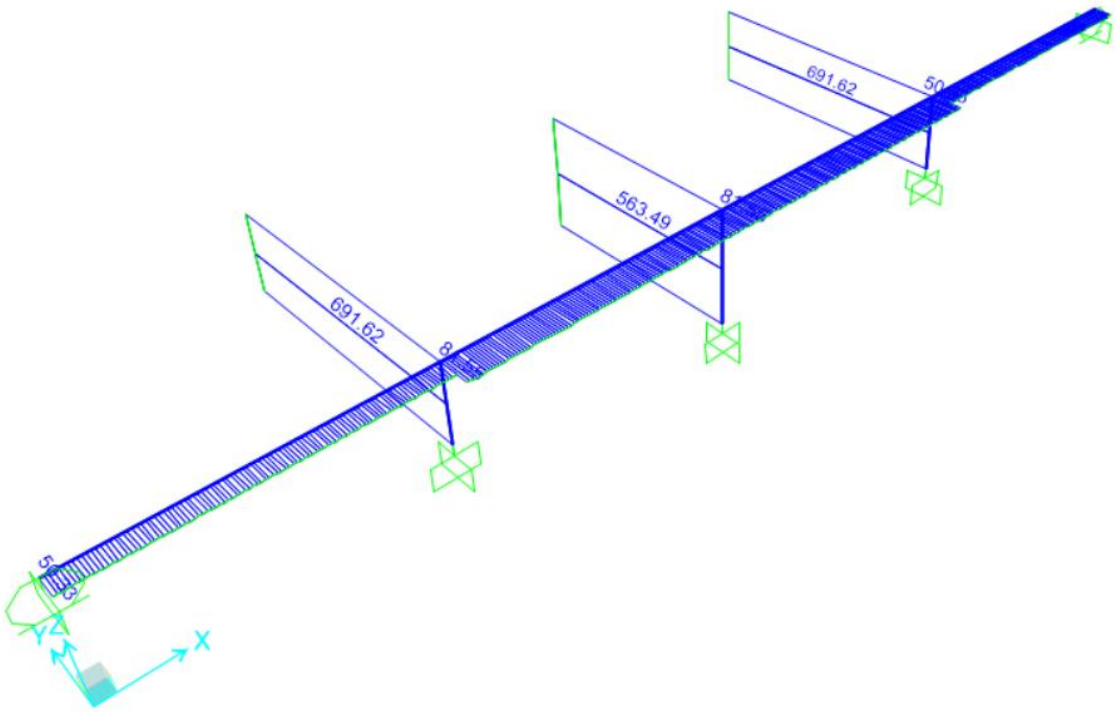

Figure 5-14: Diagrams of shear forces on Bridge 2, caused by the single action of the response spectrum for ground type A.

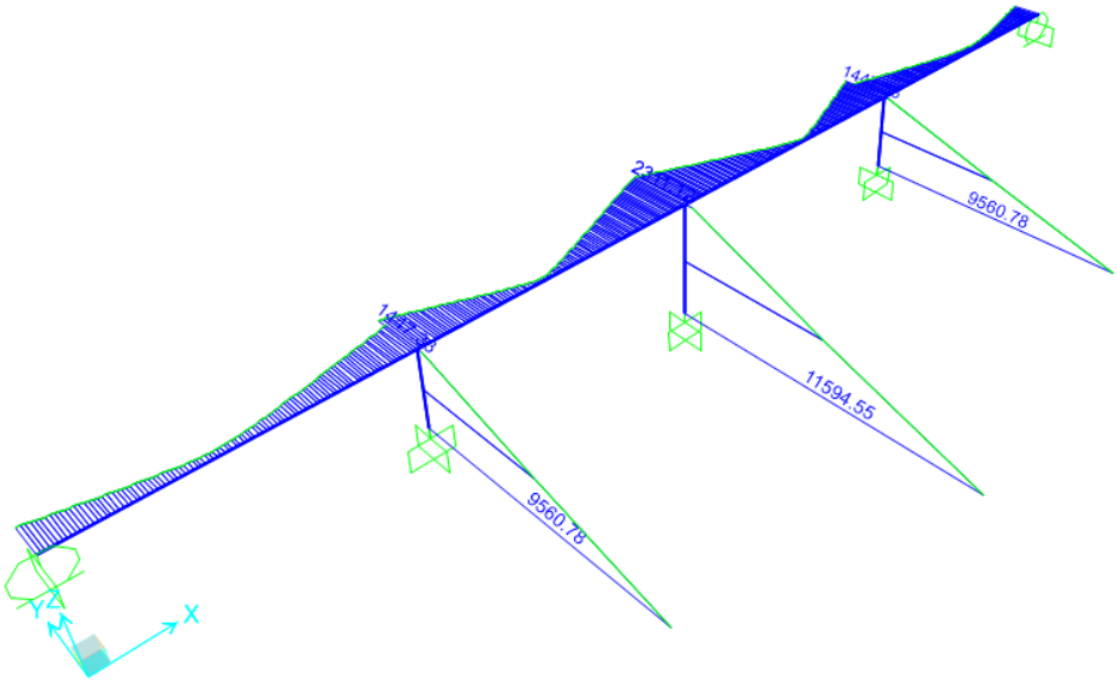

Figure 5-15: Diagrams of bending moments on Bridge 2, caused by the single action of the response spectrum for ground type A.

Piers	V (kN)	M (kN.m)
Top of pier 1	691,62	177,29
Base of pier 1	691,62	9560,78
Top of pier 2	563,49	277,17
Base of pier 2	563,49	11594,55
Top of pier 3	691,62	177,29
Base of pier 3	691,62	9560,78

Table 5-3: Values of shear forces and bending moments of the piers in Bridge 2, caused by the single action of the response spectrum for ground type A.

Deck	V (kN)	M (kN.m)
Abutment 1	50,33	1126,14
Pier 1, left	50,33	1447,33
Pier 1, right	81,55	1780,00
Pier 2, left	81,55	2311,12
Pier 2, right	81,55	2311,12
Pier 3, left	81,55	1780,00
Pier 3, right	50,33	1447,33
Abutment 2	50,33	1126,14

Table 5-4: Values of shear forces and bending moments of the deck in Bridge 2, caused by the single action of the response spectrum for ground type A.

Ground type C

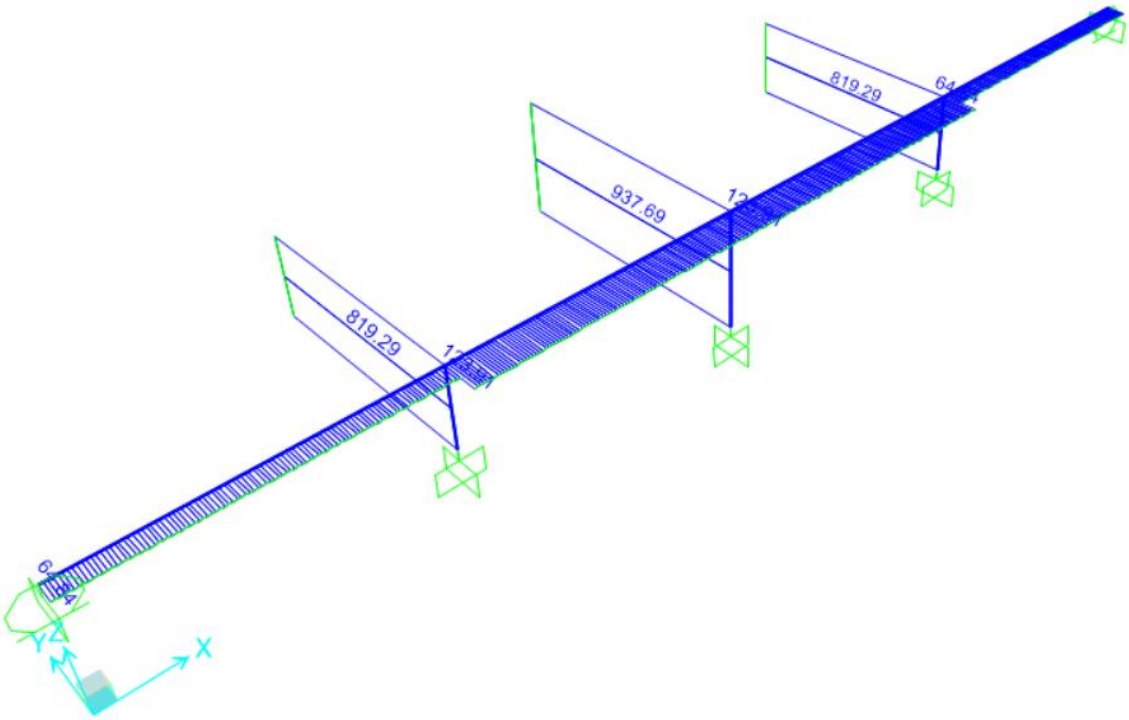

Figure 5-16: Diagrams of shear forces on Bridge 2, caused by the single action of the response spectrum for ground type C.

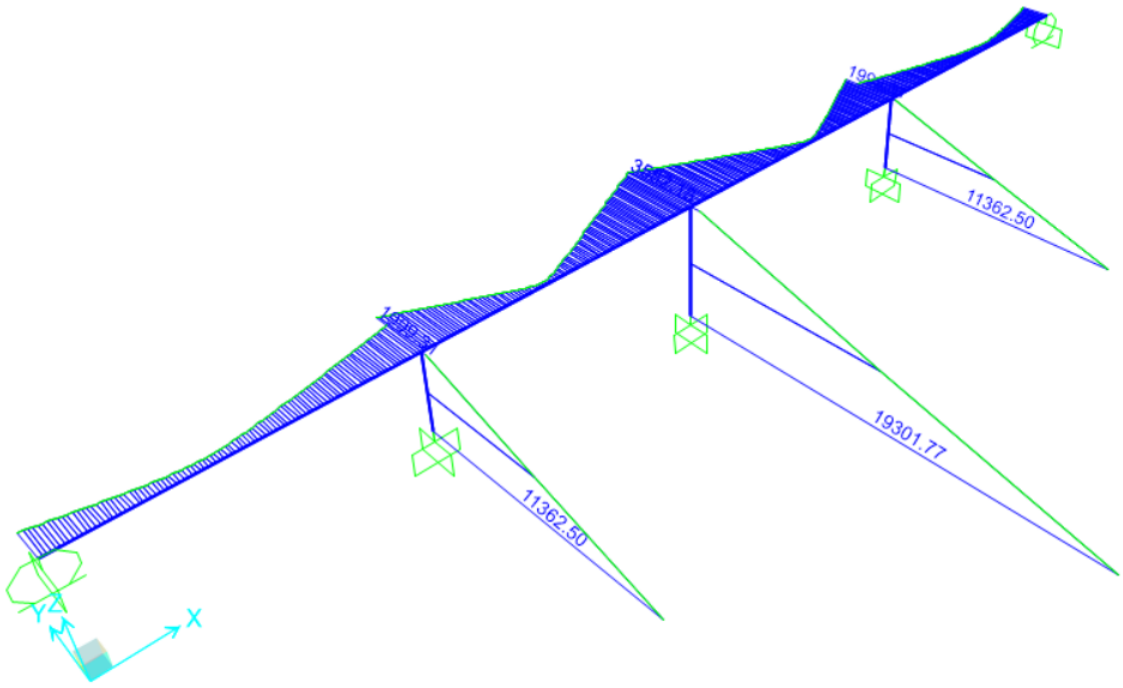

Figure 5-17: Diagrams of bending moments on Bridge 2, caused by the single action of the response spectrum for ground type C.

Piers	V (kN)	M (kN.m)
Top of pier 1	819,29	234,00
Base of pier 1	819,29	11362,50
Top of pier 2	937,69	422,16
Base of pier 2	937,69	19301,77
Top of pier 3	819,29	234,00
Base of pier 3	819,29	11362,50

Table 5-5: Values of shear forces and bending moments of the piers in Bridge 2, caused by the single action of the response spectrum for ground type C.

Deck	V (kN)	M (kN.m)
Abutment 1	64,84	1342,38
Pier 1, left	64,84	1999,31
Pier 1, right	123,91	2627,67
Pier 2, left	123,91	3582,18
Pier 2, right	123,91	3582,18
Pier 3, left	123,91	2627,67
Pier 3, right	64,84	1999,31
Abutment 2	64,84	1342,38

Table 5-6: Values of shear forces and bending moments of the deck in Bridge 2, caused by the single action of the response spectrum for ground type C.

It is possible to conclude from the table that the piers have a constant diagram of shear force and of the same value as the base shear.

During the bending moment on the piers, ground type C clearly shows higher results, with the difference between ground type A and C being particularly obvious on pier 2 (around 7700 kN). In what concerns bending moments on the deck, though these are considerable, they are less significant than the moments on piers. Once again, the highest results come also from ground type C.

5.1.3.3 Drifts of the piers

The drifts attained for each of the piers of Bridge 2 were calculated according to the method previously described in 4.3.3. For the synchronous analysis the attained results are displayed below.

	High (m)	δ_d (m)	δ_f (m)	q	θ (rad)
Pier 1	14,00	0,0026	0,0000	1,00	**1,86x10^{-4}**
Pier 2	21,00	0,0068	0,0000	1,00	**3,23x10^{-4}**
Pier 3	14,00	0,0026	0,0000	1,00	**1,86x10^{-4}**

Table 5-7: Drift of the piers due to the application of the response spectrum for ground type A.

	High (m)	δ_d (m)	δ_f (m)	q	θ (rad)
Pier 1	14,00	0,0031	0,0000	1,00	**2,22x10^{-4}**
Pier 2	21,00	0,0113	0,0000	1,00	**5,37x10^{-4}**
Pier 3	14,00	0,0031	0,0000	1,00	**2,22x10^{-4}**

Table 5-8: Drift of the piers due to the application of the response spectrum for ground type C.

From the analysis of the tables above, the conclusion points to a low drift on piers. The main pier endures the highest drift because it is the tallest and it has the same section as the others.

Similar to the previous situations, ground type C concentrates the highest values of drift.

5.1.4 Asynchronous analysis

The asynchronous analysis is previously represented in *Figures 5-7*, *5-8*, *5-12* and *5-13*, whether it concerns a ground type A or a ground type C.

5.1.4.1 Base shears and displacements of the deck

During the asynchronous analysis, the values of base shear and the displacements of the deck, attained from SAP2000 for each of the considered grounds are displayed below.

Ground type A

	Base shear (kN)	Displacements of the deck (m)
Abutment 1	79,08	0,0000
Pier 1	693,81	0,0084
Pier 2	563,49	0,0178
Pier 3	693,71	0,0250
Abutment 2	78,81	0,0329

Table 5-9: Values of base shear and displacements of the deck considering the combination of the response spectrum for ground type A with the displacements of set A.

	Base shear (kN)	Displacements of the deck (m)
Abutment 1	61,93	0,0000
Pier 1	696,13	0,0032
Pier 2	570,00	0,0069
Pier 3	696,13	0,0032
Abutment 2	61,93	0,0000

Table 5-10: Values of base shear and displacements of the deck considering the combination of the response spectrum for ground type A with the displacements of set B.

Ground type C

	Base shear (kN)	Displacements of the deck (m)
Abutment 1	171,41	0,0000
Pier 1	831,69	0,0210
Pier 2	937,69	0,0440
Pier 3	831,48	0,0644
Abutment 2	171,09	0,0851

Table 5-11: Values of base shear and displacements of the deck considering the combination of the response spectrum for ground type C with the displacements of set A.

	Base shear (kN)	Displacements of the deck (m)
Abutment 1	111,79	0,0000
Pier 1	843,23	0,0055
Pier 2	962,44	0,0116
Pier 3	843,23	0,0055
Abutment 2	111,79	0,0000

Table 5-12: Values of base shear and displacements of the deck considering the combination of the response spectrum for ground type C with the displacements of set B.

Considering the results attained, it is possible to convey that in what concerns the displacements of the deck for both ground types, the values are higher when there is a combination of the response spectrum with the displacements of set A. As for the base shears, however, the most adverse combination is the one which involves displacements of set B because it is where the highest base shears on the piers can be attained.

If the combination of set A is the only one considered, in what concerns the displacement of the deck on both ground types, the element which suffers the highest displacement is abutment 2 because this combination comprises an increase of the displacement enforced to each element, with abutment 2 having the highest imposed displacement.

In what concerns the base shears, where the combination of set B is considered, they have a distribution much similar to the synchronous case, and it is in ground type C where the highest values are attained.

5.1.4.2 Shear forces and bending moments

The efforts attained for the asynchronous analysis of Bridge 2 and their related diagrams are represented below.

Ground type A

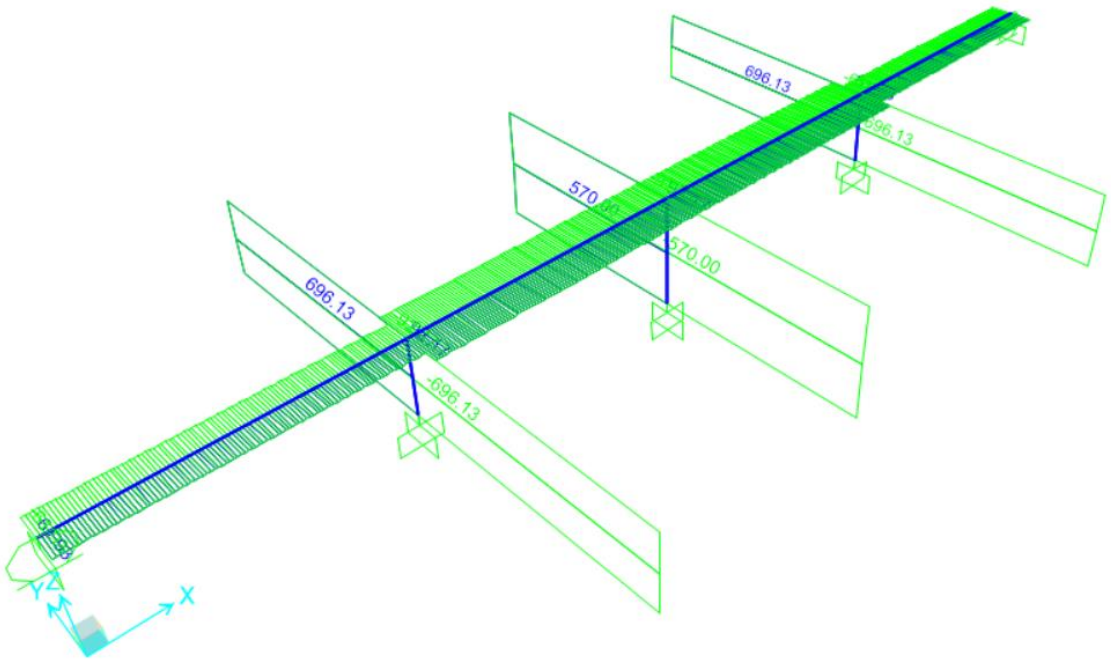

Figure 5-18: Diagrams of shear forces on Bridge 2, caused by the combination of the response spectrum for ground type A with the displacements of set B.

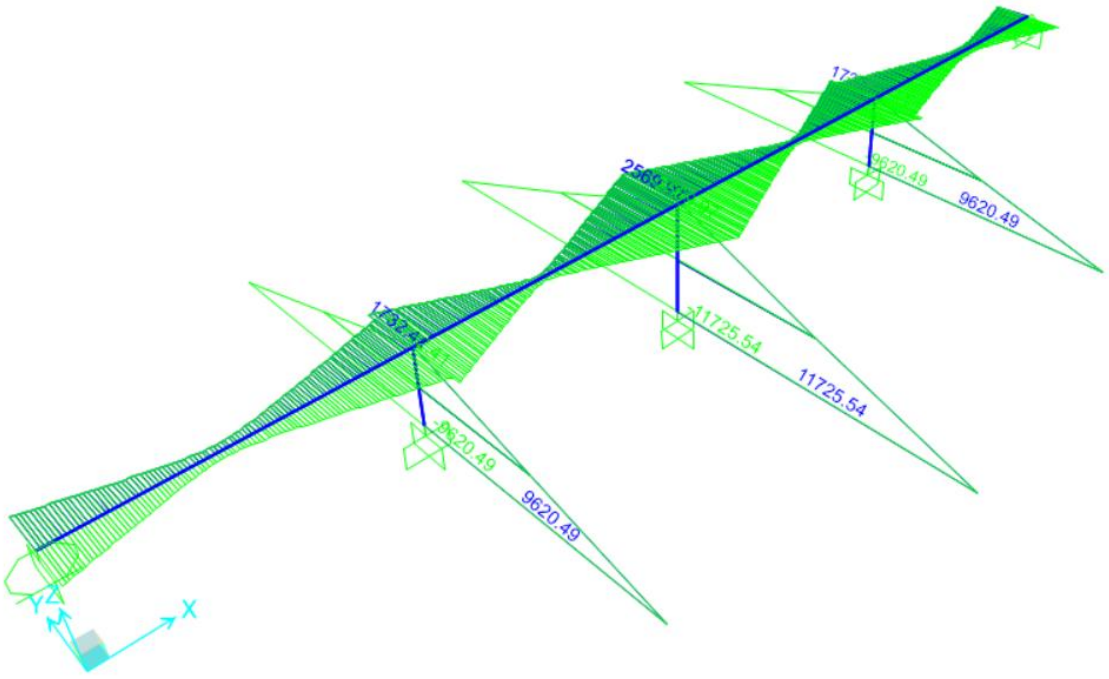

Figure 5-19: Diagrams of bending moments on Bridge 2, caused by the combination of the response spectrum for ground type A with the displacements of set B.

Piers	V (kN)	M (kN.m)
Top of pier 1	696,13	180,98
Base of pier 1	696,13	9620,49
Top of pier 2	570,00	282,84
Base of pier 2	570,00	11725,54
Top of pier 3	696,13	180,98
Base of pier 3	696,13	9620,49

Table 5-13: Values of shear forces and bending moments of the piers of Bridge 2, caused by the combination of the response spectrum for ground type A with the displacements of set B.

Deck	V (kN)	M (kN.m)
Abutment 1	61,30	1412,06
Pier 1, left	61,30	1732,41
Pier 1, right	92,18	2053,44
Pier 2, left	92,18	2569,97
Pier 2, right	92,18	2569,97
Pier 3, left	92,18	2053,44
Pier 3, right	61,30	1732,41
Abutment 2	61,30	1412,06

Table 5-14: Values of shear forces and bending moments of the deck of Bridge 2, caused by the combination of the response spectrum for ground type A with the displacements of set B.

Ground type C

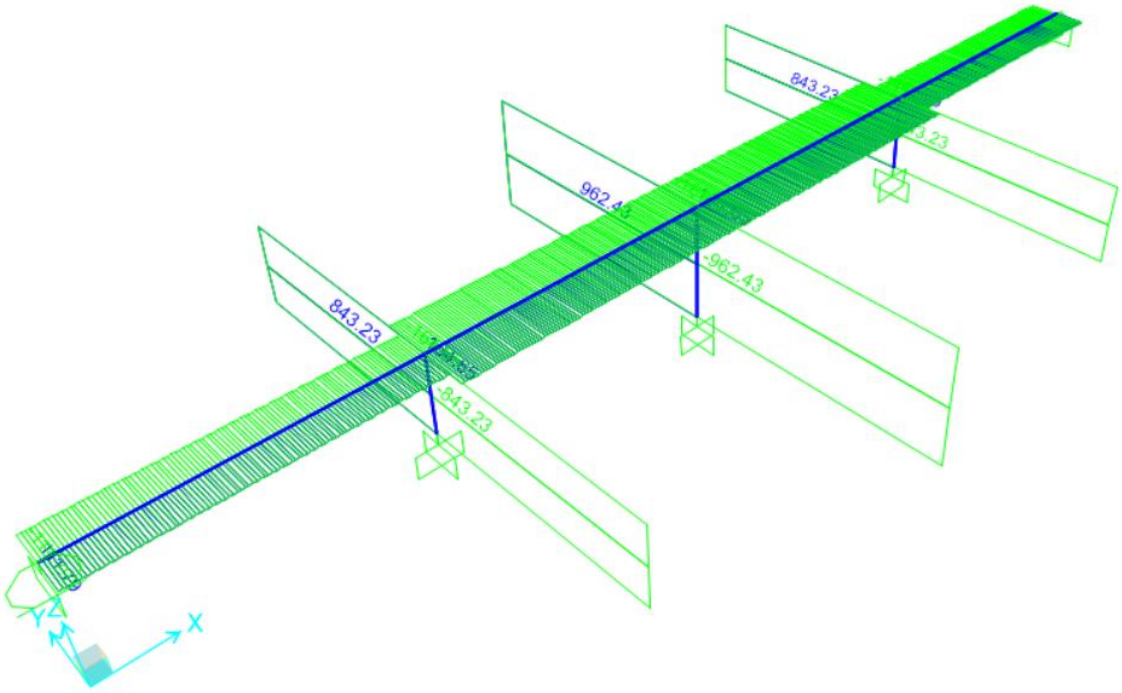

Figure 5-20: Diagrams of shear forces on Bridge 2, caused by the combination of the response spectrum for ground type C with the displacements of set B.

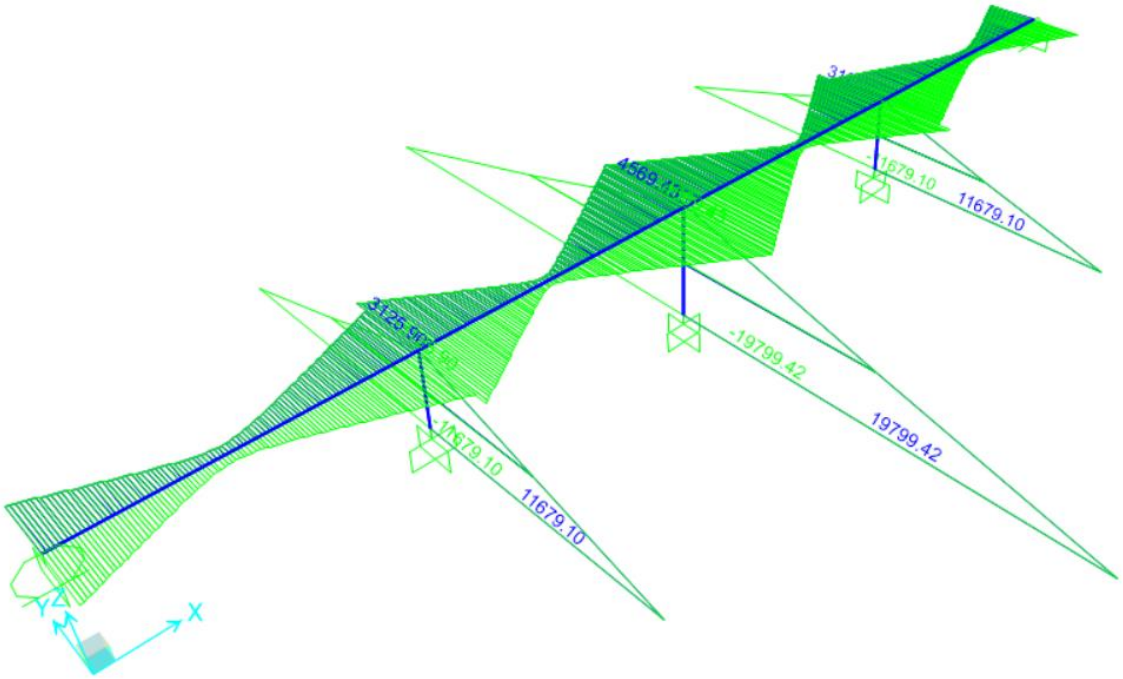

Figure 5-21: Diagrams of bending moments on Bridge 2, caused by the combination of the response spectrum for ground type C with the displacements of set B.

Piers	V (kN)	M (kN.m)
Top of pier 1	843,23	251,34
Base of pier 1	843,23	11679,10
Top of pier 2	962,44	445,49
Base of pier 2	962,44	19799,42
Top of pier 3	843,23	251,34
Base of pier 3	843,23	11679,10

Table 5-15: Values of shear forces and bending moments of the piers of Bridge 2, caused by the combination of the response spectrum for ground type C with the displacements of set B.

Deck	V (kN)	M (kN.m)
Abutment 1	111,79	2535,68
Pier 1, left	111,79	3125,90
Pier 1, right	164,65	3685,31
Pier 2, left	164,65	4569,43
Pier 2, right	164,65	4569,43
Pier 3, left	164,65	3685,31
Pier 3, right	111,79	3125,90
Abutment 2	111,79	2535,68

Table 5-16: Values of shear forces and bending moments of the deck of Bridge 2, caused by the combination of the response spectrum for ground type C with the displacements of set B.

Considering the tables and the diagrams above, it is clear that in what concerns the shear force, piers are the more loaded elements of the structure.

As for the bending moment, whether it is about the piers or the deck, it is from ground type C where the highest values are attained. It is important to state that though the bending moments of the deck are not low, they are about five times higher at the piers' platform.

5.1.4.3 Drifts of the piers

By using the calculation method explained in 4.3.3, the following drifts were attained for each pier.

	High (m)	δ_d (m)	δ_f (m)	q	θ (rad)
Pier 1	14,00	0,0084	0,0082	1,00	**1,49x10^{-5}**
Pier 2	21,00	0,0178	0,0164	1,00	**6,45x10^{-5}**
Pier 3	14,00	0,0250	0,0247	1,00	**2,41x10^{-5}**

Table 5-17: Drift of the piers due to the application of the combination of the response spectrum for ground type A with the displacements of set A.

	High (m)	δ_d (m)	δ_f (m)	q	θ (rad)
Pier 1	14,00	0,0210	0,0213	1,00	**2,19x10^{-5}**
Pier 2	21,00	0,0440	0,0425	1,00	**7,06x10^{-5}**
Pier 3	14,00	0,0644	0,0638	1,00	**4,34x10^{-5}**

Table 5-18: Drift of the piers due to the application of the combination of the response spectrum for ground type C with the displacements of set A.

The tables convey that the main pier endures more deformation because it is the highest and consequently the most flexible. The drifts of piers are low because they possess a quite sturdy section for their height, which provides them with a significant inertia. The values from this analysis, as should be remarked, are still lower than the synchronous', since for this last one needs to consider that the foundation also moves.

5.1.5 Comparison of both analysis

As a complement to the approach to Bridge 2, a comparative study between the two analysis carried out on this particular bridge is here described.

Figure 5-22 shows the displacement endured by the deck, where there is a clear difference between both analysis, synchronous and asynchronous. In the synchronous analysis, this displacement is symmetric and a sharp rise on pier 2 is noticeable, for being higher and more flexible than the others. This rise is more strongly felt when the structure lays on a ground type

C than in a ground type A. In the synchronous analysis, however, though the displacements enforced by set A have a linear growth, when they combine with the response spectrum, some of that straightness is lost (but not in a very marked way, as it can be observed in the graphic).

The displacements of the asynchronous analysis are much higher than the synchronous analysis', and in both cases ground type C comes up with the highest values.

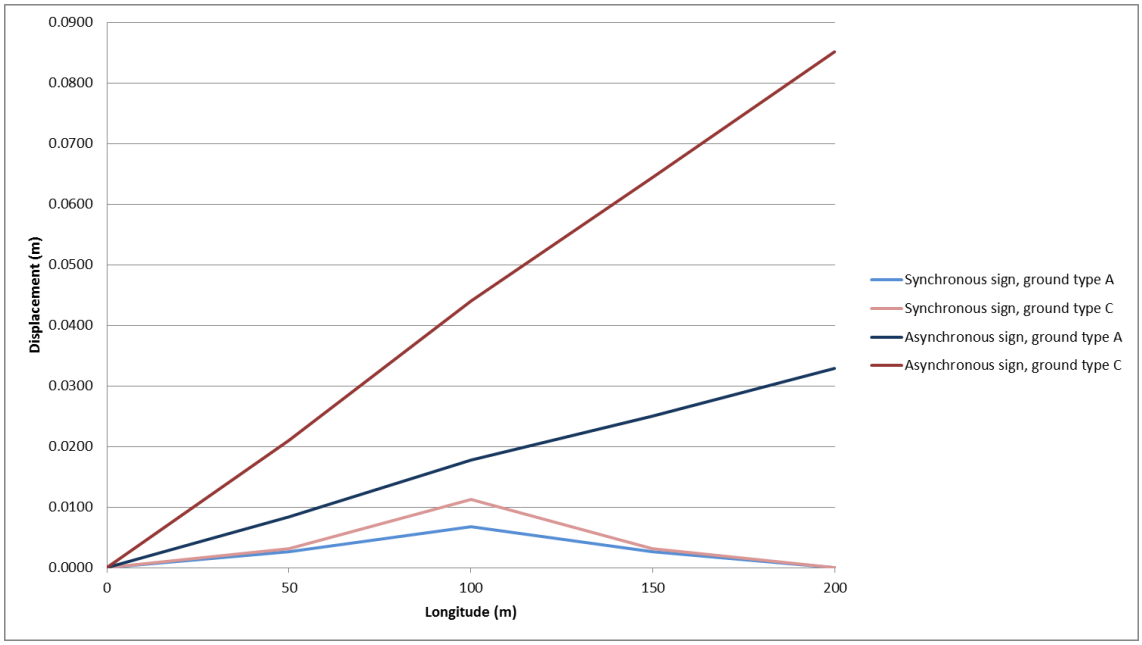

Figure 5-22: Displacements of the deck of Bridge 2.

In what concerns the shear force affecting the piers, it varies according to the ground type and not as much to the difference between the type of analysis. The difference between a synchronous analysis and an asynchronous is perfectly irrelevant considering ground type A, whereas for ground type C that difference is quite little.

In *Figure 5-23*, on pier 2, one can observe a rise and a decline in the value of the shear force, considering piers 1 and 3, whether a ground type C or A is being considered. The reason why this happens is because the response spectrum of ground type C, as observed in *Figure 4-3*, is more accelerated than the response spectrum of ground type A and also because this bridge has mode 1 as dominant vibration mode, with a corresponding period of $0{,}61\ sec$ (as displayed in *Figure 5-3*). Therefore, when $T = 0{,}61\ sec$, the acceleration of the spectrum of ground type A is of $0{,}60g$, being already in the descendant stage of the spectrum. For this same period, the acceleration of ground type C is $1{,}04g$, i.e. it is on the constant acceleration part of the spectrum. This occurrence causes the shear force of pier 2 in ground type C to rise in comparison to the values of shear force of piers 1 and 3, while in ground type A it decreases.

It is for this particular reason that most of the analyzed parameters attained in this study are higher when considering ground type C.

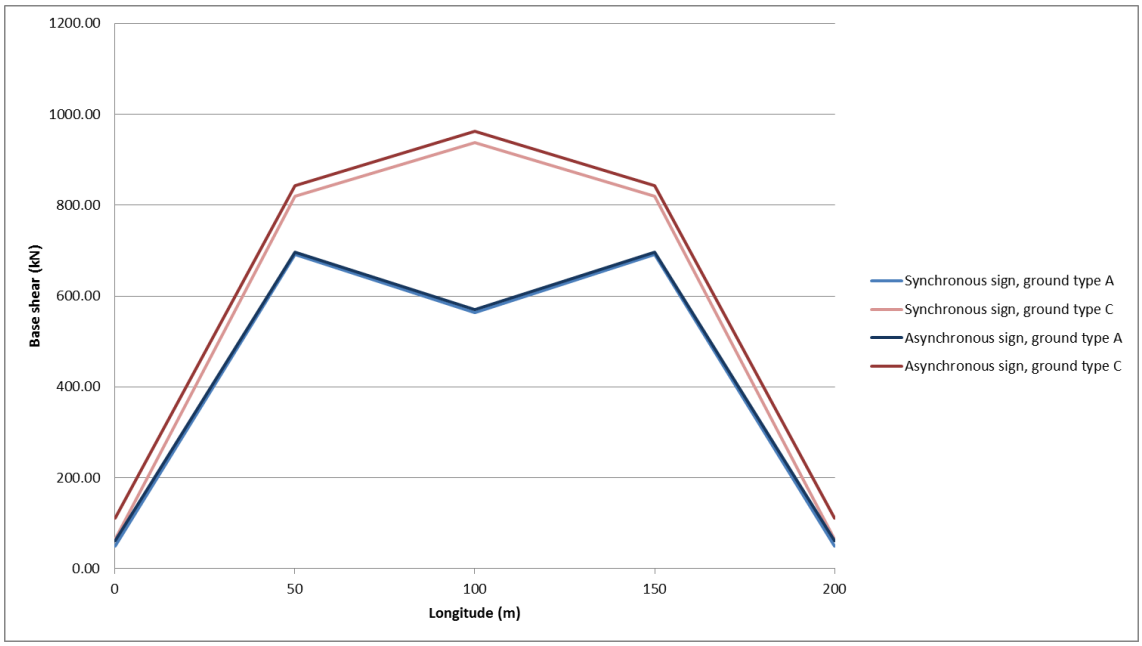

Figure 5-23: Base shear of Bridge 2.

In what concerns blending moments on piers, it is possible to conclude from *Figure 5-24*, that they achieve maximum limits on pier 2 because it is the more flexible. Once again, the difference between considering the synchronous or the asynchronous analysis is quite small, contrarily to what happens with the influence that leads to consider a ground type or the other, remembering that ground type C attains much higher values than ground type A.

As for pier 2, the moment on its platform is much higher when one considers a ground type C than a ground type A. This is due to the difference of accelerations of the response spectrum of either one or the other ground types, as previously explained.

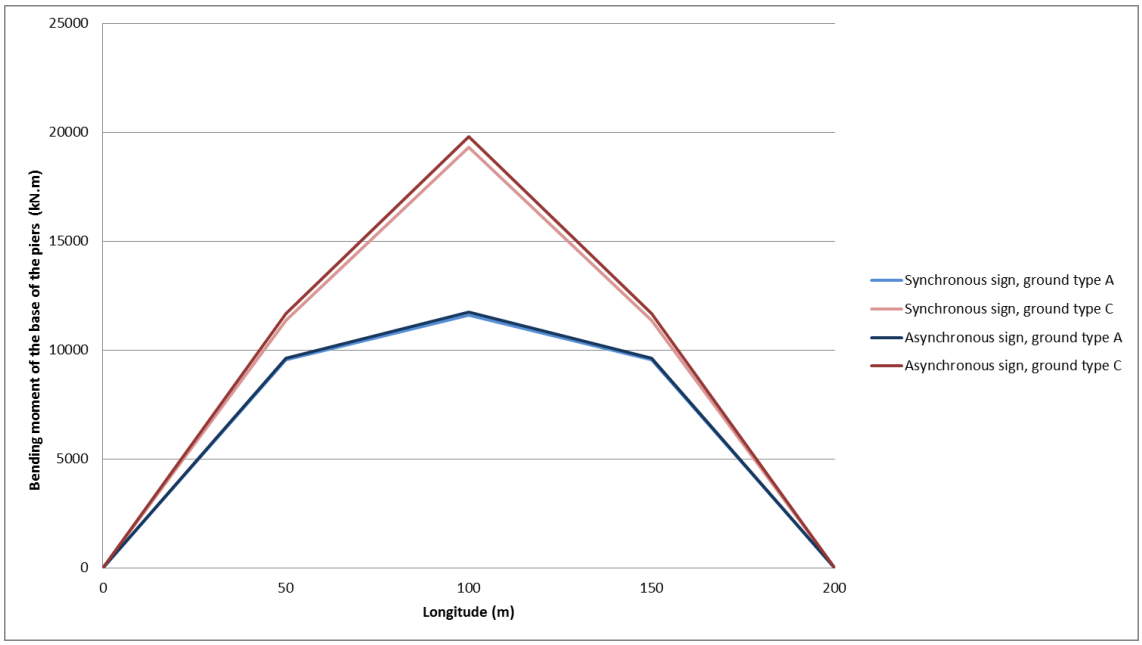

Figure 5-24: Bending moments of the base of the piers of Bridge 2.

In the blending moment felt on the deck, there is a considerable difference between considering a synchronous or an asynchronous analysis, especially in ground type C where the attained values of the asynchronous analysis are much higher, as shown in *Figure 2-25*.

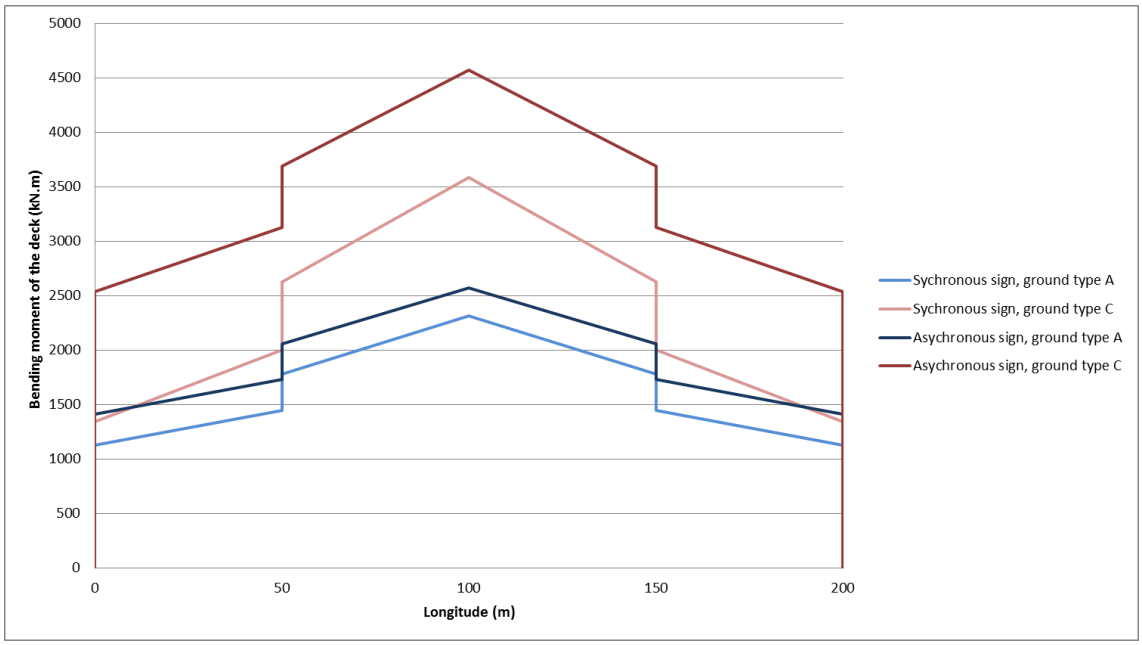

Figure 5-25: Bending moments of the deck of Bridge 2.

5.2 Long bridge crossing a mountain

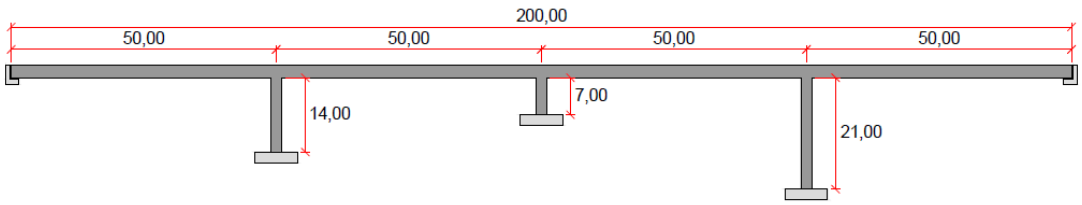

Figure 5-26: Bridge 3.

5.2.1 Displacements of the piers resulting from the seismic action

As it occurred with Bridge 2, in Bridge 3 the definition of the displacements resulting from the seismic action is in accordance to the description in 4.1. Since Bridge 3 has four spans of 50 m

each, exactly like Bridge 1 and 2, the results from theses displacements will be the same and so their display is useless repeating.

5.2.2 Modelling of Bridge 3

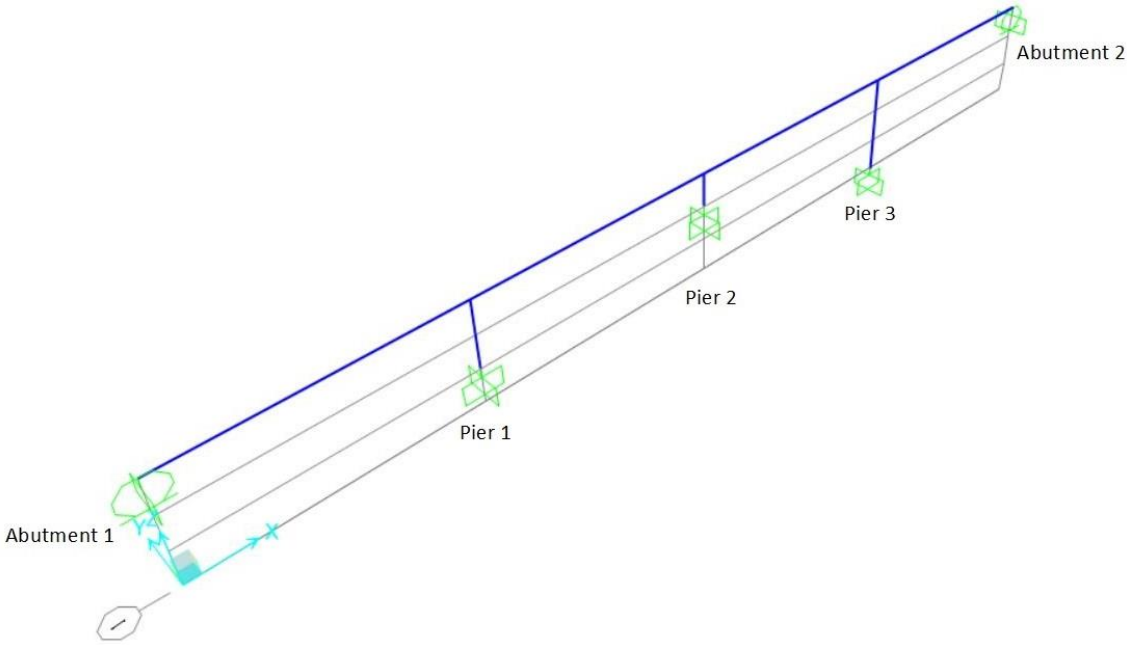

Figure 5-27: Modelling of Bridge 3 in SAP2000.

After inserting Bridge 3 model into the program and applying the actions of response spectrum and the displacements of sets A and B for each ground type, the vibration modes and deformations of the structure are displayed below.

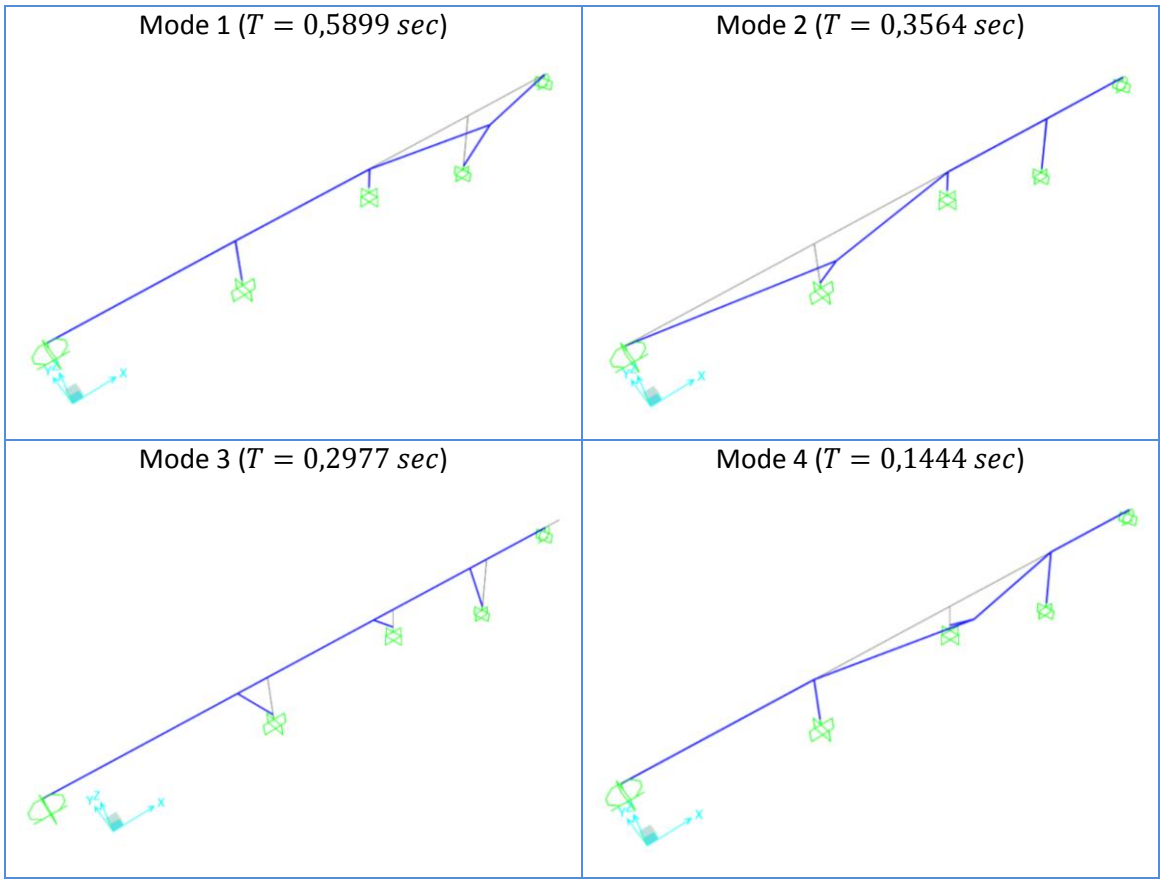

Figure 5-28: First four vibration modes of Bridge 3.

Ground type A

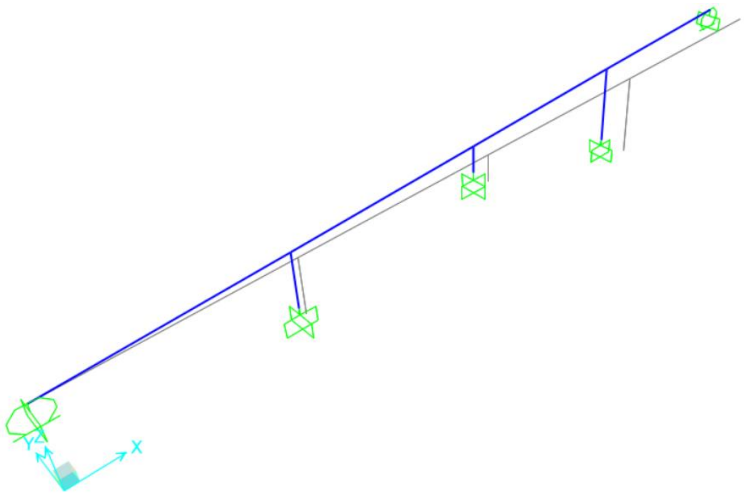

Figure 5-29: Deformation of Bridge 3 caused by the displacements of set A for ground type A.

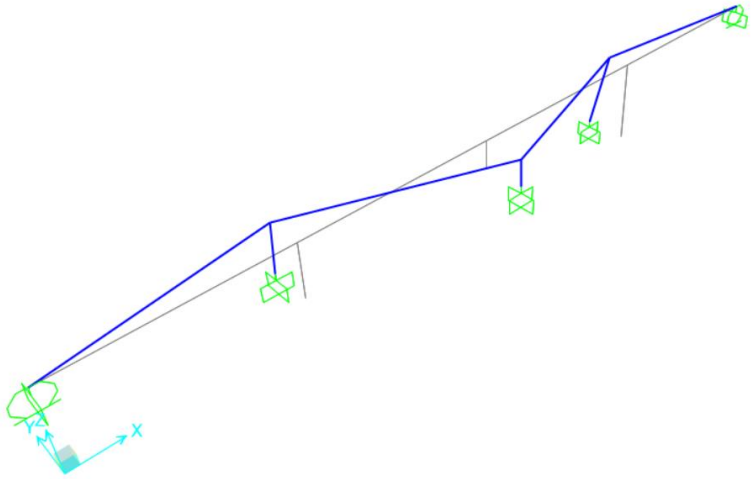

Figure 5-30: Deformation of Bridge 3 caused by the displacements of set B for ground type A.

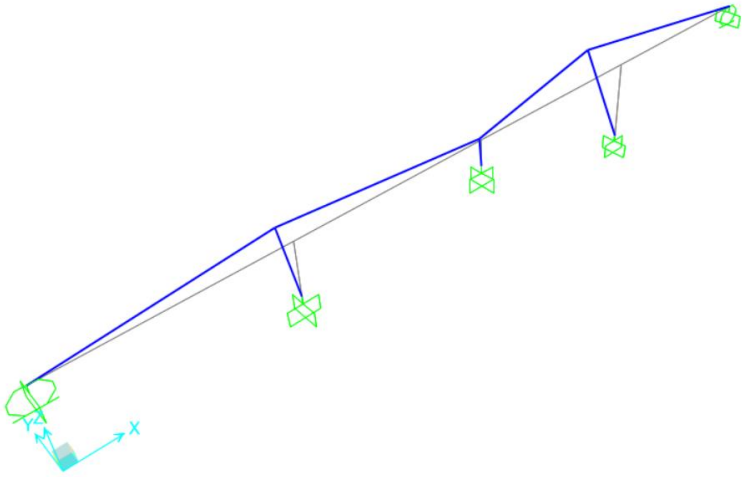

Figure 5-31: Deformation of Bridge 3 caused by the response spectrum for ground type A.

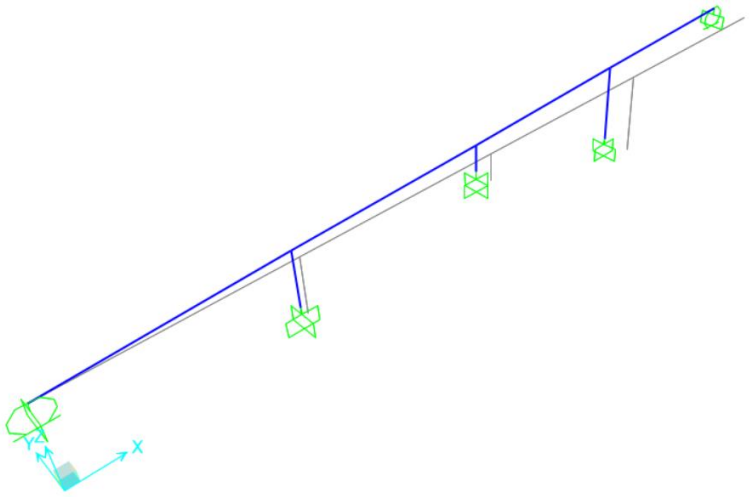

Figure 5-32: Deformation of Bridge 3 caused by the combination of the actions of the response spectrum and the displacements of set A for ground type A.

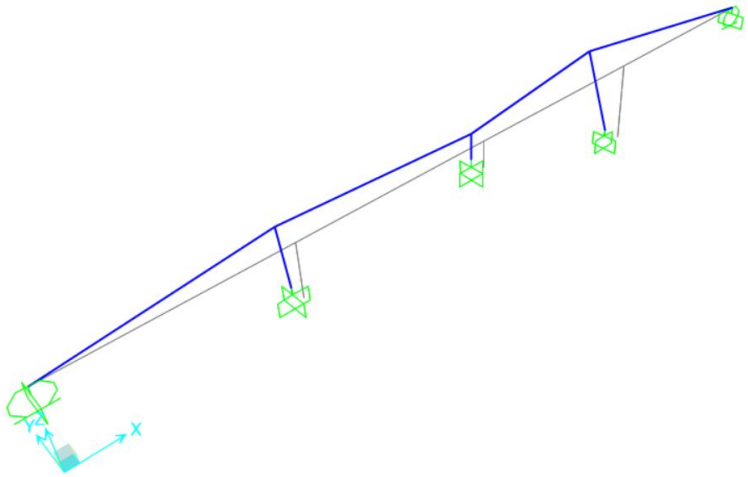

Figure 5-33: Deformation of Bridge 3 caused by the combination of the actions of the response spectrum and the displacements of set B for ground type A.

Ground type C

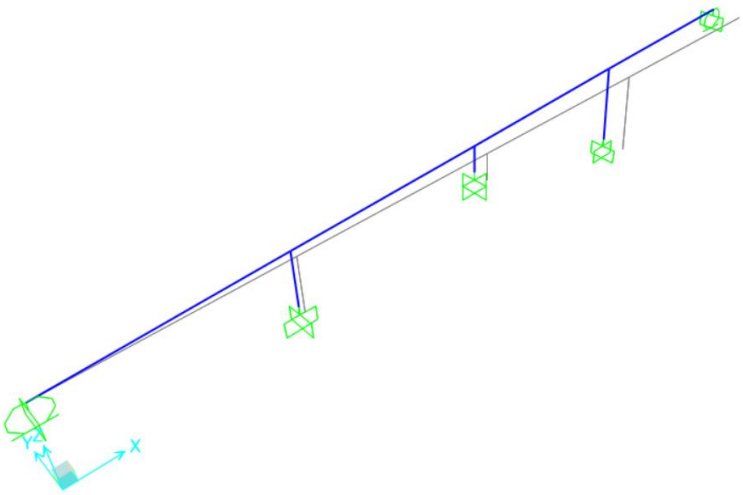

Figure 5-34: Deformation of Bridge 3 caused by the displacements of set A for ground type C.

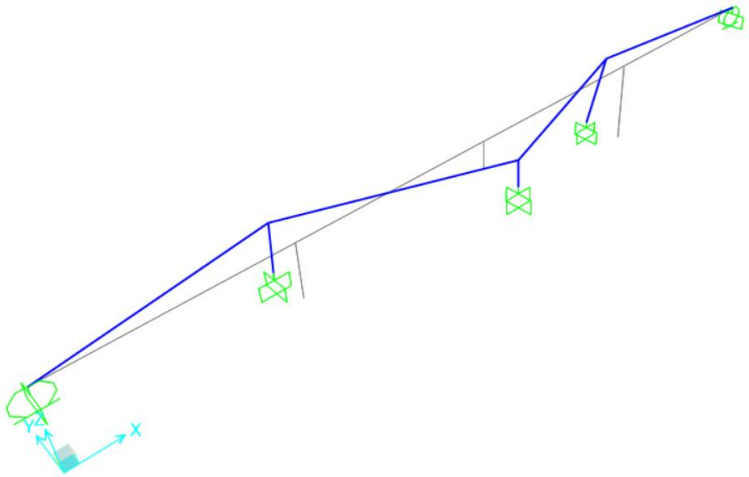

Figure 5-35: Deformation of Bridge 3 caused by the displacements of set B for ground type C.

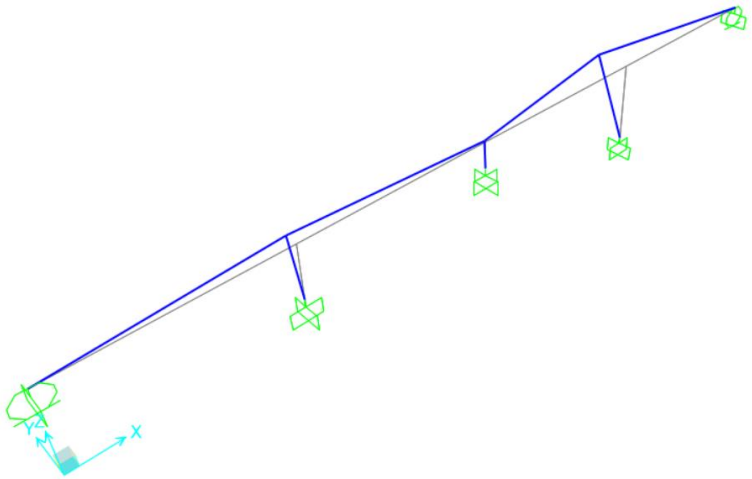

Figure 5-36: Deformation of Bridge 3 caused by the response spectrum for ground type C.

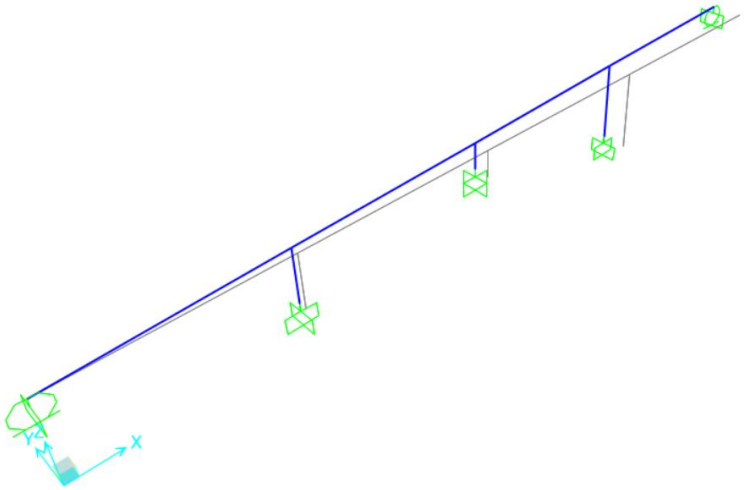

Figure 5-37: Deformation of Bridge 3 caused by the combination of the actions of the response spectrum and the displacements of set A for ground type C.

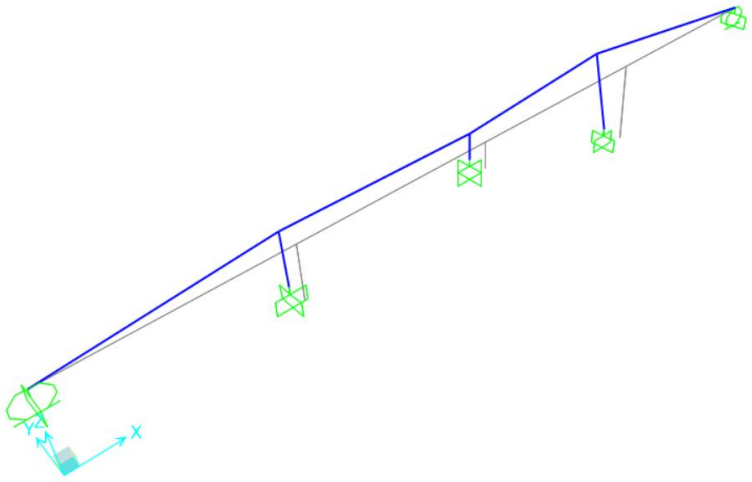

Figure 5-38: Deformation of Bridge 3 caused by the combination of the actions of the response spectrum and the displacements of set B for ground type C.

5.2.3 Synchronous analysis

The synchronous analysis is represented in *Figures 5-31* and *5-36* previously displayed, whether it concerns a ground type A or a ground type C.

5.2.3.1 Base shears and displacements of the deck

In the synchronous analysis of the structure, performed in SAP2000, the base shears and the displacements of the deck for each type of ground type are mentioned in the table below.

	Base shear (kN)	Displacements of the deck (m)
Abutment 1	47,63	0,0000
Pier 1	799,93	0,0030
Pier 2	775,52	0,0005
Pier 3	467,30	0,0056
Abutment 2	88,01	0,0000

Table 5-19: Values of base shear and displacements of the deck considering the single action of the response spectrum for ground type A.

	Base shear (kN)	Displacements of the deck (m)
Abutment 1	54,91	0,0000
Pier 1	920,25	0,0035
Pier 2	742,82	0,0004
Pier 3	751,37	0,0090
Abutment 2	141,37	0,0000

Table 5-20: Values of base shear and displacements of the deck considering the single action of the response spectrum for ground type C.

The information in the tables indicate that the displacement in the deck on each pier is proportional to the height of the piers, concerning both ground types.

It is the first time that, from all the analysis performed till this moment, ground type C shows a lower value than ground type A. The base shear of pier 2 is lower for ground type C than for ground type A. As for the rest of the piers, pier 1 and pier 3 have a higher base shear value for ground type C than for ground type A, with 120 kN and 300 kN of difference, respectively. This difference is explained by the response spectrum of ground type C being more accelerated than the response spectrum for ground type A.

5.2.3.2 Shear forces and bending moments

The efforts attained in the synchronous analysis of Bridge 3 and the related diagrams are displayed below.

Ground type A

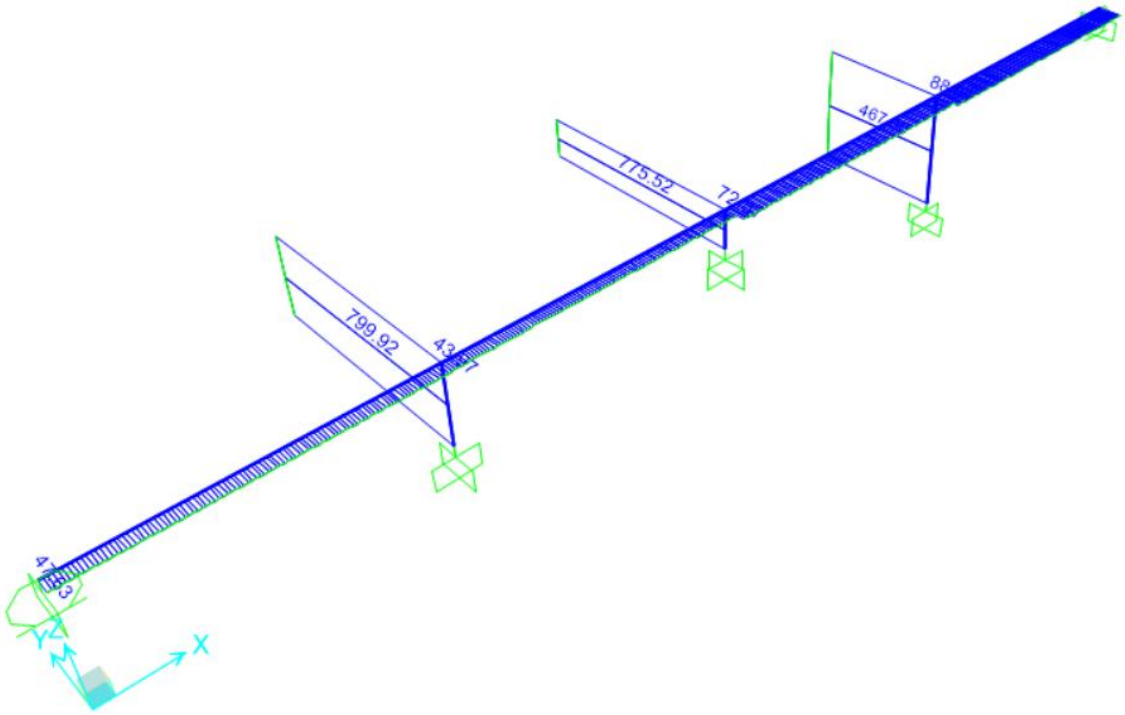

Figure 5-39: Diagrams of shear forces on Bridge 3, caused by the single action of the response spectrum for ground type A.

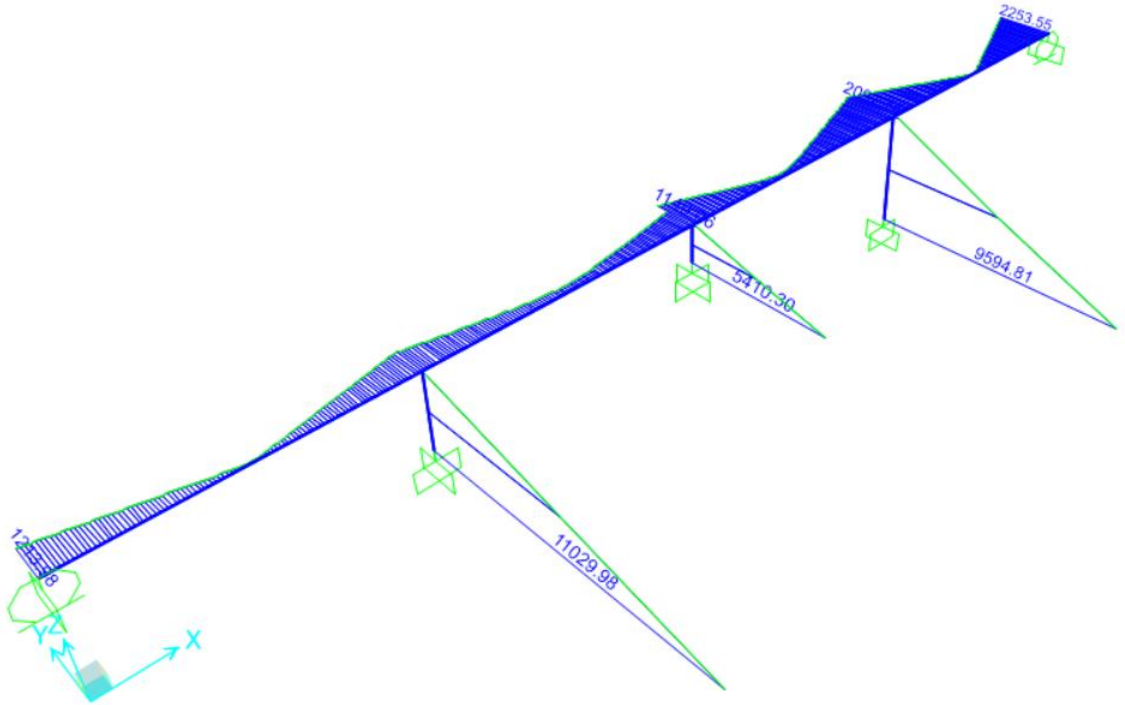

Figure 5-40: Diagrams of bending moments on Bridge 3, caused by the single action of the response spectrum for ground type A.

Piers	V (kN)	M (kN.m)
Top of pier 1	799,93	170,23
Base of pier 1	799,93	11029,98
Top of pier 2	775,52	137,99
Base of pier 2	775,52	5410,30
Top of pier 3	467,30	219,37
Base of pier 3	467,30	9594,81

Table 5-21: Values of shear forces and bending moments of the piers in Bridge 3, caused by the single action of the response spectrum for ground type A.

Deck	V (kN)	M (kN.m)
Abutment 1	47,63	1213,98
Pier 1, left	47,63	1170,00
Pier 1, right	43,97	1144,50
Pier 2, left	43,97	1149,06
Pier 2, right	72,87	1558,52
Pier 3, left	72,87	2097,74
Pier 3, right	88,01	2147,50
Abutment 2	88,01	2253,55

Table 5-22: Values of shear forces and bending moments of the deck in Bridge 3, caused by the single action of the response spectrum for ground type A.

Ground type C

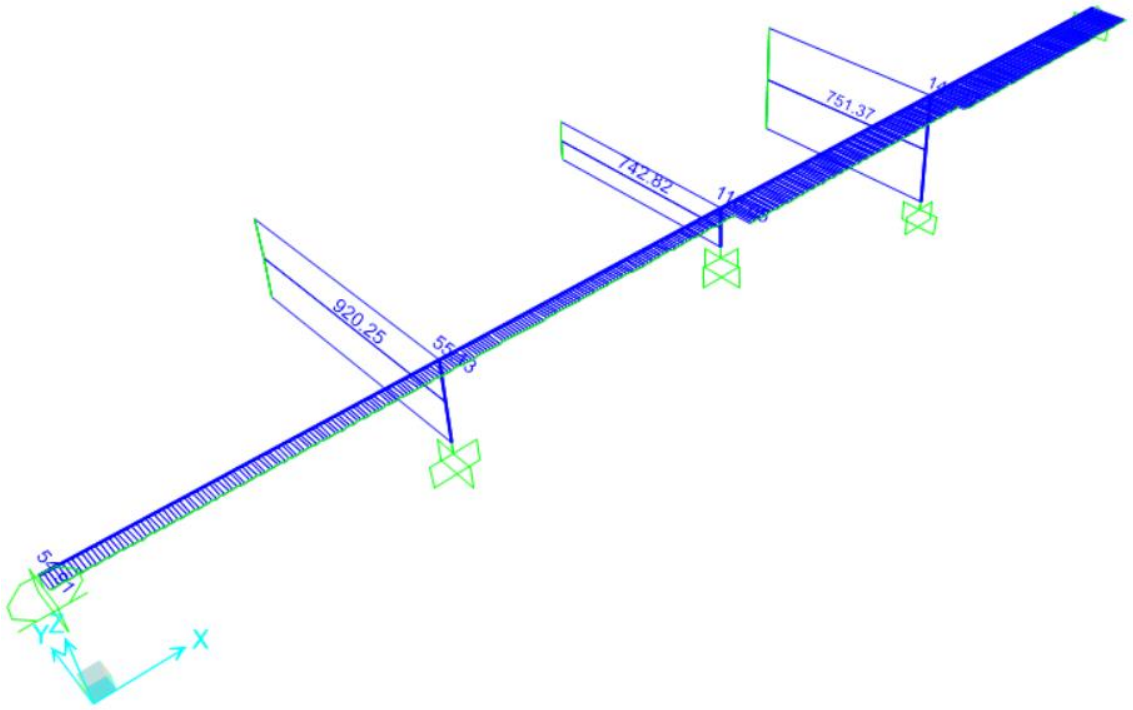

Figure 5-41: Diagrams of shear forces on Bridge 3, caused by the single action of the response spectrum for ground type C.

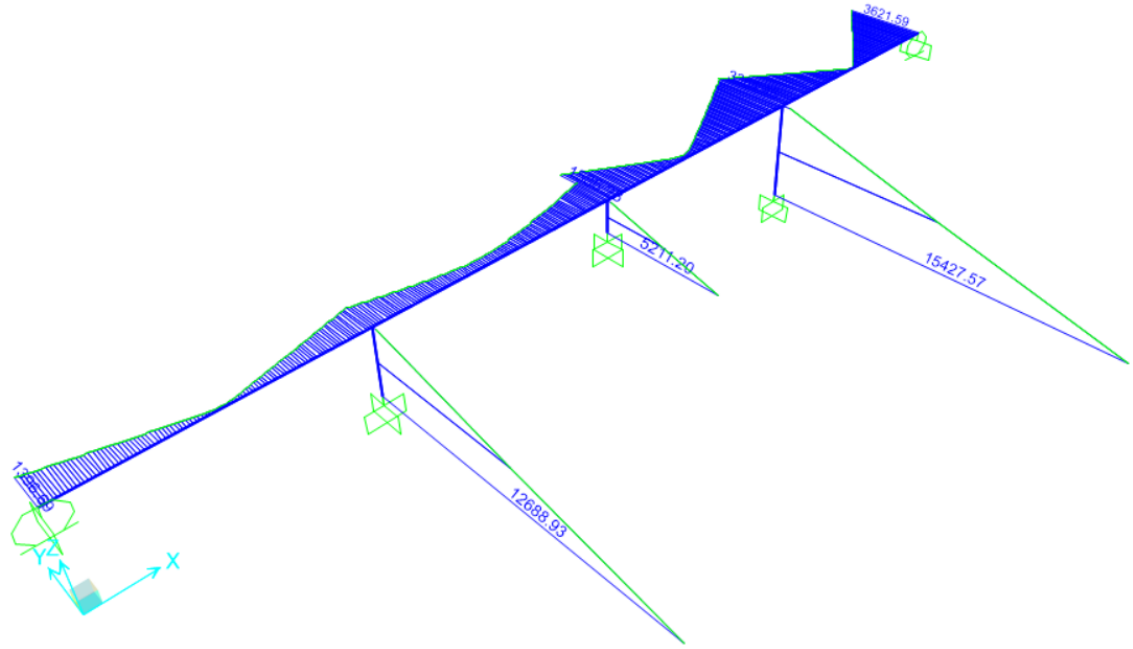

Figure 5-42: Diagrams of bending moments on Bridge 3 caused by the single action of the response spectrum for ground type C.

Piers	V (kN)	M (kN.m)
Top of pier 1	920,25	195,55
Base of pier 1	920,25	12688,93
Top of pier 2	742,82	193,41
Base of pier 2	742,82	5211,20
Top of pier 3	751,37	351,79
Base of pier 3	751,37	15427,57

Table 5-23: Values of shear forces and bending moments of the piers in Bridge 3, caused by the single action of the response spectrum for ground type C.

Deck	V (kN)	M (kN.m)
Abutment 1	54,91	1396,69
Pier 1, left	54,91	1353,32
Pier 1, right	55,13	1333,99
Pier 2, left	55,13	1586,28
Pier 2, right	116,05	2457,11
Pier 3, left	116,05	3364,46
Pier 3, right	141,37	3447,12
Abutment 2	141,37	3621,59

Table 5-24: Values of shear forces and bending moments of the deck in Bridge 3, caused by the single action of the response spectrum for ground type C.

The diagrams lead to the conclusion that the most loaded elements of the structure are clearly the piers, even though the efforts on the deck are not that irrelevant.

Considering the shear forces, since they refer to the base shears, their particular features have already been mentioned previously.

As for the bending moment on the piers, ground type C registers the highest values, except in pier 2 where the values for both ground types are the same. The bending moment in the deck, however, shows a lower value than in the piers, resulting in a similar increase for both ground types with higher values for ground type C.

5.2.3.3 Drifts of the piers

The drifts attained for each pier of Bridge 3 were calculated according to the method described in 4.3.3, with the following results for the synchronous analysis.

	High (m)	δ_d (m)	δ_f (m)	q	θ (rad)
Pier 1	14,00	0,0030	0,0000	1,00	**$2{,}15 \times 10^{-4}$**
Pier 2	7,00	0,0005	0,0000	1,00	**$6{,}53 \times 10^{-5}$**
Pier 3	21,00	0,0056	0,0000	1,00	**$2{,}67 \times 10^{-4}$**

Table 5-25: Drift of the piers due to the application of the response spectrum for ground type A.

	High (m)	δ_d (m)	δ_f (m)	q	θ (rad)
Pier 1	14,00	0,0035	0,0000	1,00	**$2{,}47 \times 10^{-4}$**
Pier 2	7,00	0,0004	0,0000	1,00	**$6{,}30 \times 10^{-5}$**
Pier 3	21,00	0,0090	0,0000	1,00	**$4{,}29 \times 10^{-4}$**

Table 5-26: Drift of the piers due to the application of the response spectrum for ground type C.

Due to the sturdy shear section of the piers providing them with a great stiffness, the drifts endured are very low, which is particularly evident in pier 2 for being the shortest and the hardest.

For both ground types, as it occurs with the displacements, the higher the pier the more flexible is becomes, resulting in a higher drift.

When a ground type C is considered, the results attained are higher than if a ground type A is used.

5.2.4 Asynchronous analysis

The asynchronous analysis is represented in *Figures 5-32*, *5-33*, *5-37* and *5-38* previously displayed, whether it refers to ground type A or ground type C.

5.2.4.1 Base shears and displacements of the deck

The values of base shears and the displacements of the deck attained in the synchronous analysis through SAP2000 for each ground type are in the tables displayed below.

Ground type A

	Base shear (kN)	Displacements of the deck (m)
Abutment 1	76,04	0,0000
Pier 1	801,16	0,0086
Pier 2	775,52	0,0164
Pier 3	468,57	0,0257
Abutment 2	101,42	0,0329

Table 5-27: Values of base shear and displacements of the deck considering the combination of the response spectrum for ground type A with the displacements of set A.

	Base shear (kN)	Displacements of the deck (m)
Abutment 1	62,00	0,0000
Pier 1	805,04	0,0035
Pier 2	781,45	0,0021
Pier 3	473,59	0,0057
Abutment 2	93,56	0,0000

Table 5-28: Values of base shear and displacements of the deck considering the combination of the response spectrum for ground type A with the displacements of set B.

Ground type C

	Base shear (kN)	Displacements of the deck (m)
Abutment 1	163,71	0,0000
Pier 1	927,49	0,0212
Pier 2	742,82	0,0425
Pier 3	756,95	0,0655
Abutment 2	193,17	0,0851

Table 5-29: Values of base shear and displacements of the deck considering the combination of the response spectrum for ground type C with the displacements of set A.

	Base shear (kN)	Displacements of the deck (m)
Abutment 1	114,21	0,0000
Pier 1	948,22	0,0056
Pier 2	781,43	0,0052
Pier 3	776,07	0,0095
Abutment 2	162,48	0,0000

Table 5-30: Values of base shear and displacements of the deck considering the combination of the response spectrum for ground type C with the displacements of set B.

Considering the displacements of the deck in both ground types, the combination which takes the displacements of set A into account is the one displaying the highest values. Although it is not linear, these displacements are constantly growing from abutment 1 to abutment 2. In base shears, however, the combination where the highest values on the piers are attained is the one considering displacements of set B for both ground types.

5.2.4.2 Shear forces and bending moments

In the asynchronous analysis of Bridge 3, the efforts and related diagrams are represented below.

Ground type A

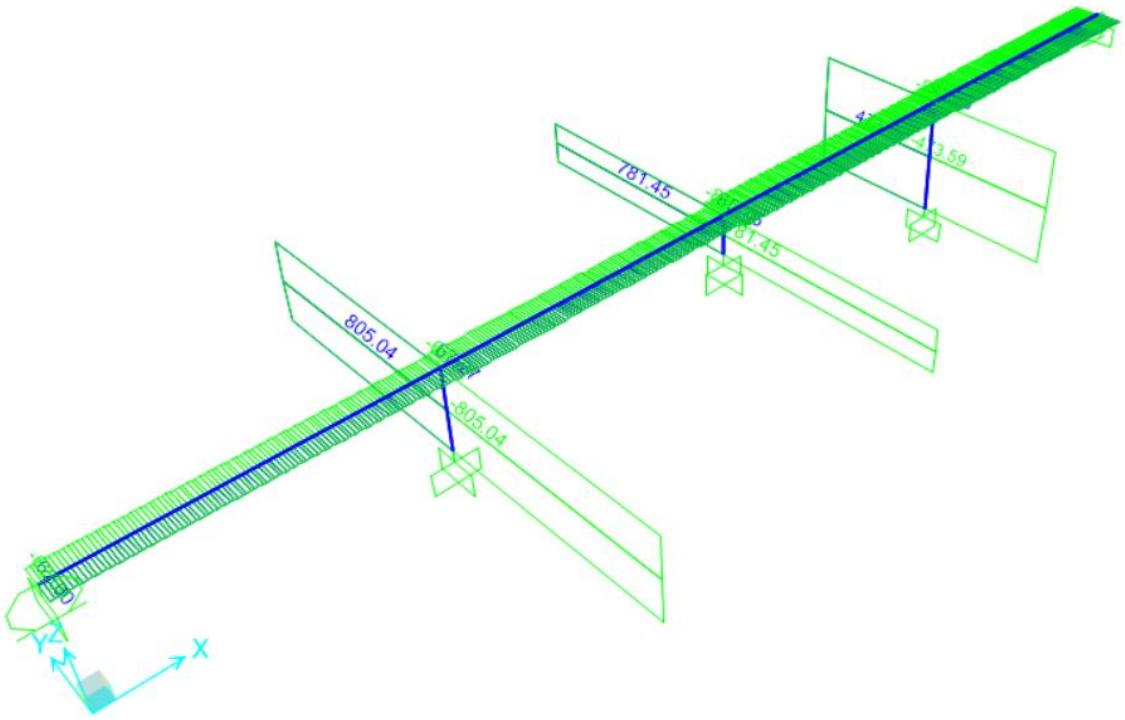

Figure 5-43: Diagrams of shear forces on Bridge 3, caused by the combination of the response spectrum for ground type A with the displacements of set B.

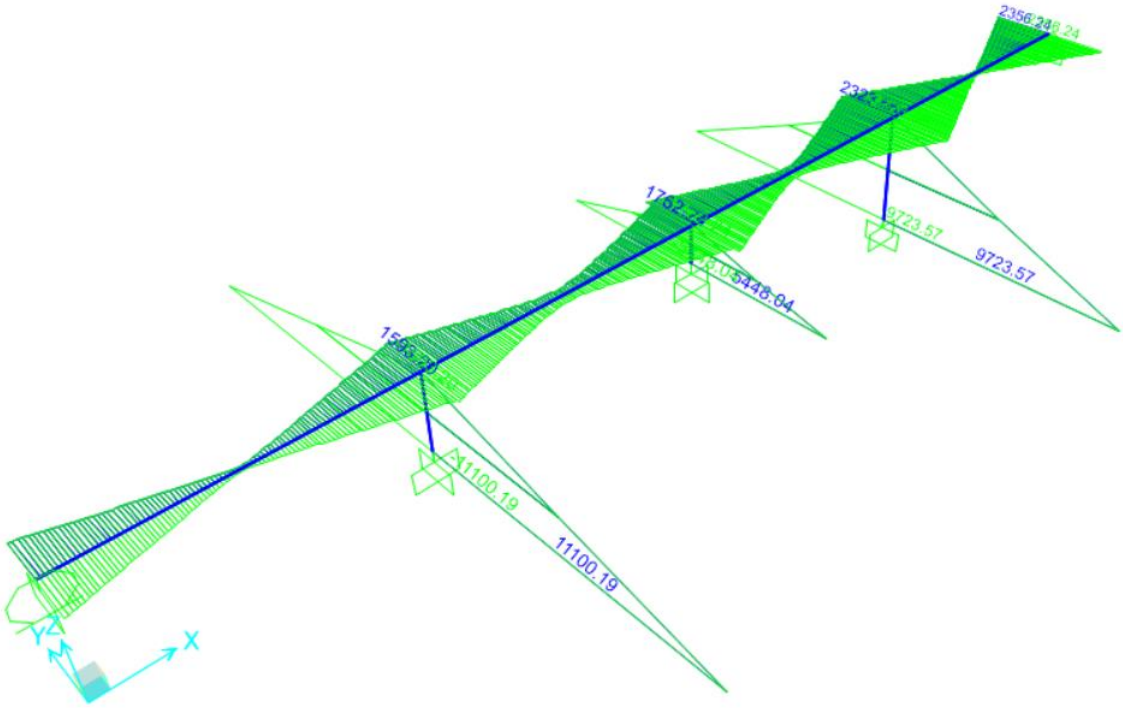

Figure 5-44: Diagrams of bending moments on Bridge 3, caused by the combination of the response spectrum for ground type A with the displacements of set B.

Piers	V (kN)	M (kN.m)
Top of pier 1	805,04	171,61
Base of pier 1	805,04	11100,19
Top of pier 2	781,45	141,80
Base of pier 2	781,45	5448,04
Top of pier 3	473,59	222,78
Base of pier 3	473,59	9723,57

Table 5-31: Values of shear forces and bending moments of the piers of Bridge 3, caused by the combination of the response spectrum for ground type A with the displacements of set B.

Deck	V (kN)	M (kN.m)
Abutment 1	62,00	1512,50
Pier 1, left	62,00	1593,20
Pier 1, right	67,27	1665,03
Pier 2, left	67,27	1762,25
Pier 2, right	85,76	2013,03
Pier 3, left	85,76	2323,55
Pier 3, right	93,56	2327,95
Abutment 2	93,56	2356,24

Table 5-32: Values of shear forces and bending moments of the deck of Bridge 3, caused by the combination of the response spectrum for ground type A with the displacements of set B.

Ground type C

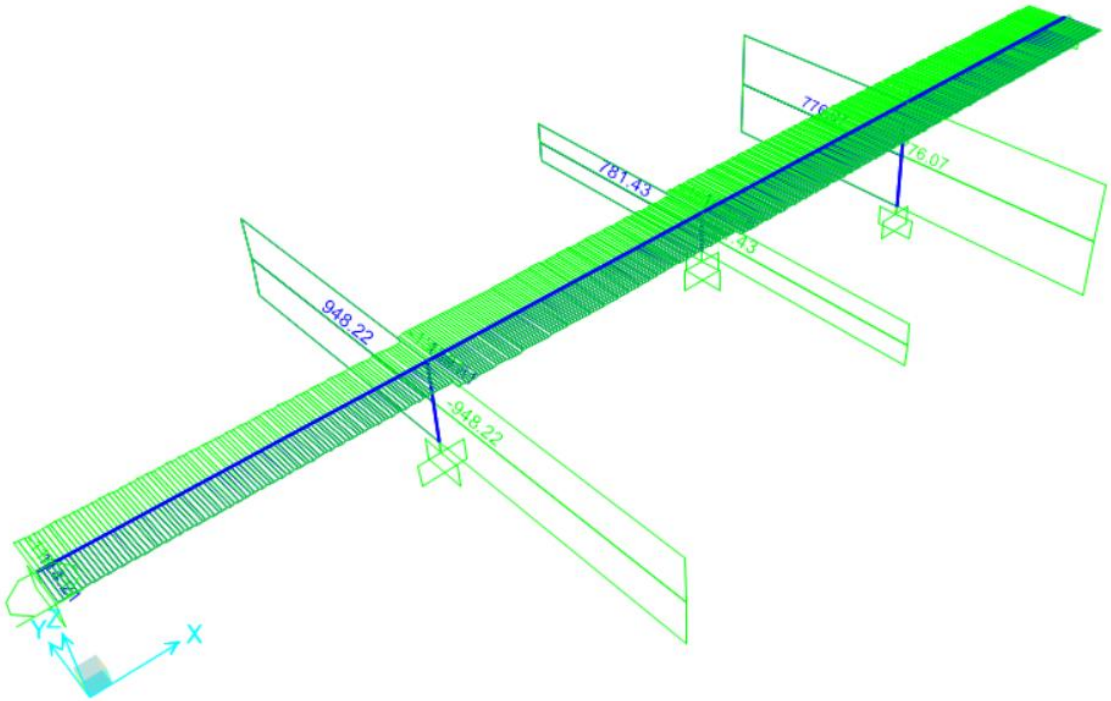

Figure 5-45: Diagrams of shear forces on Bridge 3, caused by the combination of the response spectrum for ground type C with the displacements of set B.

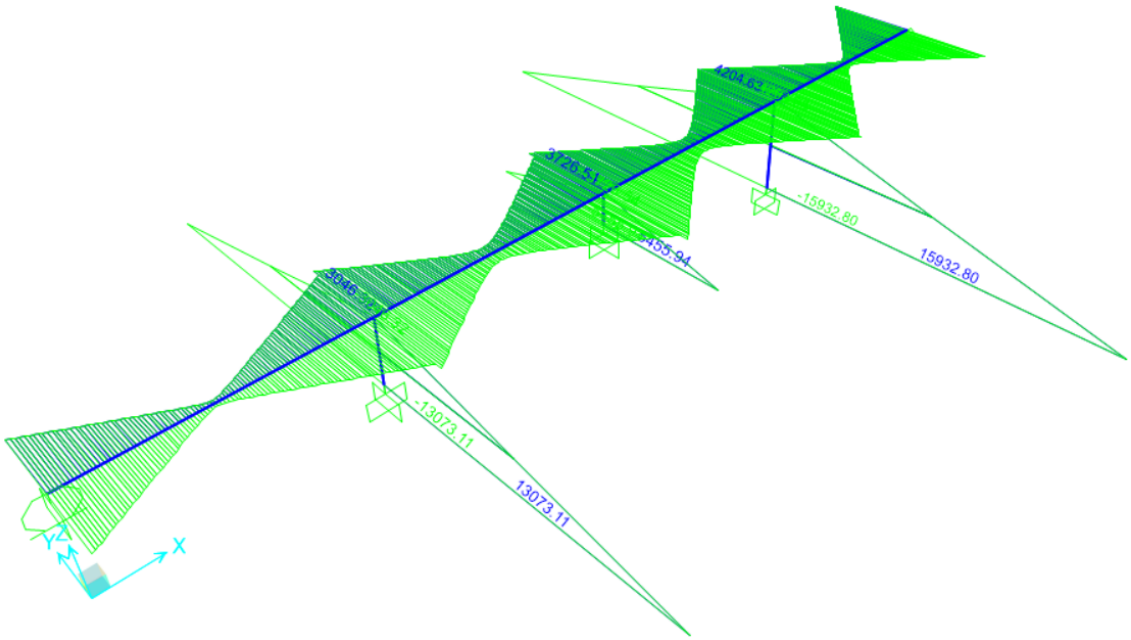

Figure 5-46: Diagrams of bending moments on Bridge 3, caused by the combination of the response spectrum for ground type C with the displacements of set B.

Piers	V (kN)	M (kN.m)
Top of pier 1	948,22	203,09
Base of pier 1	948,22	13073,11
Top of pier 2	781,43	210,26
Base of pier 2	781,43	5455,94
Top of pier 3	776,07	365,18
Base of pier 3	776,07	15932,80

Table 5-33: Values of shear forces and bending moments of the piers of Bridge 3, caused by the combination of the response spectrum for ground type C with the displacements of set B.

Deck	V (kN)	M (kN.m)
Abutment 1	114,21	2672,25
Pier 1, left	114,21	3046,32
Pier 1, right	139,81	3330,87
Pier 2, left	139,81	3726,54
Pier 2, right	162,77	4022,20
Pier 3, left	162,77	4204,63
Pier 3, right	162,48	4126,34
Abutment 2	162,48	4016,34

Table 5-34: Values of shear forces and bending moments of the deck of Bridge 3, caused by the combination of the response spectrum for ground type C with the displacements of set B.

From the observation of the results, it is possible to conclude that, as in the synchronous analysis, here piers are the elements enduring more effort. Pier 2 is the pier with the lowest efforts whether in shear forces or bending moments.

As for the bending moments of the deck, these are higher than in the synchronous analysis and display higher values when a ground type C is considered.

5.2.4.3 Drifts of the piers

By using the calculation method explained in 4.3.3, the attained drifts for each pier were the following.

	High (m)	δ_d (m)	δ_f (m)	q	θ (rad)
Pier 1	14,00	0,0086	0,0082	1,00	**$2{,}69 \times 10^{-5}$**
Pier 2	7,00	0,0164	0,0164	1,00	**$1{,}00 \times 10^{-6}$**
Pier 3	21,00	0,0257	0,0247	1,00	**$4{,}90 \times 10^{-5}$**

Table 5-35: Drift of the piers due to the application of the combination of the response spectrum for ground type A with the displacements of set A.

	High (m)	δ_d (m)	δ_f (m)	q	θ (rad)
Pier 1	14,00	0,0212	0,0213	1,00	**$1{,}07 \times 10^{-5}$**
Pier 2	7,00	0,0425	0,0425	1,00	**$5{,}71 \times 10^{-7}$**
Pier 3	21,00	0,0655	0,0638	1,00	**$8{,}20 \times 10^{-5}$**

Table 5-36: Drift of the piers due to the application of the combination of the response spectrum for ground type C with the displacements of set A.

As it occurred during the synchronous analysis, in the asynchronous it is also possible to observe that in both ground types, A or C, the drift of each pier is as broad as its height. However, the values are low for both cases, considering that the sturdy shear section possessed by piers provides them with a higher stiffness which becomes more noticeable when the pier is less high.

The results attained for ground type C are higher than for ground type A, likewise the synchronous analysis.

5.2.5 Comparison of both analysis

With the purpose of closing the approach to Bridge 3, this part focus on the comparison between the results from the two analysis carried out on this particular bridge.

Figure 5-47 is a graphic of the displacement occurred in the deck of Bridge 3 depending on its longitude, for both the analysis carried out and also the ground types. It is possible to observe

that the results attained in the synchronous analysis are similar for either ground type A or ground type C, and the fact that the displacement endured by the deck on each pier is as higher as the pier's height. It is important to notice that, differently from what happened till this moment, these displacements are not symmetric because despite the action of the response spectrum being constant in the whole structure, Bridge 3's piers have different heights, which causes different flexibilities and the consequent asymmetry in the displacements occurring in the deck.

In what concerns the displacements of the synchronous analysis, they are the result of the combination of the response spectrum with the displacements enforced by set A from Eurocode 8. In this particular situation, one can notice that the displacement of the deck increases with the longitude of the bridge, in an almost regular growth due to the different heights of the bridge's piers which do not allow for a total regularity.

Still in what refers to the displacements of the deck in the asynchronous analysis, ground type C shows the higher results, whereas in the synchronous analysis, both ground types on pier 2 display similar values, as it is a short pier with a quite sturdy shear section considering its height and so providing it with a considerable stiffness. In the remaining piers, as occurred in the asynchronous analysis ground type C displays the highest values, though the difference between the results from ground type A and ground type C is not as significant as in the synchronous analysis.

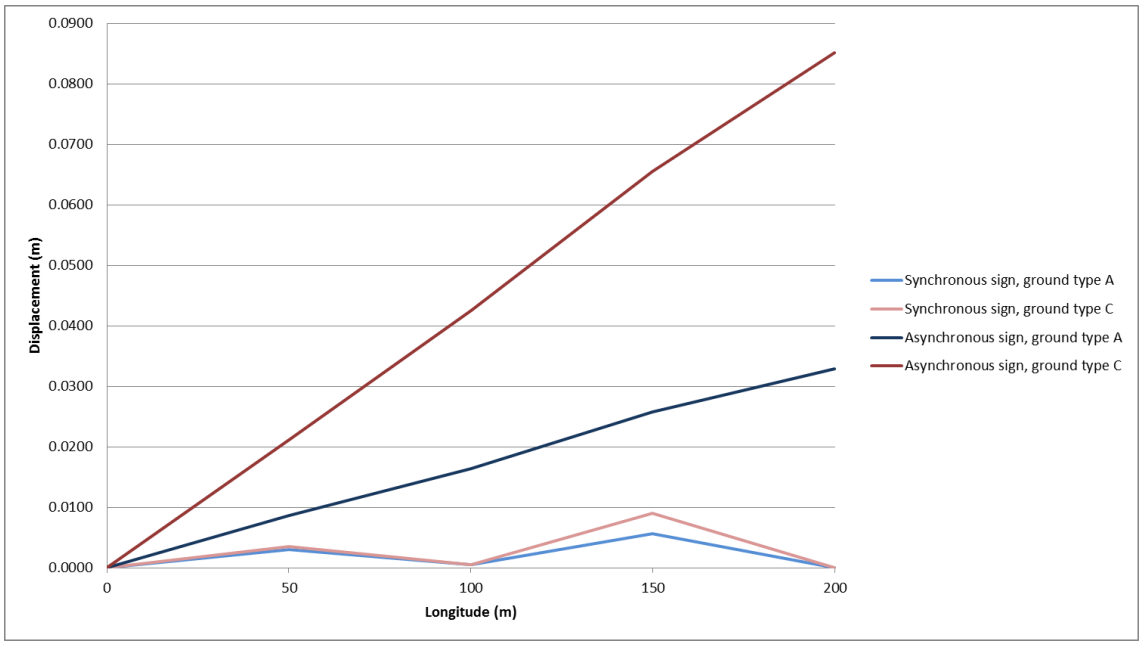

Figure 5-47: Displacements of the deck of Bridge 3.

The shear force endured by piers does not change a lot when it concerns a synchronous or an asynchronous analysis, varying according to the ground type considered.

Considering ground type C, the values attained are higher than ground type A's, as the first reveals a faster spectrum than A's. Influenced by vibration mode 2, pier 1 is the only one moving and it is where the highest shear forces in both ground forces are noticeable. Pier 2

comes next because it is the sturdiest, concentrating more efforts than Pier 3. In Pier 3 there's a significant difference between considering a ground type A and a ground type C, of about 300 kN.

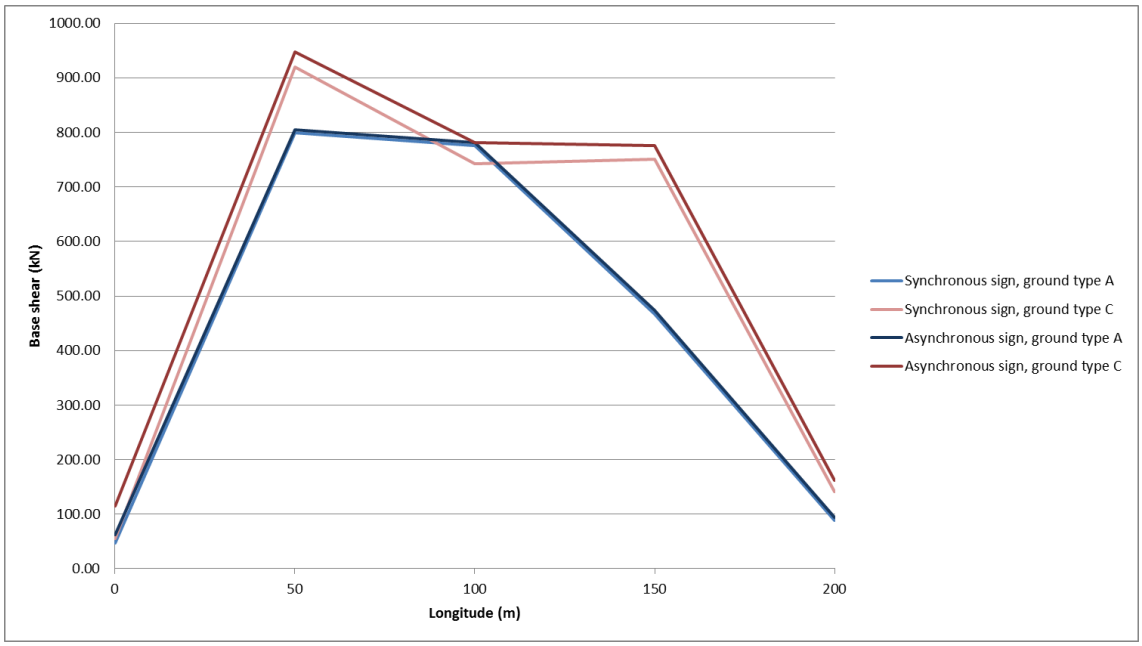

Figure 5-48: Base shear of Bridge 3.

The bending moments undergone by each pier's platform almost don't change with the different analysis, as it happened with the shear forces. However, considering a ground type A or C represents a great change, as it is in ground type C where the highest values are attained except in pier 2 where the values are the same for both ground types.

When it refers to ground type A, the highest value comes from pier 1, whereas in ground type C the highest result is on pier 3.

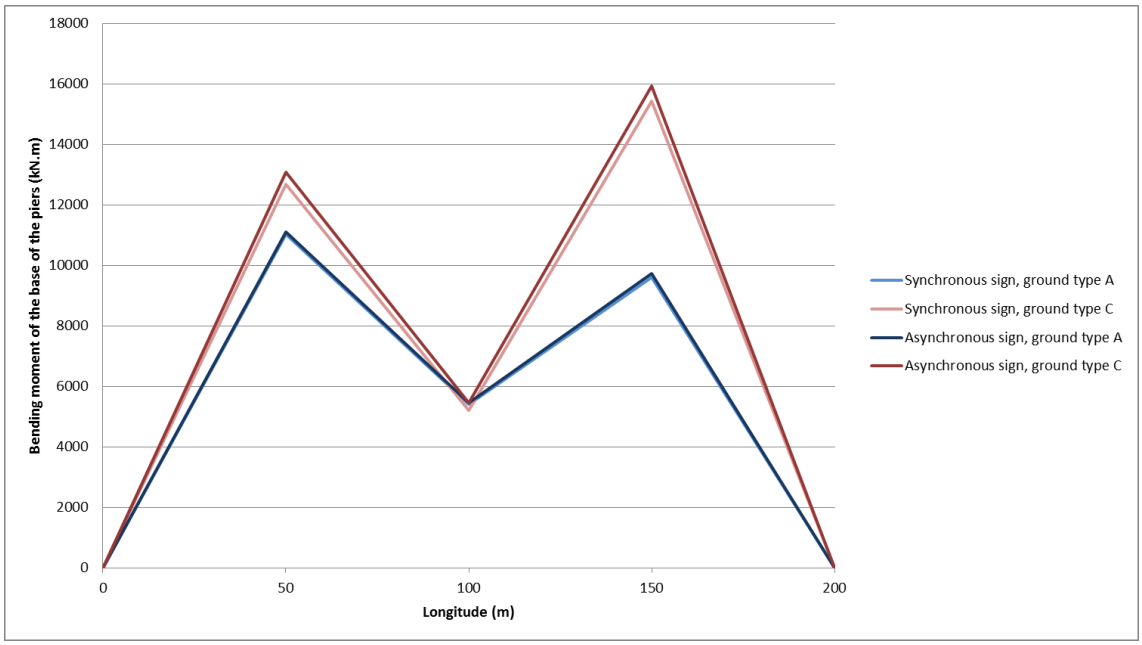

Figure 5-49: Bending moments of the base of the piers of Bridge 3.

As for the bending moments on the deck, despite showing significant values, they are quite below the ones resulting from the bending moment occurred in the pier's platform. In this case, the difference between considering the asynchrony of seismic waves or not is very important, as it is in the synchronous analysis that the highest values are attained. The values of ground type C, especially considering the asynchronous analysis, are much higher than the ground type A's.

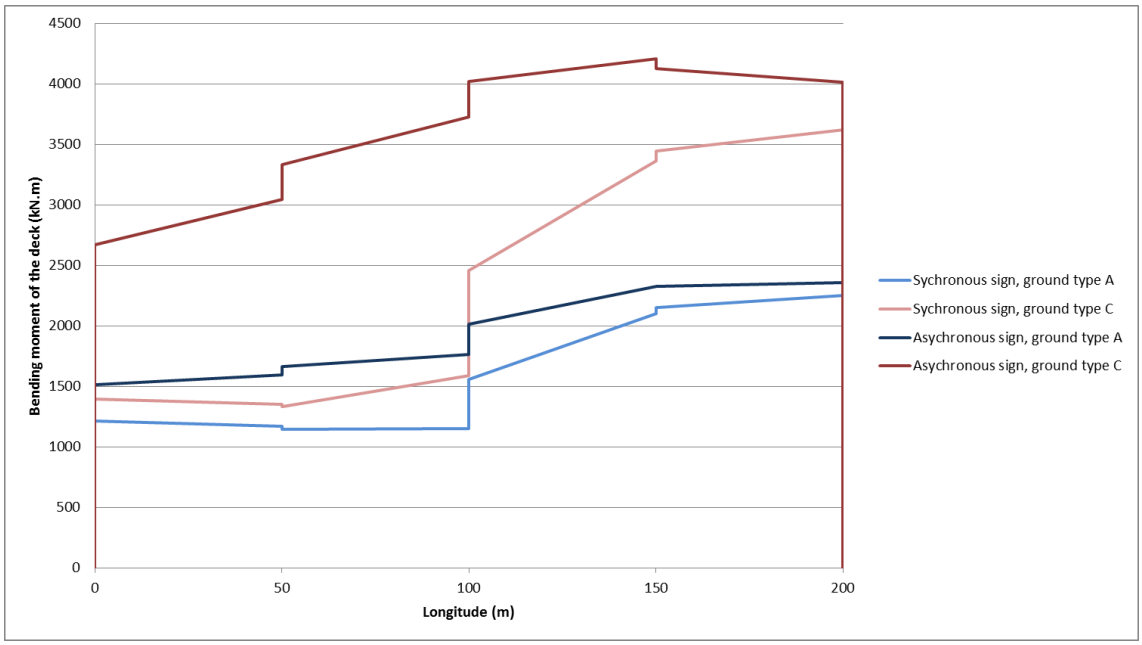

Figure 5-50: Bending moments of the deck of Bridge 3.

6. Effect of the length variation

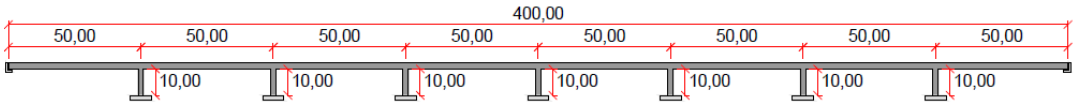

Figure 6-1: Bridge 4.

6.1 Displacements of the piers resulting from the seismic action

As in the previous situations, the calculation of the displacements of the piers resulting from the seismic action can be found in 4.1. With respect to Bridge 4, considering that it doubles the longitude of the others, the attained results for these displacements are displayed in the tables below.

Displacements of set A

	Abutment 1	Pier 1	Pier 2	Pier 3	Pier 4	Pier 5	Pier 6	Pier 7	Abutment 2
d_{ri} (m)	**0,0000**	**0,0082**	**0,0164**	**0,0247**	**0,0329**	**0,0411**	**0,0493**	**0,0575**	**0,0658**
$\varepsilon_r \cdot L_i$ (m)	–	0,0082	0,0164	0,0247	0,0329	0,0411	0,0493	0,0575	0,0658
ε_r	–	$1{,}6\text{x}10^{-4}$	$1{,}6\text{x}10^{-4}$	$1{,}6\text{x}10^{-4}$	$1{,}6\text{x}10^{-4}$	$1{,}6\text{x}10^{-4}$	$1{,}6\text{x}10^{-4}$	$1{,}6\text{x}10^{-4}$	$1{,}6\text{x}10^{-4}$
L_i (m)	–	50,00	100,00	150,00	200,00	250,00	300,0	350,00	400,00
$d_g\sqrt{2}$ (m)	–	0,0986	0,0986	0,0986	0,0986	0,0986	0,0986	0,0986	0,0986

Table 6-1: Displacements of set A for ground type A.

	Abutment 1	Pier 1	Pier 2	Pier 3	Pier 4	Pier 5	Pier 6	Pier 7	Abutment 2
d_{ri} (m)	**0,0000**	**0,0213**	**0,0425**	**0,0638**	**0,0851**	**0,1063**	**0,1276**	**0,1489**	**0,1702**
$\varepsilon_r \cdot L_i$ (m)	–	0,0213	0,0425	0,0638	0,0851	0,1063	0,1276	0,1489	0,1702
ε_r	–	$4{,}3\text{x}10^{-4}$	$4{,}3\text{x}10^{-4}$	$4{,}3\text{x}10^{-4}$	$4{,}3\text{x}10^{-4}$	$4{,}3\text{x}10^{-4}$	$4{,}3\text{x}10^{-4}$	$4{,}3\text{x}10^{-4}$	$4{,}3\text{x}10^{-4}$
L_i (m)	–	50,00	100,00	150,00	200,00	250,00	300,0	350,00	400,00
$d_g\sqrt{2}$ (m)	–	0,1702	0,1702	0,1702	0,1702	0,1702	0,1702	0,1702	0,1702

Table 6-2: Displacements of set A for ground type C.

Displacements of set B

	Ground type A	Ground type C
Δd_i (m)	**0,0041**	**0,0106**
β_r	0,50	0,50
ε_r	$1{,}64\text{x}10^{-4}$	$4{,}25\text{x}10^{-4}$
$L_{\alpha v,i}$ (m)	50,00	50,00

Table 6-3: Displacements Δd_i, of set B for ground types A and C.

	Ground type A d_i (m)	Ground type C d_i (m)
Abutment 1	0,0000	0,0000
Pier 1	0,0021	0,0053
Pier 2	-0,0021	-0,0053
Pier 3	0,0021	0,0053
Pier 4	-0,0021	-0,0053
Pier 5	0,0021	0,0053
Pier 6	-0,0021	-0,0053
Pier 7	0,0021	0,0053
Abutment 2	0,0000	0,0000

Table 6-4: Displacements of set B for ground type A and C.

6.2 Modelling of Bridge 4

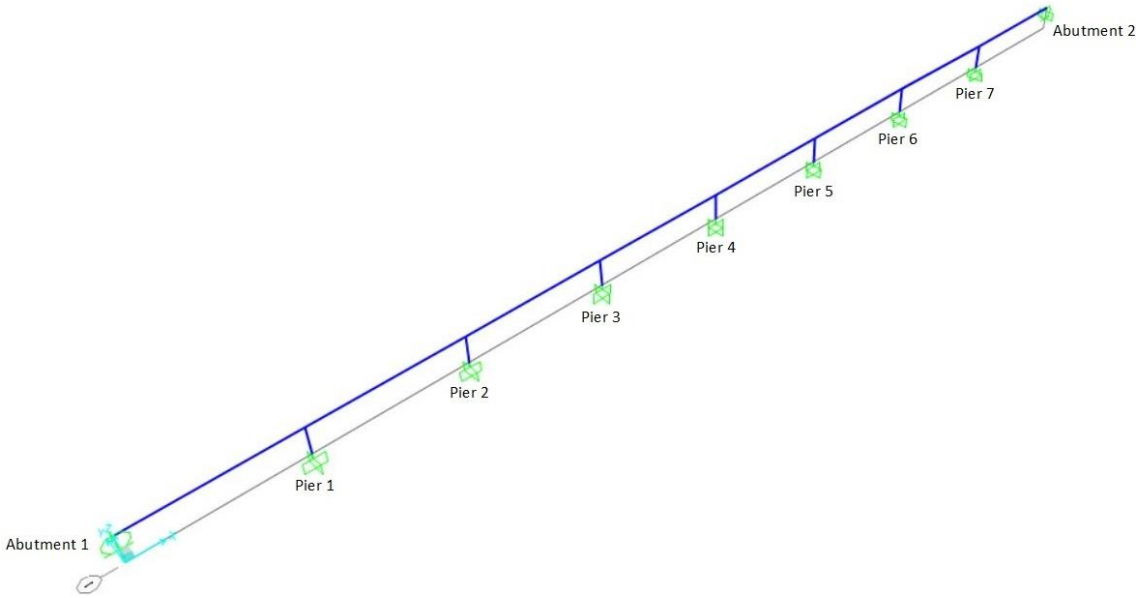

Figure 6-2: Modelling of Bridge 4 in SAP2000.

After inserting Bridge 4 model and its actions and combinations in SAP2000, for both ground types, the vibration modes and deformations for each of loading situation were attained and displayed below.

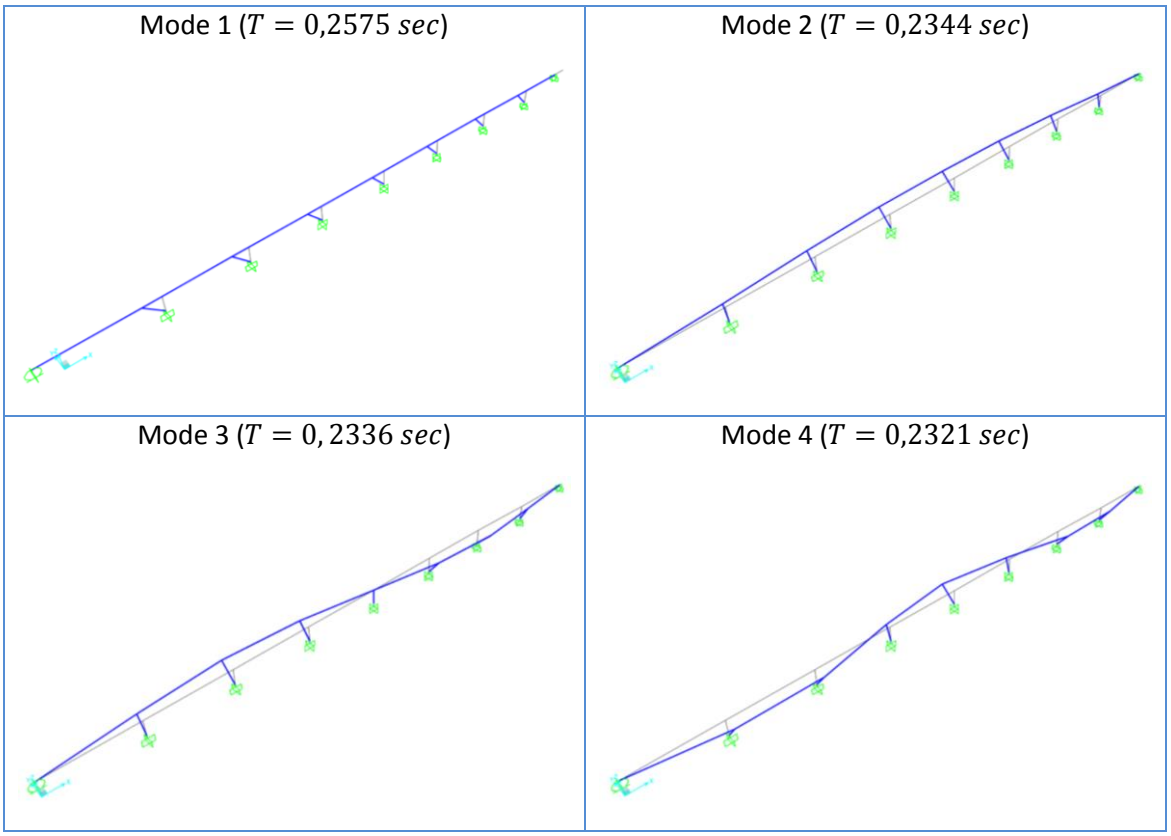

Figure 6-3: First four vibration modes of Bridge 4.

Ground type A

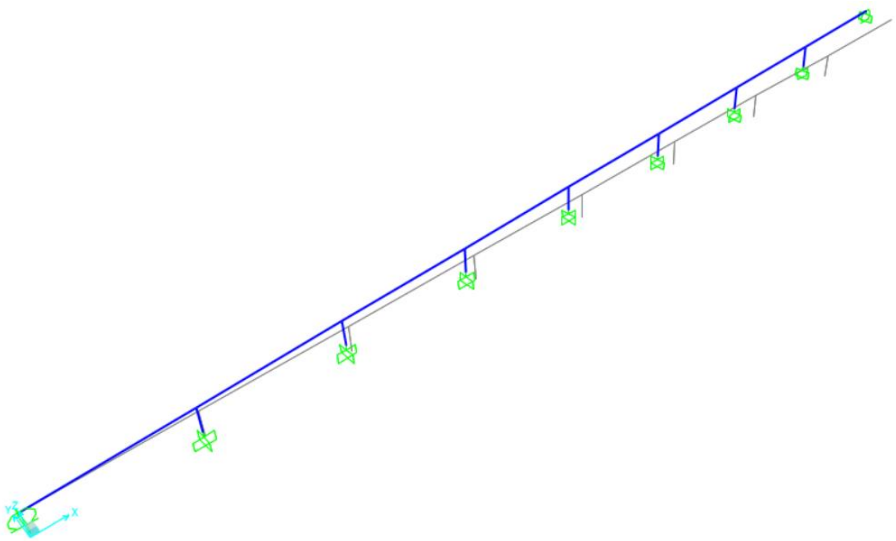

Figure 6-4: Deformation of Bridge 4 caused by the displacements of set A for ground type A.

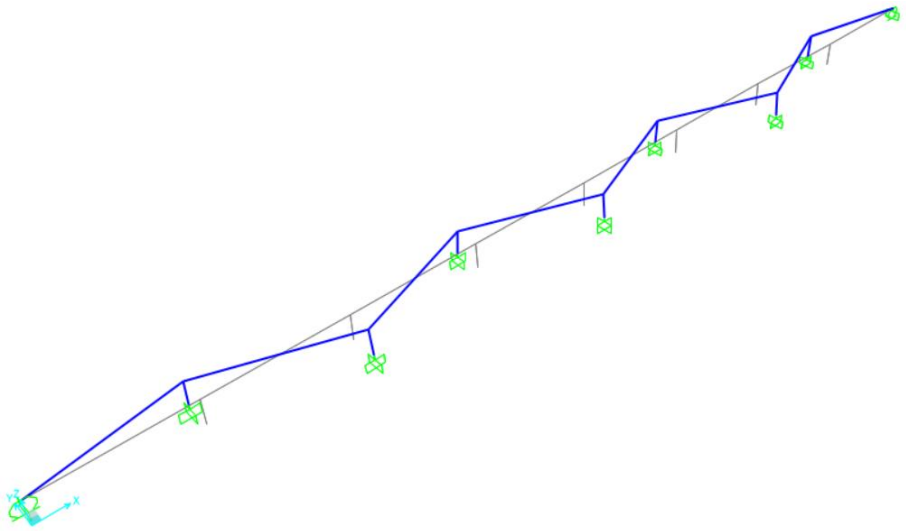

Figure 6-5: Deformation of Bridge 4 caused by the displacements of set B for ground type A.

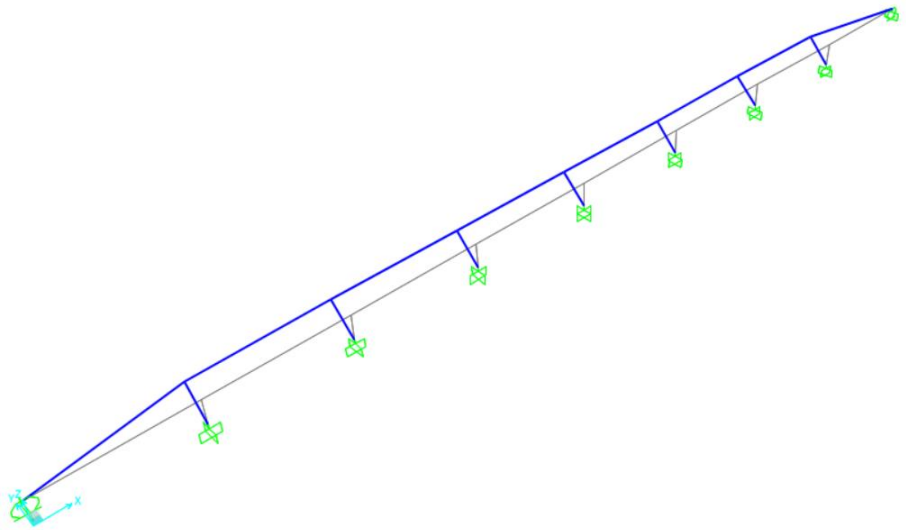

Figure 6-6: Deformation of Bridge 4 caused by the response spectrum for ground type A.

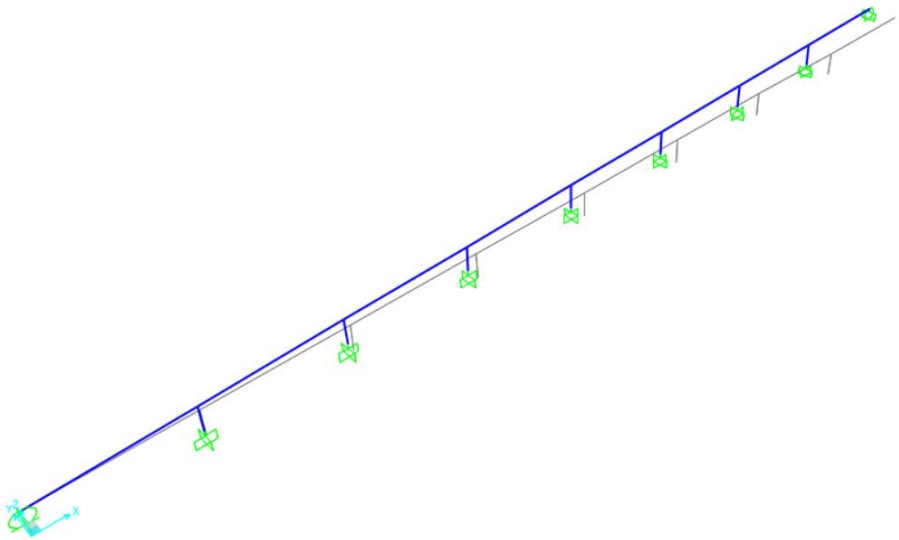

Figure 6-7: Deformation of Bridge 4 caused by the combination of the actions of the response spectrum and the displacements of set A for ground type A.

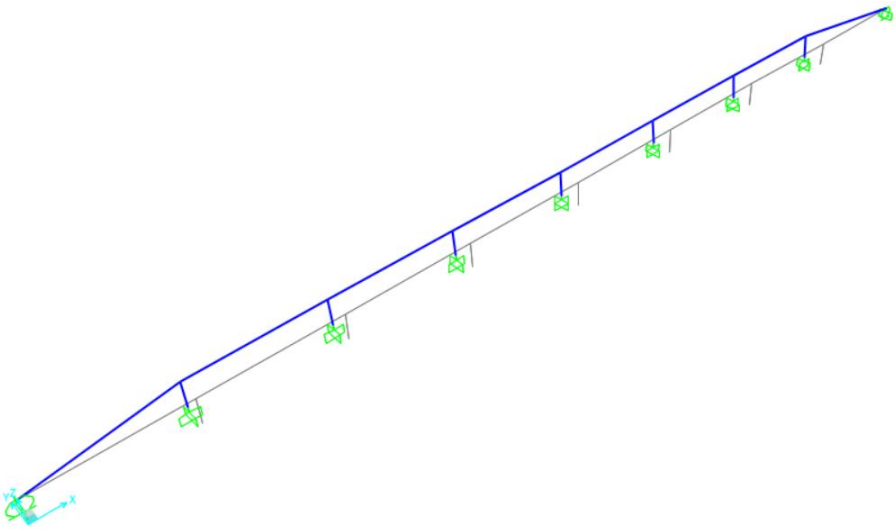

Figure 6-8: Deformation of Bridge 4 caused by the combination of the actions of the response spectrum and the displacements of set B for ground type A.

Ground type C

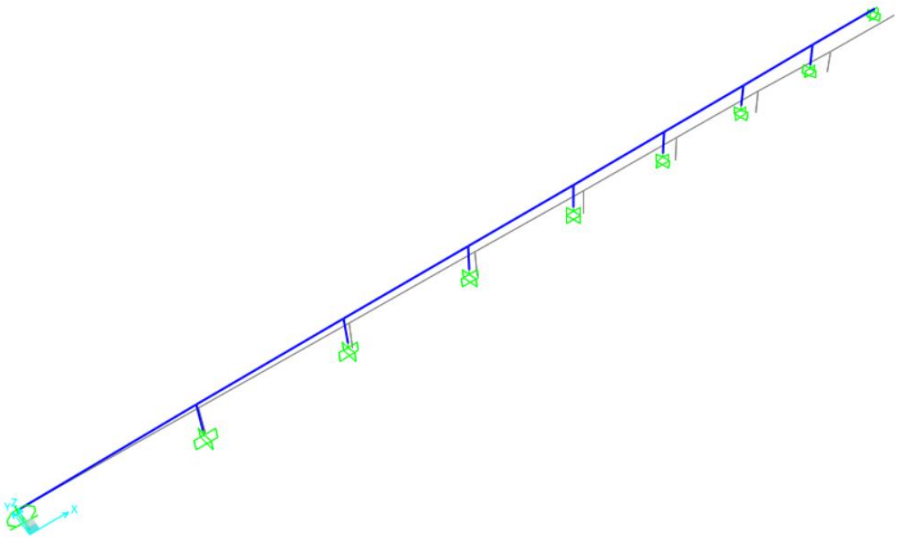

Figure 6-9: Deformation of Bridge 4 caused by the displacements of set A for ground type C.

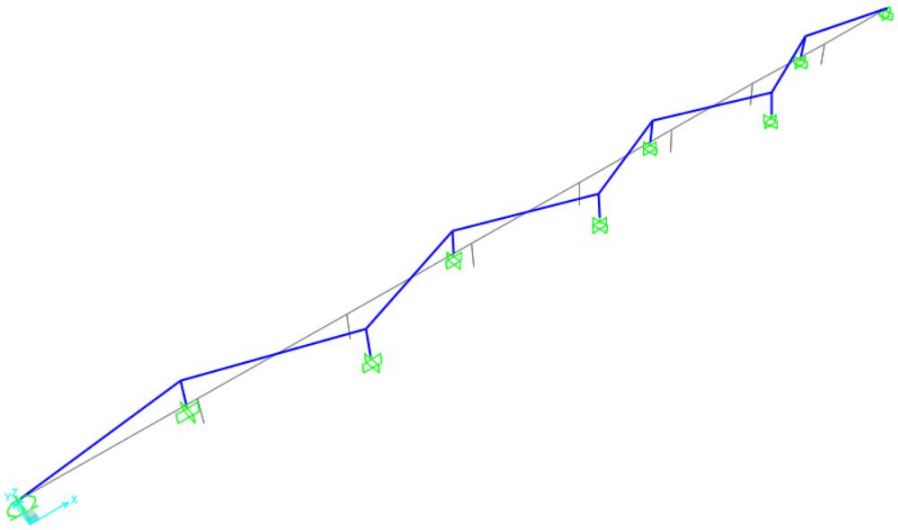

Figure 6-10: Deformation of Bridge 4 caused by the displacements of set B for ground type C.

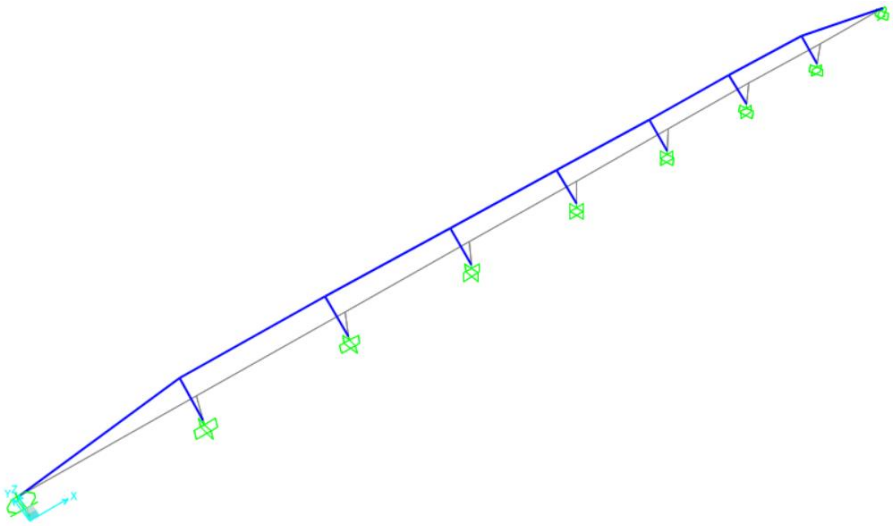

Figure 6-11: Deformation of Bridge 4 caused by the response spectrum for ground type C.

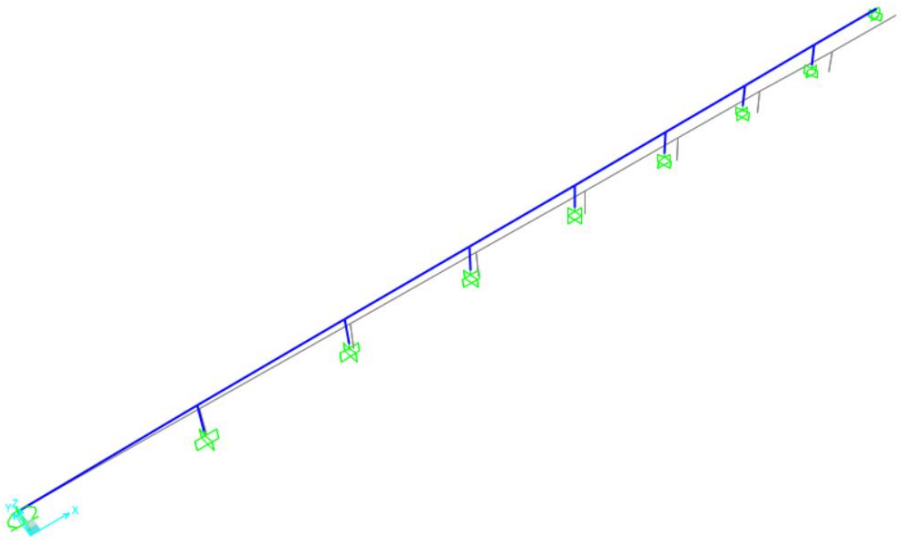

Figure 6-12: Deformation of Bridge 4 caused by the combination of the actions of the response spectrum and the displacements of set A for ground type C.

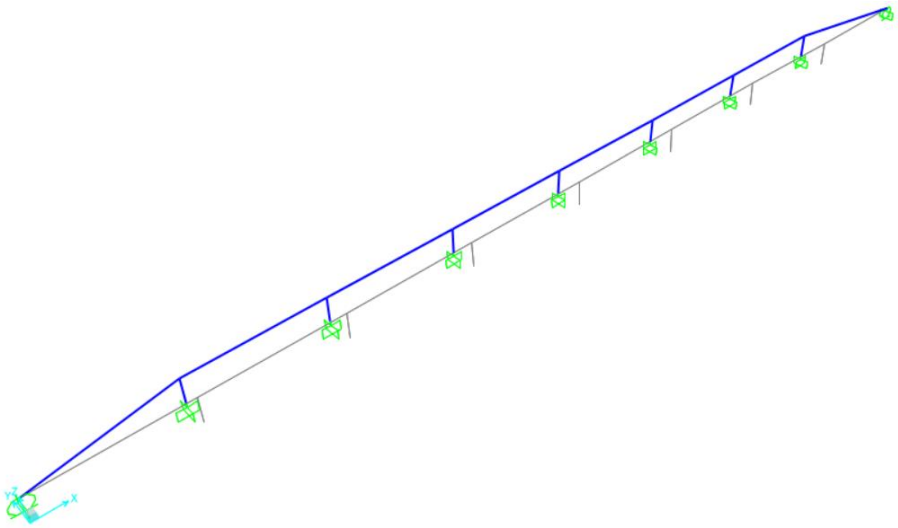

Figure 6-13: Deformation of Bridge 4 caused by the combination of the actions of the response spectrum and the displacements of set B for ground type C.

6.3 Synchronous analysis

The synchronous analysis is represented in *Figures 6-6* and *6-11* previously presented, whether it is a ground type A or a ground type C.

6.3.1 Base shears and displacements of the deck

For carrying out the synchronous analysis, the base shears and the displacements of the deck, attained through SAP2000 are displayed in the following tables.

	Base shear (kN)	Displacements of the deck (m)
Abutment 1	13,69	0,0000
Pier 1	799,24	0,0012
Pier 2	860,57	0,0013
Pier 3	829,09	0,0012
Pier 4	836,23	0,0013
Pier 5	829,09	0,0012
Pier 6	860,57	0,0013
Pier 7	799,24	0,0012
Abutment 2	13,69	0,0000

Table 6-5: Values of base shear and displacements of the deck considering the single action of the response spectrum for ground type A.

	Base shear (kN)	Displacements of the deck (m)
Abutment 1	15,74	0,0000
Pier 1	919,12	0,0014
Pier 2	989,66	0,0015
Pier 3	953,45	0,0014
Pier 4	961,67	0,0014
Pier 5	953,45	0,0014
Pier 6	989,66	0,0015
Pier 7	919,12	0,0014
Abutment 2	15,74	0,0000

Table 6-6: Values of base shear and displacements of the deck considering the single action of the response spectrum for ground type C.

It is possible to conclude, from observing the tables that for both the base shear and the displacements of the deck, it is from ground type C that the highest values are attained. With respect to the base shears, there is a great difference between considering a ground type A or

a ground type C (around 100 kN), whereas in the displacements of the deck, the difference is so insignificant (0,2 mm) that it can despised.

Whether we are considering the base shear or the displacements of the deck for both ground types, the values are symmetric and achieve their maximum expression in piers 2 and 6.

6.3.2 Shear forces and bending moments

The efforts attained by the synchronous analysis of Bridge 4 and the related diagrams are all included in the table below.

Ground type A

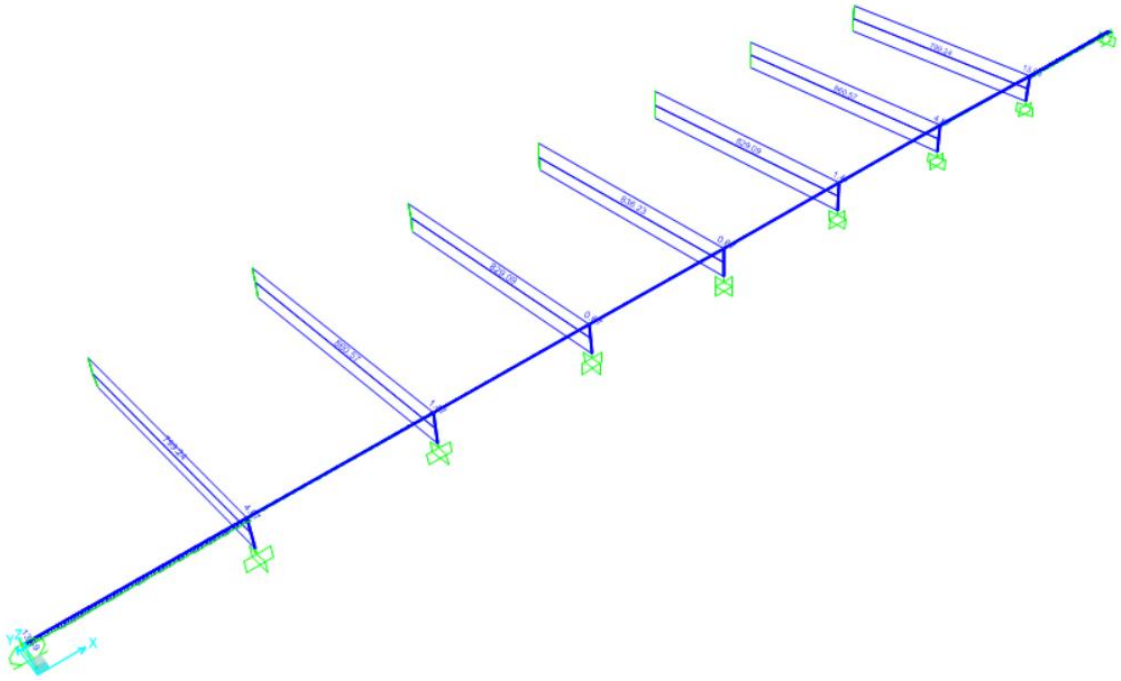

Figure 6-14: Diagrams of shear forces on Bridge 4, caused by the single action of the response spectrum for ground type A.

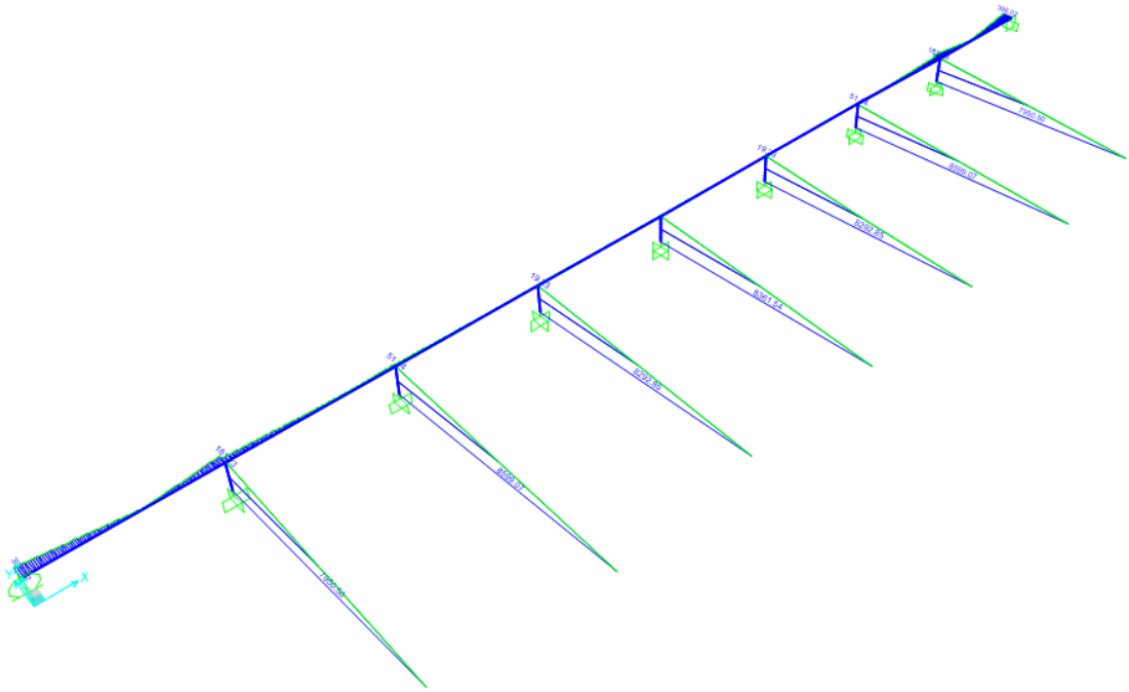

Figure 6-15: Diagrams of bending moments on Bridge 4, caused by the single action of the response spectrum for ground type A.

Piers	V (kN)	M (kN.m)
Top of pier 1	799,24	43,14
Base of pier 1	799,24	7950,50
Top of pier 2	860,57	12,87
Base of pier 2	860,57	8599,07
Top of pier 3	829,09	3,94
Base of pier 3	829,09	8292,85
Top of pier 4	836,23	2,73
Base of pier 4	836,23	8361,54
Top of pier 5	829,09	3,94
Base of pier 5	829,09	8292,85
Top of pier 6	860,57	12,87
Base of pier 6	860,57	8599,07
Top of pier 7	799,24	43,14
Base of pier 7	799,24	7950,50

Table 6-7: Values of shear forces and bending moments of the piers in Bridge 4, caused by the single action of the response spectrum for ground type A.

Deck	V (kN)	M (kN.m)
Abutment 1	13,69	398,02
Pier 1, left	13,69	287,04
Pier 1, right	4,87	181,23
Pier 2, left	4,87	74,76
Pier 2, right	1,47	25,60
Pier 3, left	1,47	51,13
Pier 3, right	0,67	19,23
Pier 4, left	0,67	15,31
Pier 4, right	0,67	15,31
Pier 5, left	0,67	19,23
Pier 5, right	1,47	51,13
Pier 6, left	1,47	25,60
Pier 6, right	4,87	74,76
Pier 7, left	4,87	181,23
Pier 7, right	13,69	287,04
Abutment 2	13,69	398,02

Table 6-8: Values of shear forces and bending moments of the deck in Bridge 4, caused by the single action of the response spectrum for ground type A.

Ground type C

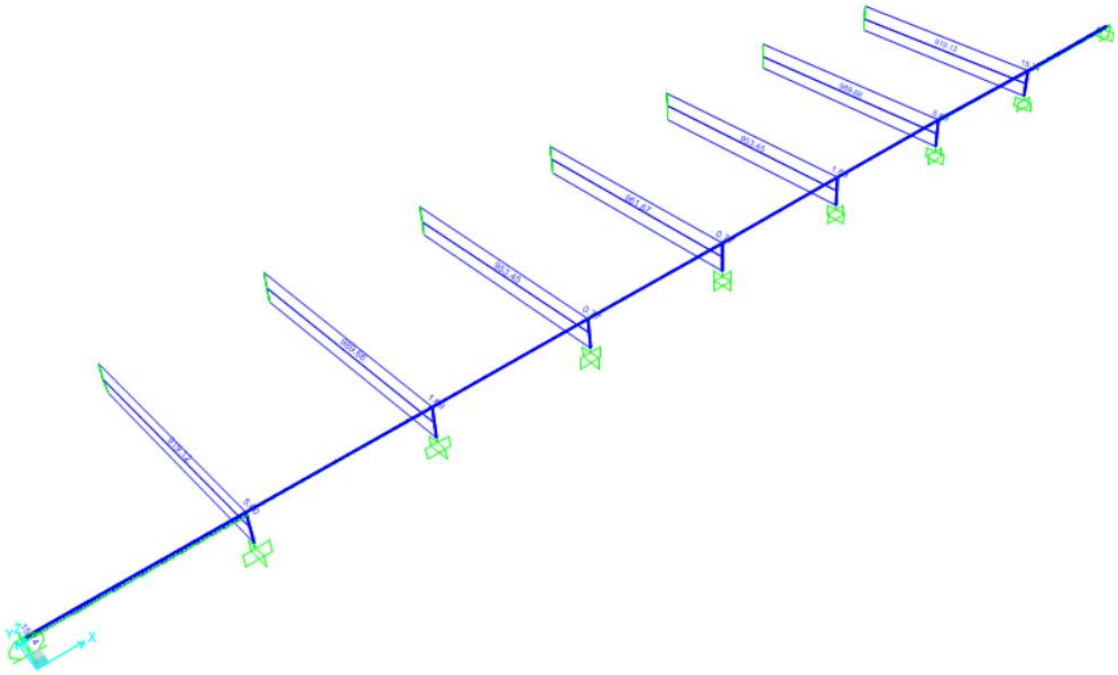

Figure 6-16: Diagrams of shear forces on Bridge 4, caused by the single action of the response spectrum for ground type C.

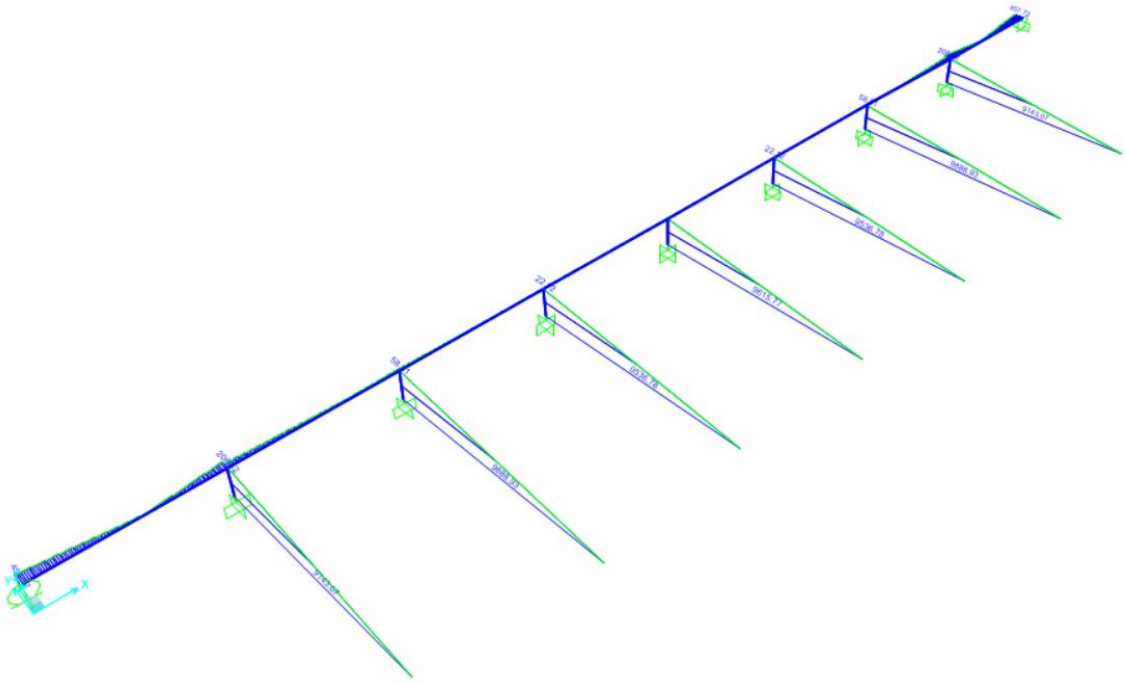

Figure 6-17: Diagrams of bending moments on Bridge 4, caused by the single action of the response spectrum for ground type C.

Piers	V (kN)	M (kN.m)
Top of pier 1	919,12	49,61
Base of pier 1	919,12	9143,07
Top of pier 2	989,66	14,80
Base of pier 2	989,66	9888,93
Top of pier 3	953,45	4,53
Base of pier 3	953,45	9536,78
Top of pier 4	961,67	3,14
Base of pier 4	961,67	9615,77
Top of pier 5	953,45	4,53
Base of pier 5	953,45	9536,78
Top of pier 6	989,66	14,80
Base of pier 6	989,66	9888,93
Top of pier 7	919,12	49,61
Base of pier 7	919,12	9143,07

Table 6-9: Values of shear forces and bending moments of the piers in Bridge 4, caused by the single action of the response spectrum for ground type C.

Deck	V (kN)	M (kN.m)
Abutment 1	15,74	457,72
Pier 1, left	15,74	330,10
Pier 1, right	5,60	208,42
Pier 2, left	5,60	85,97
Pier 2, right	1,69	58,81
Pier 3, left	1,69	29,44
Pier 3, right	0,76	22,12
Pier 4, left	0,76	17,61
Pier 4, right	0,76	17,61
Pier 5, left	0,76	22,12
Pier 5, right	1,69	29,44
Pier 6, left	1,69	58,81
Pier 6, right	5,60	85,97
Pier 7, left	5,60	208,42
Pier 7, right	15,74	330,10
Abutment 2	15,74	457,72

Table 6-10: Values of shear forces and bending moments of the deck in Bridge 4, caused by the single action of the response spectrum for ground type C.

The structure's piers are the elements enduring the highest efforts in the whole structure, whether it considers the shear force or bending moments. The shear force of the deck is depreciable, and the bending moments very low, especially in the center of the structure.

As for the bending moments of the deck, they are higher next to the abutments and lower in the center of the structure with few value changes whether it refers to a ground type A or a ground type C.

The highest values are attained for the ground type C, since it possesses a more accelerated response spectrum than ground type A.

6.3.3 Drifts of the piers

The drifts attained for each of the piers of Bridge 4 were calculated using the method presented in 4.3.3. For the synchronous analysis the attained results are displayed below.

	High (m)	δ_d (m)	δ_f (m)	q	θ (rad)
Pier 1	10,00	0,0012	0,0000	1,00	**1,19x10^{-4}**
Pier 2	10,00	0,0013	0,0000	1,00	**1,29x10^{-4}**
Pier 3	10,00	0,0012	0,0000	1,00	**1,25x10^{-4}**
Pier 4	10,00	0,0013	0,0000	1,00	**1,26x10^{-4}**
Pier 5	10,00	0,0012	0,0000	1,00	**1,25x10^{-4}**
Pier 6	10,00	0,0013	0,0000	1,00	**1,29x10^{-4}**
Pier 7	10,00	0,0012	0,0000	1,00	**1,19x10^{-4}**

Table 6-11: Drift of the piers due to the application of the response spectrum for ground type A.

	High (m)	δ_d (m)	δ_f (m)	q	θ (rad)
Pier 1	10,00	0,0014	0,0000	1,00	**1,37x10^{-4}**
Pier 2	10,00	0,0015	0,0000	1,00	**1,49x10^{-4}**
Pier 3	10,00	0,0014	0,0000	1,00	**1,43x10^{-4}**
Pier 4	10,00	0,0014	0,0000	1,00	**1,45x10^{-4}**
Pier 5	10,00	0,0014	0,0000	1,00	**1,43x10^{-4}**
Pier 6	10,00	0,0015	0,0000	1,00	**1,49x10^{-4}**
Pier 7	10,00	0,0014	0,0000	1,00	**1,37x10^{-4}**

Table 6-12: Drift of the piers due to the application of the response spectrum for ground type C.

As in the previous explanations, the values in this situation are symmetric and the maximum is attained in piers 2 and 6, for both ground types. The highest values are attained when the ground is type C.

It is important to remark that these values are very low due to the bending stiffness provided from the pier section, keeping them from deforming too much.

6.4 Asynchronous analysis

The asynchronous analysis is previously represented in *Figures 6-7*, *6-8*, *6-12* and *6-13*, whether it concerns a ground type A or a ground type C.

6.4.1 Base shears and displacements of the deck

During the asynchronous analysis, the values of base shear and the displacements of the deck, attained from SAP2000 for each of the considered grounds are displayed below.

Ground type A

	Base shear (kN)	Displacements of the deck (m)
Abutment 1	67,88	0,0000
Pier 1	801,07	0,0082
Pier 2	860,64	0,0165
Pier 3	829,09	0,0247
Pier 4	836,23	0,0329
Pier 5	829,09	0,0411
Pier 6	860,63	0,0493
Pier 7	801,15	0,0576
Abutment 2	68,93	0,0658

Table 6-13: Values of base shear and displacements of the deck considering the combination of the response spectrum for ground type A with the displacements of set A.

	Base shear (kN)	Displacements of the deck (m)
Abutment 1	44,75	0,00000
Pier 1	805,43	0,00229
Pier 2	868,91	0,00232
Pier 3	838,77	0,00228
Pier 4	845,98	0,00229
Pier 5	838,77	0,00228
Pier 6	868,91	0,00232
Pier 7	805,43	0,00229
Abutment 2	44,75	0,00000

Table 6-14: Values of base shear and displacements of the deck considering the combination of the response spectrum for ground type A with the displacements of set B.

Ground type C

	Base shear (kN)	Displacements of the deck (m)
Abutment 1	173,63	0,0000
Pier 1	929,85	0,0211
Pier 2	989,98	0,0426
Pier 3	953,46	0,0638
Pier 4	961,67	0,0851
Pier 5	953,47	0,1063
Pier 6	989,97	0,1276
Pier 7	929,68	0,1491
Abutment 2	173,27	0,1702

Table 6-15: Values of base shear and displacements of the deck considering the combination of the response spectrum for ground type C with the displacements of set A.

	Base shear (kN)	Displacements of the deck (m)
Abutment 1	108,66	0,00000
Pier 1	952,92	0,00512
Pier 2	1035,04	0,00508
Pier 3	1005,94	0,00504
Pier 4	1014,51	0,00504
Pier 5	1005,94	0,00504
Pier 6	1035,04	0,00508
Pier 7	952,92	0,00512
Abutment 2	108,66	0,00000

Table 6-16: Values of base shear and displacements of the deck considering the combination of the response spectrum for ground type C with the displacements of set B.

It is possible to conclude from observing the tables, that the combination of the response spectrum with the displacements of set A, in both ground types, is the one responsible for the highest displacements of the deck. As for shear forces, it is from the combination considering the displacements of set B that the highest values for the piers are attained.

The displacements attained from set A are much higher than in the synchronous analysis, providing for the linear increase from abutment 1 to abutment 2. Considering the shear forces, they have a similar development to the synchronous situation, but with slightly higher values, being the highest attained on piers 2 and 6.

In both situations, only when a ground type C was considered, were the highest results attained.

6.4.2 Shear forces and bending moments

The efforts attained for the asynchronous analysis of Bridge 4 and their related diagrams are represented below.

Ground type A

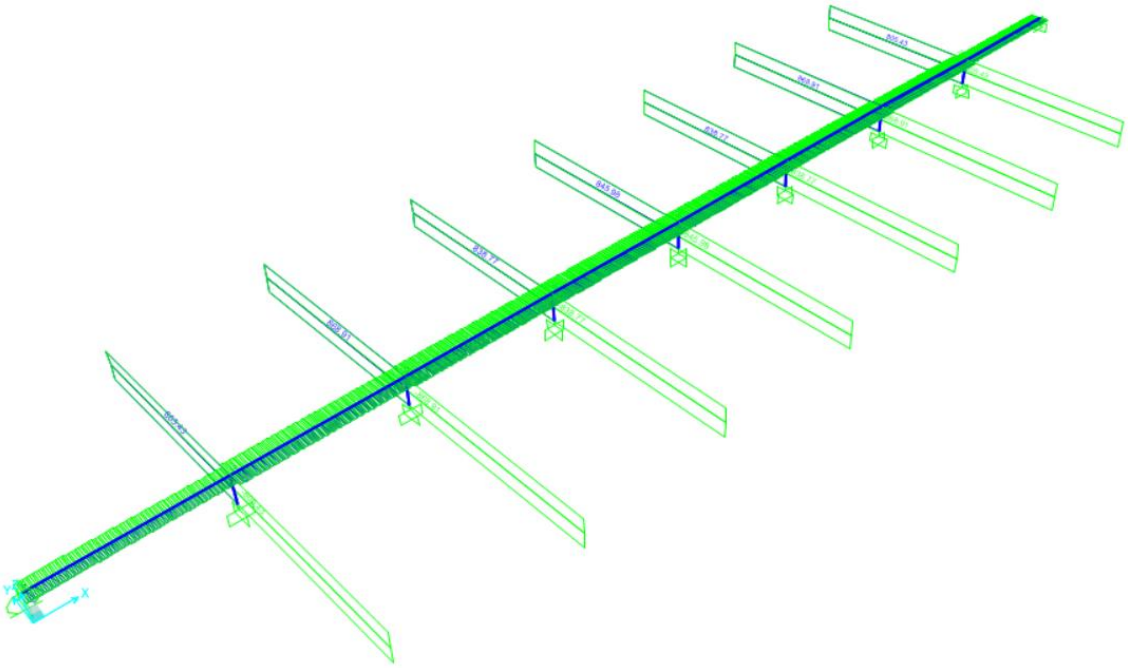

Figure 6-18: Diagrams of shear forces on Bridge 4, caused by the combination of the response spectrum for ground type A with the displacements of set B.

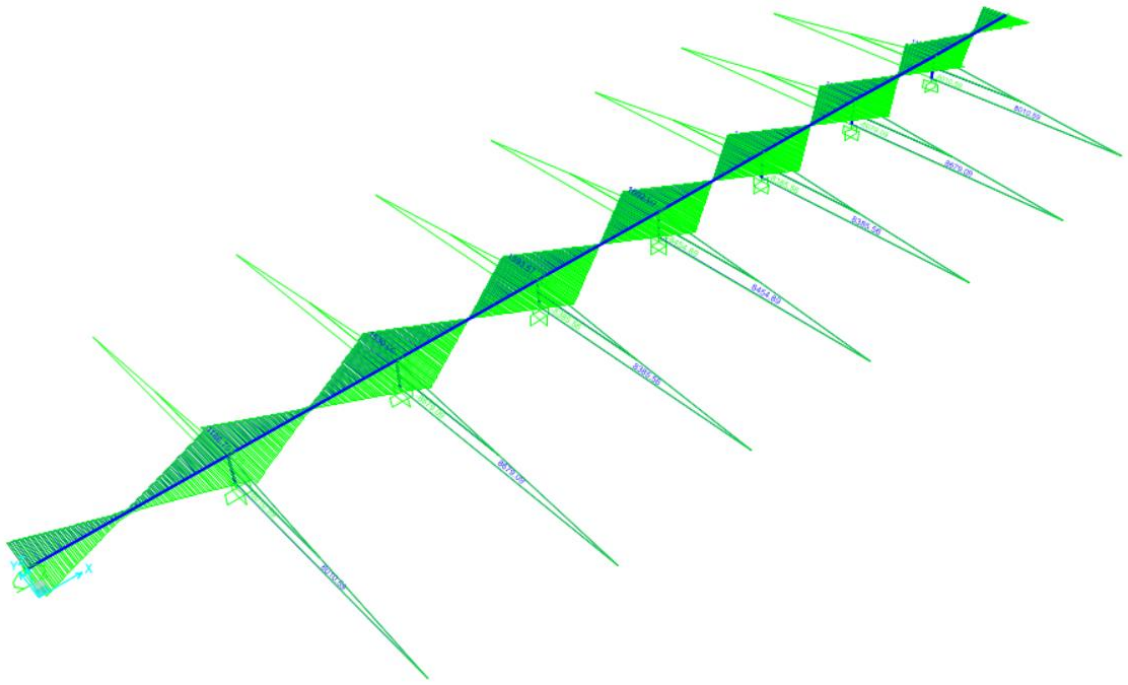

Figure 6-19: Diagrams of bending moments on Bridge 4, caused by the combination of the response spectrum for ground type A with the displacements of set B.

Piers	V (kN)	M (kN.m)
Top of pier 1	805,43	46,49
Base of pier 1	805,43	8010,59
Top of pier 2	868,91	28,34
Base of pier 2	868,91	8679,08
Top of pier 3	838,77	27,40
Base of pier 3	838,77	8385,56
Top of pier 4	845,98	27,67
Base of pier 4	845,98	8454,89
Top of pier 5	838,77	27,40
Base of pier 5	838,77	8385,56
Top of pier 6	868,91	28,34
Base of pier 6	868,91	8679,08
Top of pier 7	805,43	46,49
Base of pier 7	805,43	8010,59

Table 6-17: Values of shear forces and bending moments of the piers of Bridge 4, caused by the combination of the response spectrum for ground type A with the displacements of set B.

Deck	V (kN)	M (kN.m)
Abutment 1	44,75	1056,36
Pier 1, left	44,75	1186,79
Pier 1, right	57,27	1337,33
Pier 2, left	57,27	1530,09
Pier 2, right	63,06	1559,38
Pier 3, left	63,06	1593,67
Pier 3, right	64,03	1598,31
Pier 4, left	64,03	1602,99
Pier 4, right	64,03	1602,99
Pier 5, left	64,03	1598,31
Pier 5, right	63,06	1593,67
Pier 6, left	63,06	1559,38
Pier 6, right	57,27	1530,09
Pier 7, left	57,27	1337,33
Pier 7, right	44,75	1186,79
Abutment 2	44,75	1056,36

Table 6-18: Values of shear forces and bending moments of the deck of Bridge 4, caused by the combination of the response spectrum for ground type A with the displacements of set B.

Ground type C

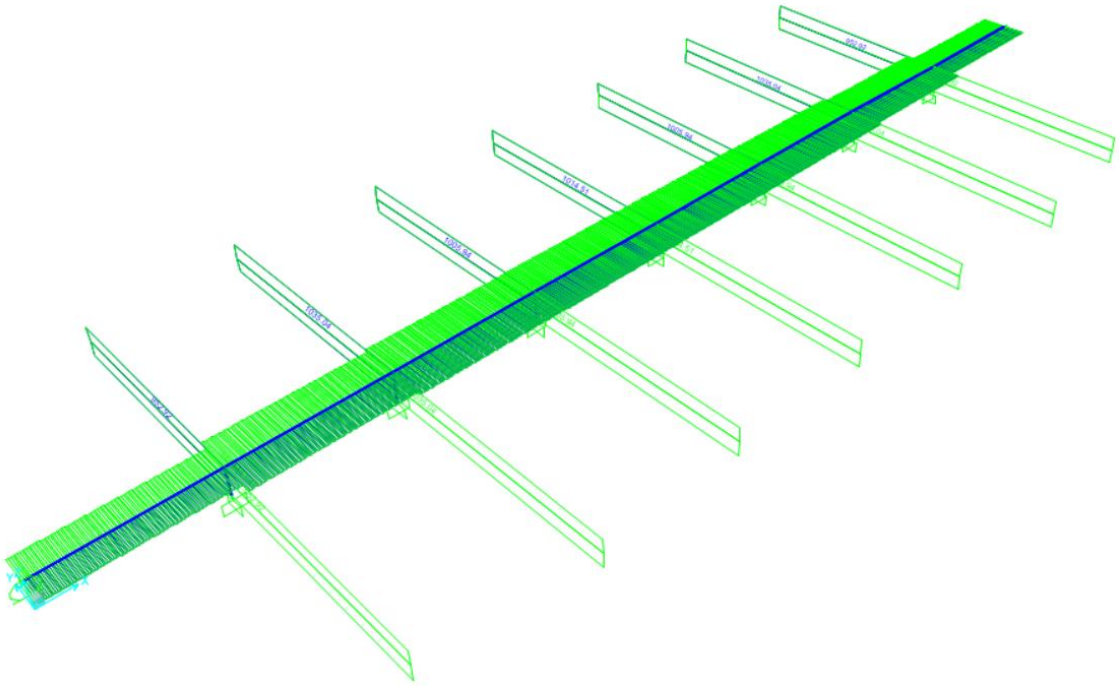

Figure 6-20: Diagrams of shear forces on Bridge 4, caused by the combination of the response spectrum for ground type C with the displacements of set B.

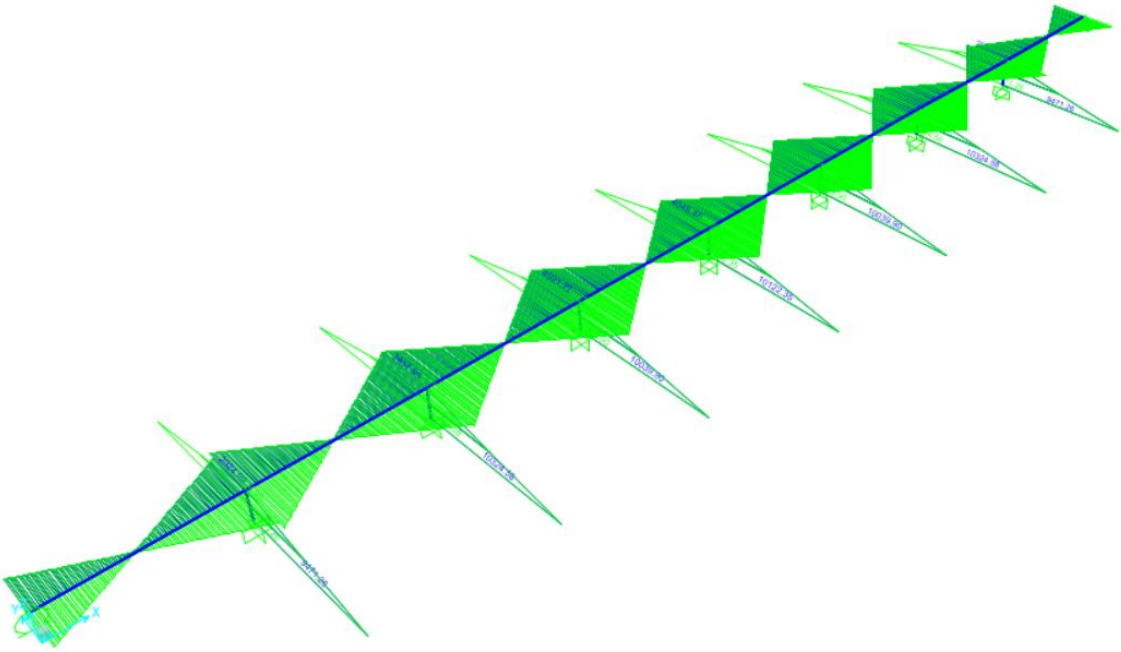

Figure 6-21: Diagrams of bending moments on Bridge 4, caused by the combination of the response spectrum for ground type C with the displacements of set B.

Piers	V (kN)	M (kN.m)
Top of pier 1	952,92	66,15
Base of pier 1	952,92	9471,26
Top of pier 2	1035,04	65,44
Base of pier 2	1035,04	10324,58
Top of pier 3	1005,94	68,58
Base of pier 3	1005,94	10039,90
Top of pier 4	1014,51	69,56
Base of pier 4	1014,51	10122,35
Top of pier 5	1005,94	68,58
Base of pier 5	1005,94	10039,90
Top of pier 6	1035,04	65,44
Base of pier 6	1035,04	10324,58
Top of pier 7	952,92	66,15
Base of pier 7	952,92	9471,26

Table 6-19: Values of shear forces and bending moments of the piers of Bridge 4, caused by the combination of the response spectrum for ground type C with the displacements of set B.

Deck	V (kN)	M (kN.m)
Abutment 1	108,66	2511,62
Pier 1, left	108,66	2924,99
Pier 1, right	144,13	3350,53
Pier 2, left	144,13	3857,99
Pier 2, right	159,11	3933,90
Pier 3, left	159,11	4021,72
Pier 3, right	161,58	4033,60
Pier 4, left	161,58	4045,48
Pier 4, right	161,58	4045,48
Pier 5, left	161,58	4033,60
Pier 5, right	159,11	4021,72
Pier 6, left	159,11	3933,90
Pier 6, right	144,13	3857,99
Pier 7, left	144,13	3350,53
Pier 7, right	108,66	2924,99
Abutment 2	108,66	2511,62

Table 6-20: Values of shear forces and bending moments of the deck of Bridge 4, caused by the combination of the response spectrum for ground type C with the displacements of set B.

As it had occurred during the synchronous analysis, piers are still the most loaded elements of the structure. However, one should notice that the values attained whether for the shear force or for the bending moment of the deck are much higher than previously. When a ground type C is considered the highest results are attained.

For the piers, as it happened in the synchronous analysis, the values attained are symmetric for both the shear force and the bending moment, achieving its maximum in piers 2 and 6.

With respect to the bending moment of the deck, this is much higher when a ground type C is considered rather than a ground type A (around 2450 kN on pier 2). These bending moments have a symmetric distribution, with the highest values concentrate in the center of the bridge.

6.4.3 Drifts of the piers

By using the calculation method explained in 4.3.3, the following drifts for the asynchronous analysis of Bridge 4 were attained for each pier.

	High (m)	δ_d (m)	δ_f (m)	q	θ (rad)
Pier 1	10,00	0,0082	0,0082	1,00	**$1{,}30\times10^{-6}$**
Pier 2	10,00	0,0165	0,0164	1,00	**$6{,}60\times10^{-6}$**
Pier 3	10,00	0,0247	0,0247	1,00	**$2{,}80\times10^{-6}$**
Pier 4	10,00	0,0329	0,0023	1,00	**$3{,}06\times10^{-3}$**
Pier 5	10,00	0,0411	0,0411	1,00	**$2{,}10\times10^{-6}$**
Pier 6	10,00	0,0493	0,0493	1,00	**$3{,}00\times10^{-7}$**
Pier 7	10,00	0,0576	0,0575	1,00	**$9{,}40\times10^{-6}$**

Table 6-21: Drift of the piers due to the application of the combination of the response spectrum for ground type A with the displacements of set A.

	High (m)	δ_d (m)	δ_f (m)	q	θ (rad)
Pier 1	10,00	0,0211	0,0213	1,00	**$1{,}64\times10^{-5}$**
Pier 2	10,00	0,0426	0,0425	1,00	**$6{,}20\times10^{-6}$**
Pier 3	10,00	0,0638	0,0638	1,00	**$1{,}10\times10^{-6}$**
Pier 4	10,00	0,0851	0,0851	1,00	**$1{,}10\times10^{-6}$**
Pier 5	10,00	0,1063	0,1063	1,00	**$1{,}70\times10^{-6}$**
Pier 6	10,00	0,1276	0,1276	1,00	**$2{,}60\times10^{-6}$**
Pier 7	10,00	0,1491	0,1489	1,00	**$1{,}13\times10^{-5}$**

Table 6-22: Drift of the piers due to the application of the combination of the response spectrum for ground type C with the displacements of set A.

From the observation of the tables, it is possible to conclude that the attained values are much lower than during the asynchronous analysis, because for the calculation of this drift the displacement of the ground caused by set A is considered.

As it occurred in the synchronous situation, the attained values for ground type C are higher than those of ground type A, as ground type C has a more accelerated spectrum than ground type A.

6.5 Comparison of both analysis

This part of the chapter focus on the comparative study between the two analysis performed over Bridge 4, with the purpose of completing the approach to the considered bridge.

Figure 6-22 represents the variation of the displacements of both analysis and of both ground types throughout the longitudinal development of the bridge. As it can be observed there is a huge difference between considering the asynchrony of seismic waves or not. In the synchronous situation, displacements are quite constant along the whole bridge, leaving no differences between the ground type to consider, A or C. As for the asynchronous analysis, the values grow from abutment 1 to abutment 2, and it is in ground type C where the highest values are clearly attained.

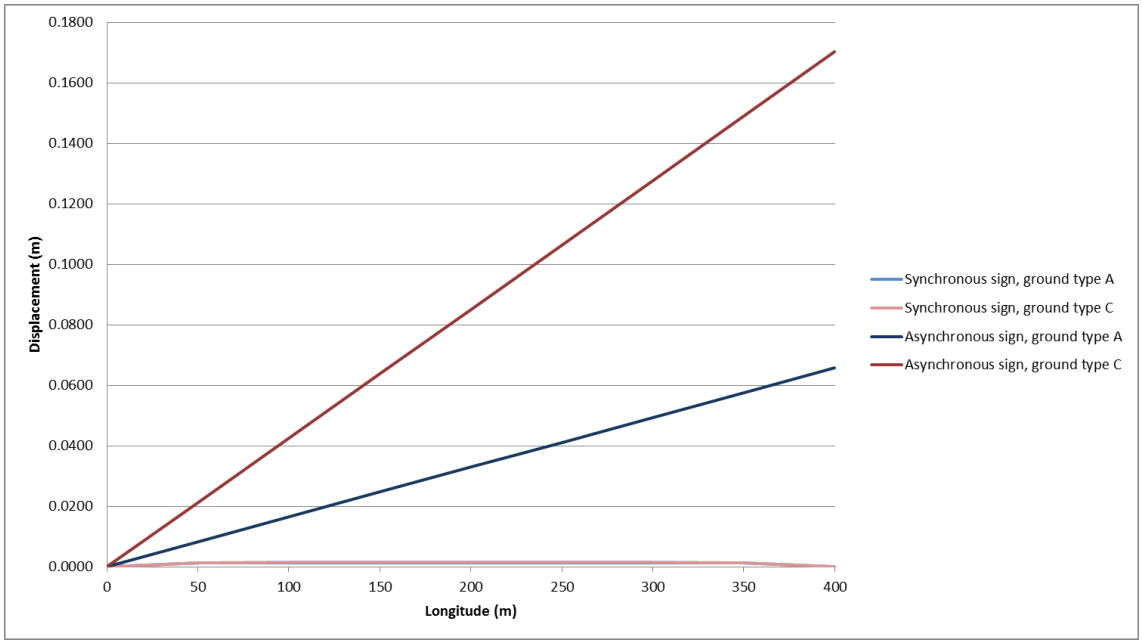

Figure 6-22: Displacements of the deck of Bridge 4.

As mentioned before and represented in *Figures 6-23* and *6-24*, there is hardly no difference between taking on a synchronous or an asynchronous analysis when considering the shear forces and bending moments in piers, especially when the ground is type C. In both situations it is on ground type C that the highest values are attained, with the maximum on piers 2 and 6.

The observation of the structure's vibration modes, represented in *Figure 6-3* leads to the conclusion that each pier can be calculated in a separate way due to the great longitude of the bridge in question. It is important to notice that central piers are not included in certain modes, whereas the outward piers participate in all the modes. This is why the highest values are attained on piers 2 and 6.

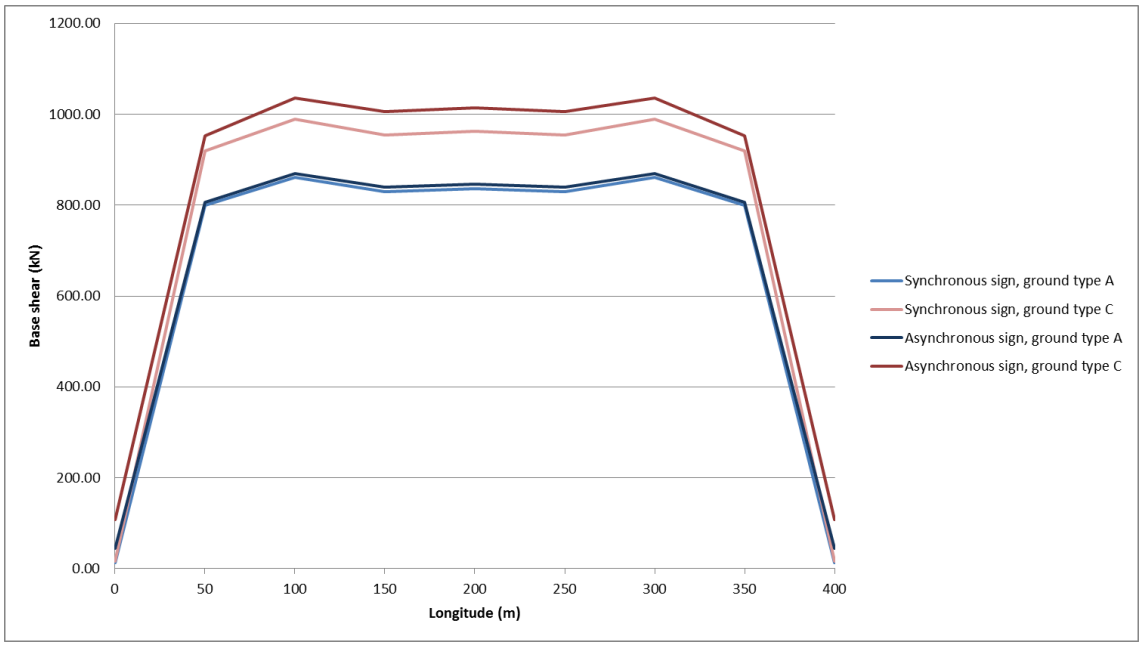

Figure 6-23: Base shear of Bridge 4.

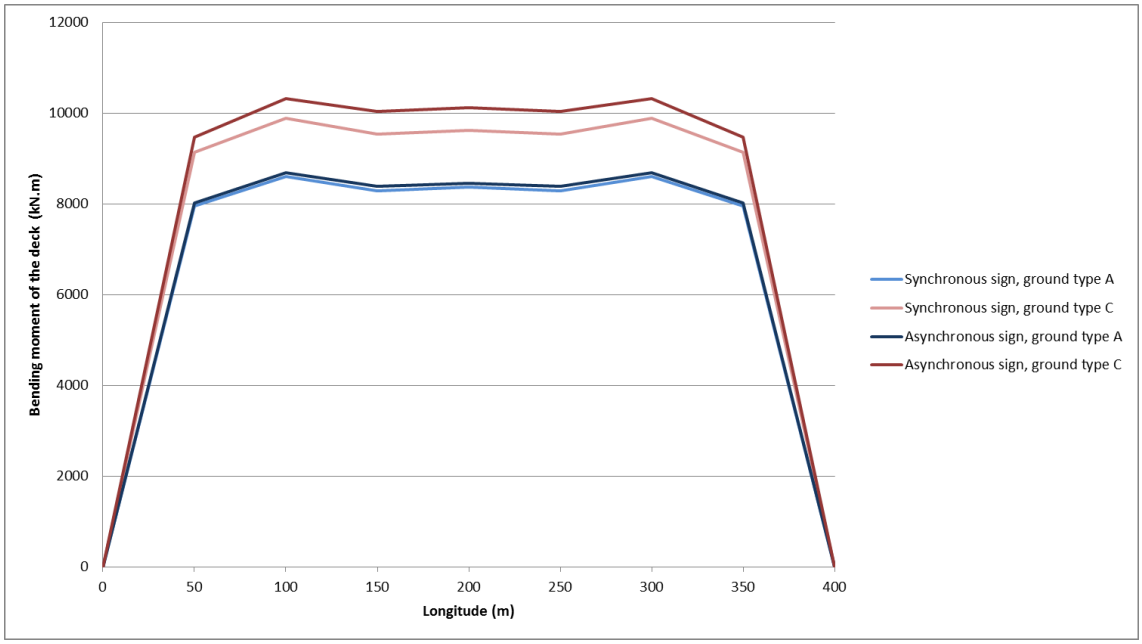

Figure 6-24: Bending moments of the base of the piers of Bridge 4.

As for the bending moments of the deck, as represented in *Figure 6-25*, they have a significant influence on whether to apply the synchrony or asynchrony of seismic waves. In the synchronous analysis lower values are attained, especially in the center of the structure where the difference between considering a ground type A or C is almost none. In the asynchronous analysis, however, the attained moments are much higher and it is clear to conclude that the highest values come from a ground type C.

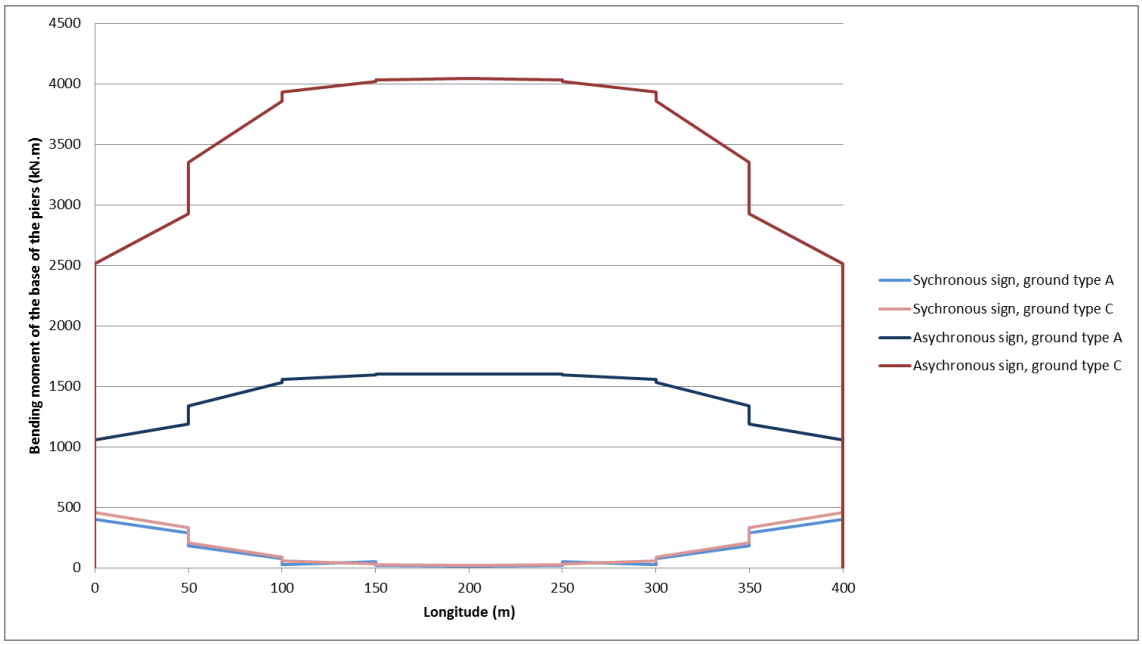

Figure 6-25: Bending moments of the deck of Bridge 4.

7. Comparison of the analysis performed

7.1 Displacements of the deck

The following figures, *Figure 7-1* and *Figure 7-2*, show the evolution of the displacements of the deck according to the longitude, for the four bridges analysed, whereas it is a synchronous or an asynchronous analysis.

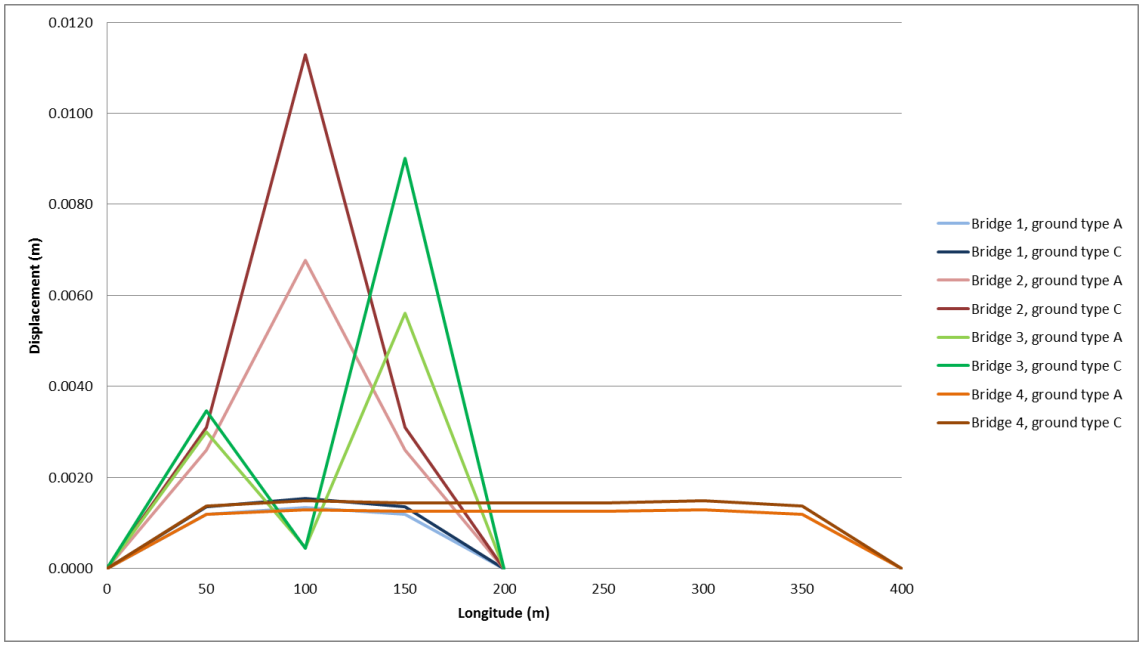

Figure 7-1: Displacements of synchronous analysis of the four bridges and both ground types.

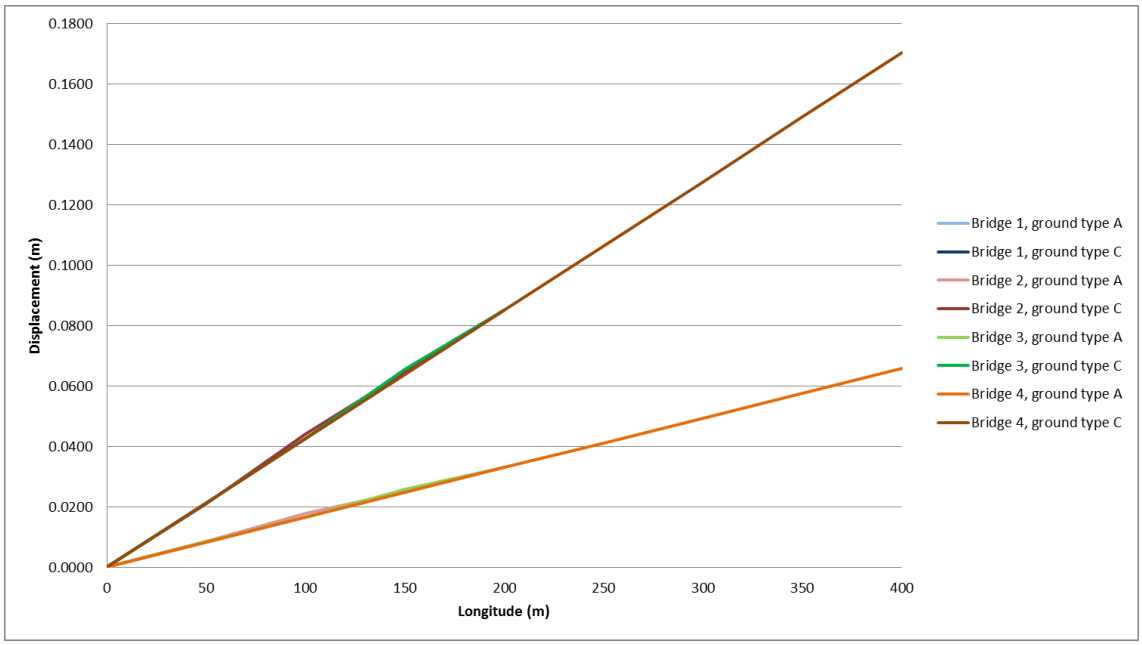

Figure 7-2: Displacements of asynchronous analysis of the four bridges and both ground types.

The analysis of the two figures above leads to the immediate conclusion that the displacements attained in the asynchronous analysis are much higher than the synchronous'.

The variation of the results from bridge to bridge is also a very remarkable difference. As it can be observed, in the synchronous analysis each bridge has its own displacements varying according to the bridge in question and caused only by the action of the response spectrum of the considered ground type. As for the asynchronous analysis, since the displacements attained during its performance are the result of the combination of the response spectrum of the considered ground type with a set of displacements enforced by Eurocode 8 (which imposes a displacement in the piers' foundations), the displacements attained from each bridge are an almost straight line common to all of them, whether they relate to ground type A or ground type C.

Therefore, it is possible to come to the conclusion that the effect of the asynchrony of seismic waves has a significant influence in what concerns the displacements which occur in the deck. As for the variation between considering a ground type A or a ground type C, it does not have a considerable expression for this particular case.

7.2 Base shear

The *Figures 7-3* and *7-4* presented below represent the evolution of the base shear of the piers according to the longitude for the four bridges analysed, whereas it is a synchronous or an asynchronous analysis.

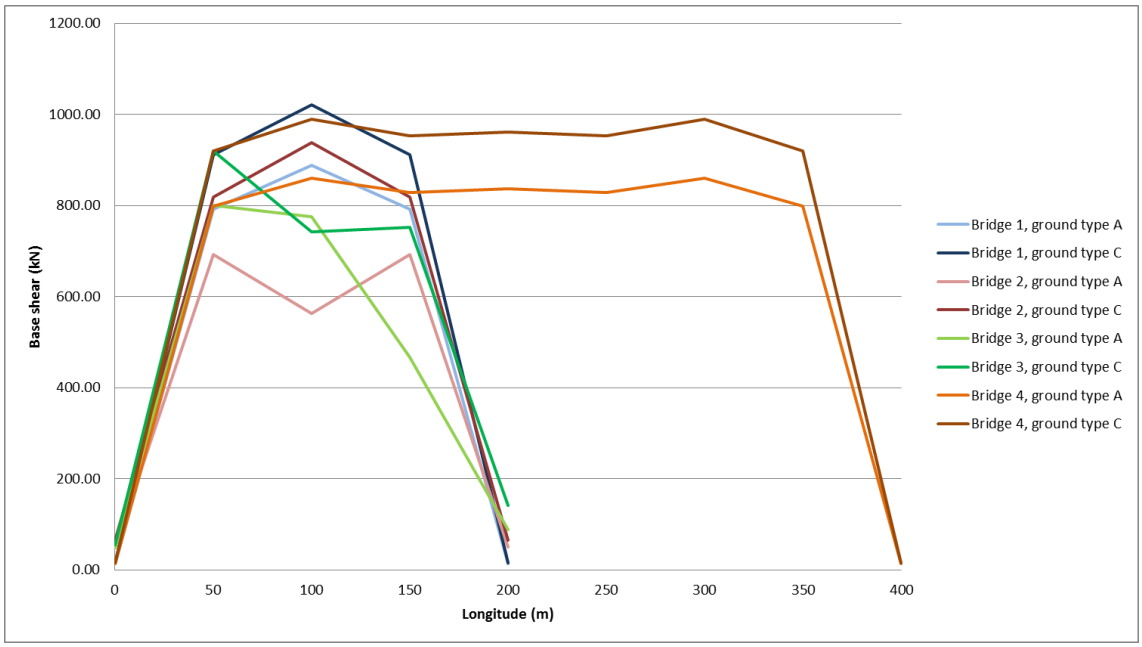

Figure 7-3: Base shear of synchronous analysis of the four bridges and both ground types.

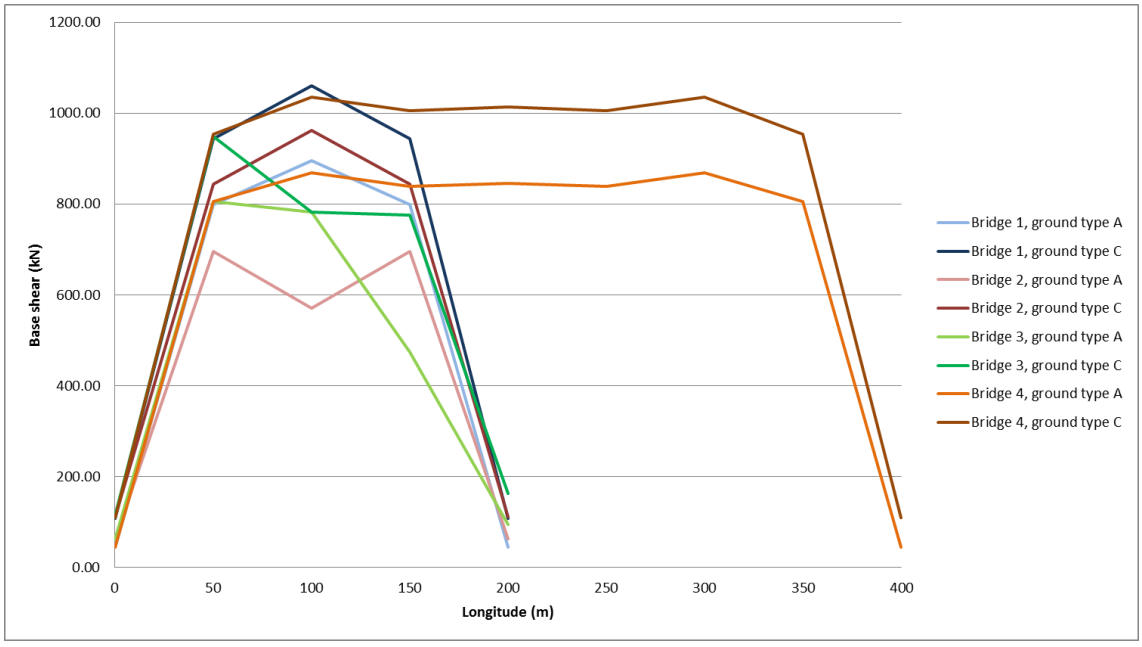

Figure 7-4: Base shear of asynchronous analysis of the four bridges and both ground types.

From the observation of both graphics, it is possible to verify that in all the four studied bridges, whether it is a synchronous or an asynchronous analysis, the order of magnitude of the results is quite close. However, in what concerns the ground type considered, whether type A or C, its influence is quite significant.

7.3 Bending moment

Throughout this study, the values of the bending moments in the piers and in the deck of each one of the four bridges considered for the current study were evaluated.

Bending moment of the base of the piers

Figures 4-5 and *4-6*, represent the bending moments attained for the base of each pier in the synchronous and asynchronous analysis, in each of the studied bridges.

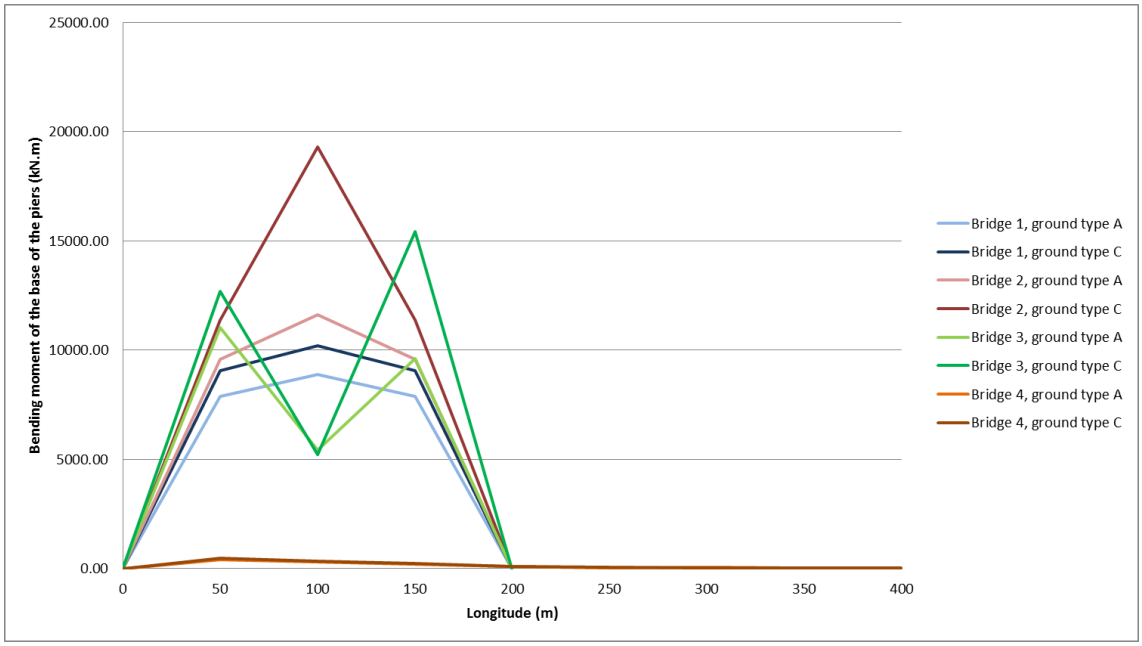

Figure 7-5: Bending moments of the base of the piers of synchronous analysis of the four bridges and both ground types.

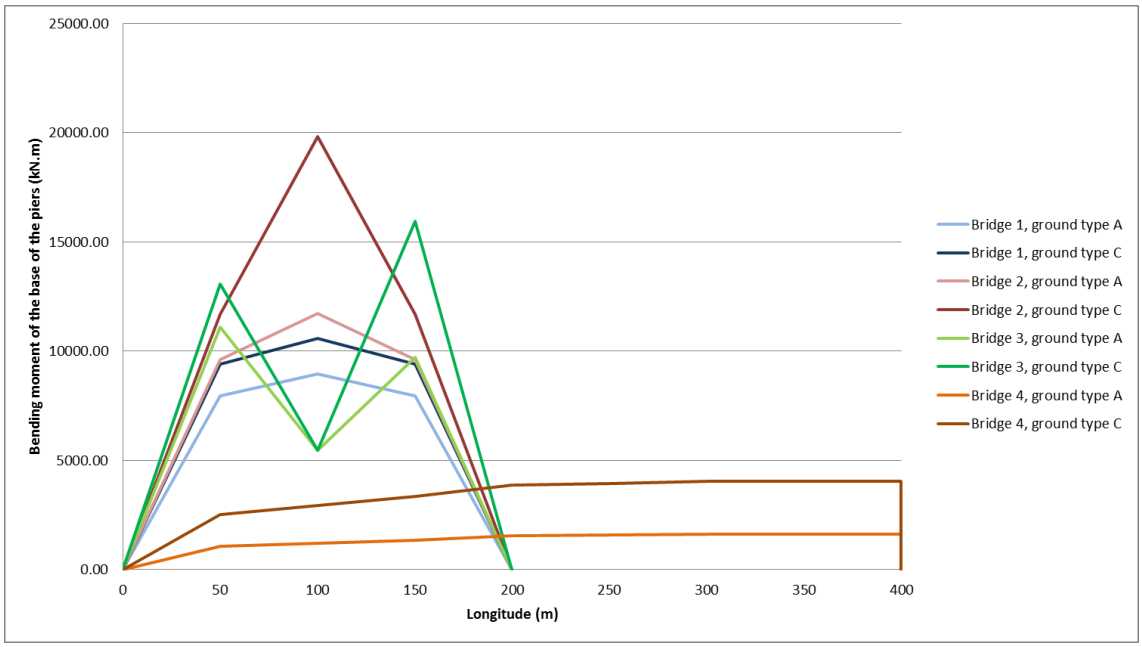

Figure 7-6: Bending moments of the base of the piers of asynchronous analysis of the four bridges and both ground types.

As it happens with the base shear, in the bending moments at the base of the piers the difference between considering the asynchrony of seismic waves is not significant with the results varying mostly according to the ground type.

Bending moments of the deck

Figures 4-7 and *4-8*, represent the bending moments of the deck attained in the synchronous and asynchronous analysis, in each one of the studied bridges.

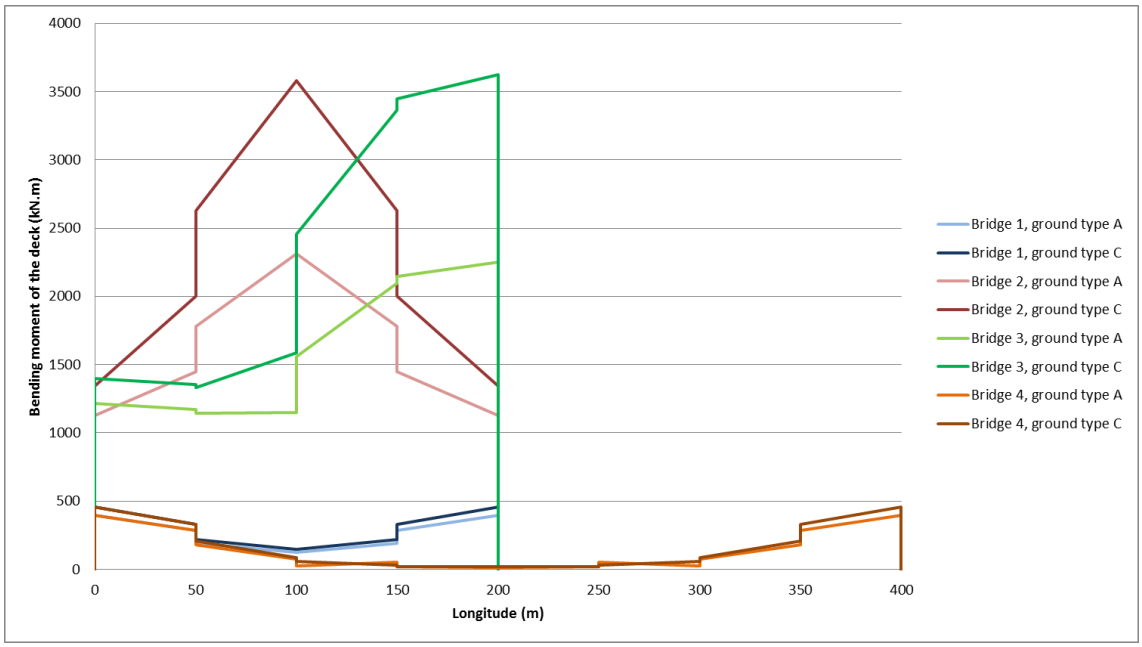

Figure 7-7: Bending moments of the deck of synchronous analysis of the four bridges and both ground types.

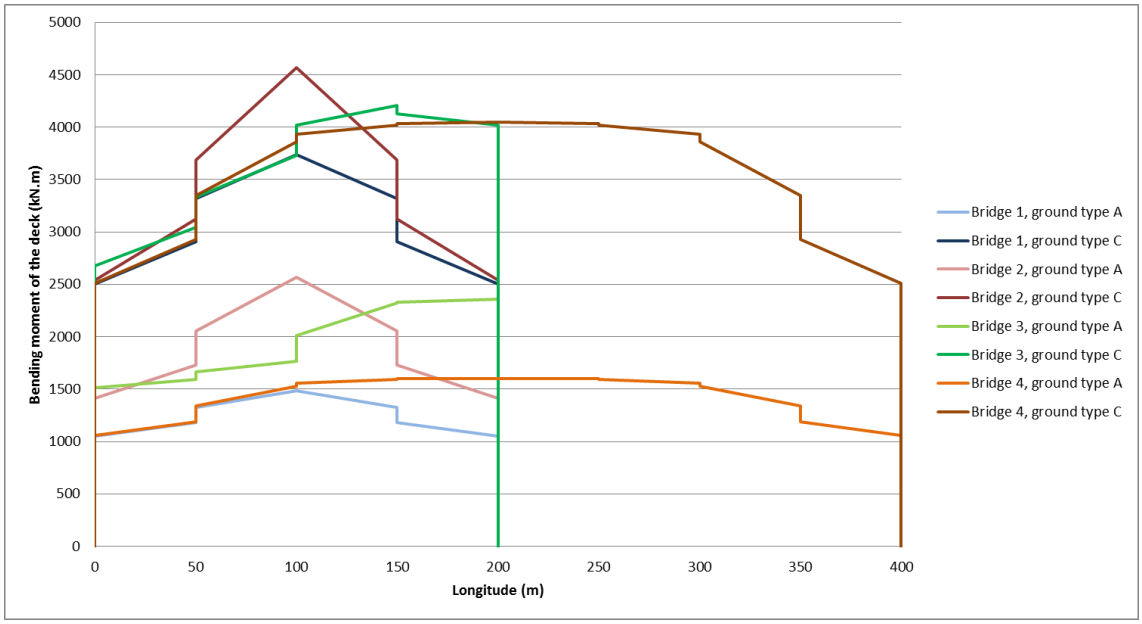

Figure 7-8: Bending moments of the deck of asynchronous analysis of the four bridges and both ground types.

From the observation of the graphics, one can conclude that the values attained when the asynchrony of the seismic sign is considered are much higher than when it is not considered. Therefore, during the design of the deck of a bridge against seismic action, it is necessary to consider the effect of the asynchrony.

As for the influence of the ground type, especially in the asynchronous case, there is a significant difference, in a general way, which should be considered.

7.4 Drift of the piers

Table 7-1 represents all the drifts obtained in both of the performed analysis, for each bridge.

		Synchronous analysis		Asynchronous analysis	
		Ground type A	Ground type C	Ground type A	Ground type C
Bridge 1	Pier 1	$1{,}18\text{x}10^{-4}$	$1{,}36\text{x}10^{-4}$	$8{,}00\text{x}10^{-7}$	$1{,}59\text{x}10^{-5}$
	Pier 2	$1{,}33\text{x}10^{-4}$	$1{,}53\text{x}10^{-4}$	$5{,}60\text{x}10^{-6}$	$2{,}90\text{x}10^{-6}$
	Pier 3	$1{,}18\text{x}10^{-4}$	$1{,}36\text{x}10^{-4}$	$1{,}04\text{x}10^{-5}$	$2{,}15\text{x}10^{-5}$
Bridge 2	Pier 1	$1{,}86\text{x}10^{-4}$	$2{,}22\text{x}10^{-4}$	$1{,}49\text{x}10^{-5}$	$2{,}19\text{x}10^{-5}$
	Pier 2	$3{,}23\text{x}10^{-4}$	$5{,}37\text{x}10^{-4}$	$6{,}45\text{x}10^{-5}$	$7{,}06\text{x}10^{-5}$
	Pier 3	$1{,}86\text{x}10^{-4}$	$2{,}22\text{x}10^{-4}$	$2{,}41\text{x}10^{-5}$	$4{,}34\text{x}10^{-5}$
Bridge 3	Pier 1	$2{,}15\text{x}10^{-4}$	$2{,}47\text{x}10^{-4}$	$2{,}69\text{x}10^{-5}$	$1{,}07\text{x}10^{-5}$
	Pier 2	$6{,}53\text{x}10^{-5}$	$6{,}30\text{x}10^{-5}$	$1{,}00\text{x}10^{-6}$	$5{,}71\text{x}10^{-7}$
	Pier 3	$2{,}67\text{x}10^{-4}$	$4{,}29\text{x}10^{-4}$	$4{,}90\text{x}10^{-5}$	$8{,}20\text{x}10^{-5}$
Bridge 4	Pier 1	$1{,}19\text{x}10^{-4}$	$1{,}37\text{x}10^{-4}$	$1{,}30\text{x}10^{-6}$	$1{,}64\text{x}10^{-5}$
	Pier 2	$1{,}29\text{x}10^{-4}$	$1{,}49\text{x}10^{-4}$	$6{,}60\text{x}10^{-6}$	$6{,}20\text{x}10^{-6}$
	Pier 3	$1{,}25\text{x}10^{-4}$	$1{,}43\text{x}10^{-4}$	$2{,}80\text{x}10^{-6}$	$1{,}10\text{x}10^{-6}$
	Pier 4	$1{,}26\text{x}10^{-4}$	$1{,}45\text{x}10^{-4}$	$3{,}06\text{x}10^{-3}$	$1{,}10\text{x}10^{-6}$
	Pier 5	$1{,}25\text{x}10^{-4}$	$1{,}43\text{x}10^{-4}$	$2{,}10\text{x}10^{-6}$	$1{,}70\text{x}10^{-6}$
	Pier 6	$1{,}29\text{x}10^{-4}$	$1{,}49\text{x}10^{-4}$	$3{,}00\text{x}10^{-7}$	$2{,}60\text{x}10^{-6}$
	Pier 7	$1{,}19\text{x}10^{-4}$	$1{,}37\text{x}10^{-4}$	$9{,}40\text{x}10^{-6}$	$2{,}13\text{x}10^{-5}$

Table 7-1: Drifts of the piers of the four bridges in study, for both analysis and both ground types.

The values displayed in the tables are extremely low. This happens not only because piers have a quite sturdy section despite its height, providing it with a considerable stiffness, but also because the actions of the response spectrum and the displacements of set A are combined according to SRSS rule. When this rule is applied in the calculation of the drift the maximum values will be deducted, hiding some of the true greatness of the drift.

To turn the results more trustworthy, the analysis should have been carried out according to the time history method. However, to confirm the importance of considering the asynchrony of seismic waves, the results attained throughout this study are sufficient.

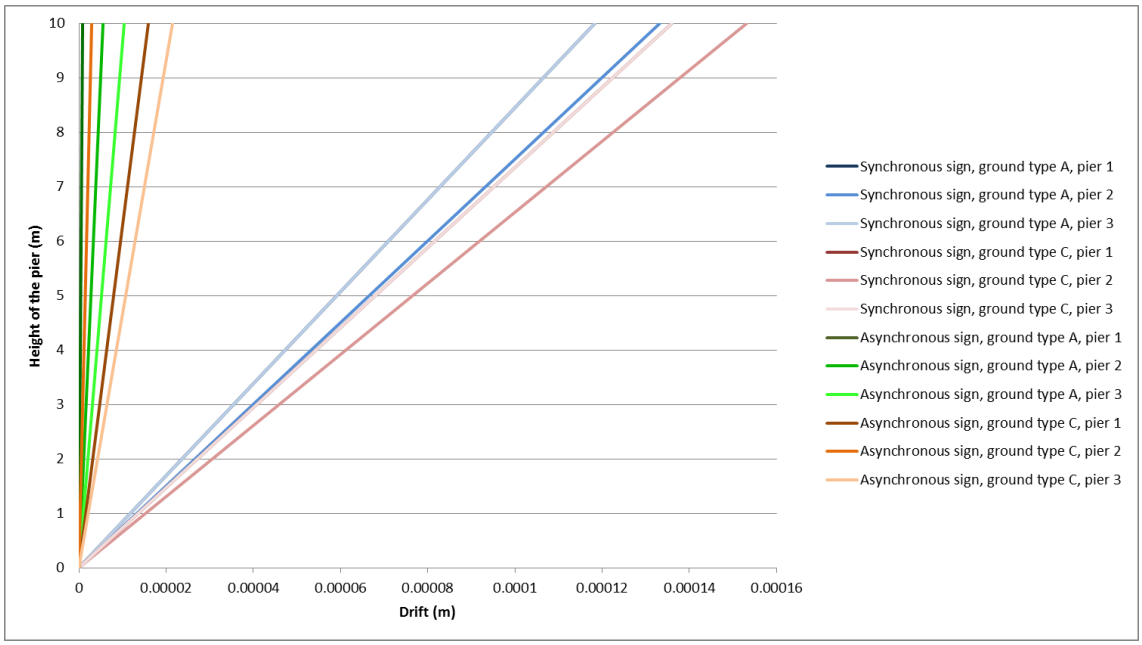

Figure 7-9: Drifts of the piers of Bridge 1, for a synchronous and asynchronous analysis.

Figure 7-9 intends to represent the effect that considering an asynchronous seismic sign has on the drift of the piers in a graphic, taking Bridge 1 as an example. As it can be observed, the results are lower when the asynchrony is not considered. Moreover, it is important to add that in none of the analysis do the attained values have the appreciable dimensions.

It should yet be stated that in all other cases it is in the synchronous analysis that the most adverse results are attained.

8. Conclusions and Recommendations

Based on the research carried out throughout this study, it is possible to state that the main purpose of any seismic guideline is to establish design and construction provisions for bridges to minimize their susceptibility to damage from earthquakes.

The design earthquake motions and forces of the norm studied in this research are based on a low probability of their being exceeded during the normal life expectancy of a bridge. Bridges and their components that are designed to resist these forces and that are built in accordance to the design details contained in the norms may suffer damage, but should have low probability of collapse due to seismically induced ground shaking.

Structural failures which have occurred during earthquakes and are directly traceable to poor quality control during construction are innumerable. Literature is replete with reports pointing out that collapse may have been prevented if a proper inspection had been exercised (Cooper, 1986). To ensure an adequate level of resistance of the structure when facing a seismic event, the engineer specifies the quality assurance requirements, the contractor exercises the control to achieve the desired quality and the owner measures the construction process through special inspection. It is essential that each part recognizes its responsibilities, understands the procedures and has the capability to carry them out. Because the contractor does the work and exercises quality control it is essential that the inspection be performed by someone approved by the owner and not the contractor's direct employee.

In what concerns the SVEGM, the performance of this study leads to the conclusion that the uniform seismic excitation is not able to control the seismic design for long prestressed concrete bridge, and the influence of the multi-support excitations on the seismic responses of the long prestressed concrete bridge must be considered.

The current study enables the possibility to state that, except for Bridge 3 in which the main pier has two slightly higher values when the effect of SVEGM are not considered, in all other situations the moment the asynchronous effect of seismic waves is taken into account is when

the results are more adverse. Therefore, the design of a large bridge should be calculated having the effect of the spatial variability of ground motion in mind.

In what concerns the ground type, it was also proven that the better the ground type of the foundation of the bridge is, the least adverse will be the damage caused by the earthquake on the structure. It is important to say that this study always comprised a single ground type for the whole bridge. Considering that these are all bridges with a considerable longitudinal development, it would be logical to assume that the ground type of the foundation varies depending on the cementation. Although this variation was not comprised in this study, its future study will be very appropriate and can lead to extend the knowledge on the SVEGM effect on large bridges.

As it was demonstrated before, the seismic excitation of a large structure is quite complex having a high variability in time and space. In the calculations of the dynamic response about these long structures, the assumption of the uniform ground supports motion cannot be considered valid. For long bridges, many researchers have studied about multi-support and traveling seismic wave effects like Li and Yang (2008), among others, and therefore it has been concluded that the use of identical excitations is generally unacceptable.

References

BRAILE, L. (2006). *UPSeis an educational site for budding seismologists*. Michigan Technological University, Houghton. <http://www.geo.mtu.edu/UPSeis/waves.html>.

CALTRANS (2013). Caltrans *Seismic Design Criteria – version 1.7*. California Department of Transportation, Sacramento, CA.

CEN (2004). *Eurocode 8: Design of structures for earthquake resistance – Part 1: General rules, seismic actions and rules for buildings*. European Committee for Standardization, Brussels. EN 1998-1.

CEN (2005). *Eurocode 8: Design of structures for earthquake resistance – Part 2: Bridges*. European Committee for Standardization, Brussels. EN 1998-2.

COOPER, J. D. (1986). *Seismic design guidelines for highway bridges*. ATC – Applied Technology Council, Federal highway administration department o transportation, second edition, Redwood City, California.

ELNASHAI, A. S. and MWAFY, A. M. (n.d.). Seismic response and design. University of Illinois, USA and UAE University. Gerard Park and Nigel Hewson. *ICE manual of bridge engineering*. Thomas Telford, London, 2008, 158 – 162.

KIUREGHIAN, A. (1996). A coherency model for spatially varying ground motions. University of California, Berkeley.

LI, J. and YANG, Q. (2008). Seismic responses analysis of long continuous rigid-framed bridge subjected to multi-support excitations. School of Civil Engineering Beijing Jiaotong University, Beijing.

LUPOI, A., FRANCHIN, P., PINTO, P. and MONTI, G. (2005). Seismic design of bridges accounting for spatial variability of ground motion. University of Rome 'La Sapienza', Rome.

PAPADOPOULOS, S., LEKIDIS, V., SEXTOS, A., and KARAKOSTAS, C. (2013). Assessment of EC8 procedures for the asynchronous excitation of bridges based on numerical analysis and recorded data. Department of Civil Engineering Aristotle University of Thessaloniki and Earthquake Planning and Protection Organization (EPPO- ITSAK), Thessaloniki.

PENNINGTON, W., ENDSLEY, K. and ASIALA, C. (2007). *UPSeis an educational site for budding seismologists*. Michigan Technological University, Houghton. <http://www.geo.mtu.edu/UPSeis/waves.html>.

PINTO, P. (coordinator) Task Group 7.4 (2007). Seismic bridge design and retrofit – structural solutions. fib CEB-FIP, Lausanne, bulletin 39, chapter 7.

RYALL, M. J. (n.d.). Loads and load distribution. University of Surrey. Gerard Park and Nigel Hewson. *ICE manual of bridge engineering*. Thomas Telford, London, 2008, 38 – 39.

SILVA, D. (2009). Análise sísmica de pontes contemplando a acção sísmica assíncrona. Faculdade de Engenharia da Universidade do Porto, Porto.

VANMARCKE, E. H. (1996). Random processes and random fields in earthquake engineering. Princeton University, Princeton.